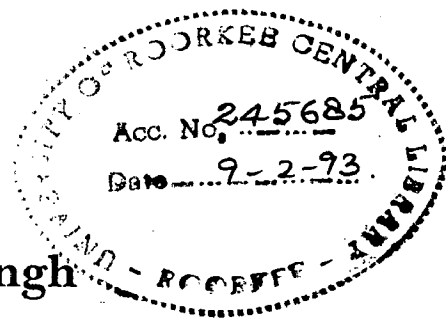


T.
F 97-90
SIN

SURFACE CHARACTERIZATION OF PRINTING PAPERS

by

Surendra Pal Singh



A Thesis submitted in Fulfilment
of the Requirement for the Degree of

Doctor of Philosophy

(Pulp and Paper Technology)

at the

University of Roorkee, Roorkee, INDIA

Swedish Pulp and Paper Research Institute, Stockholm, Sweden
June - 1990



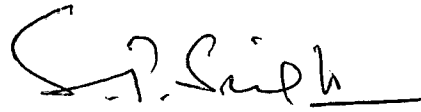
UNIVERSITY OF ROORKEE

CANDIDATES DECLARATION


I hereby certify that the work which is being presented in the thesis entitled SURFACE CHARACTERIZATION OF PRINTING PAPERS in fulfilment of the requirement for the award of the degree of Doctor of Philosophy, submitted at the Institute of Paper Technology, Saharanpur, is an authentic record of my own work carried out at the Swedish Pulp and Paper Research Institute, Stockholm, Sweden and the Institute of Paper Technology, Saharanpur under the guidance of Dr J. A. Bristow and Dr N. J. Rao. *The work was carried out during the period from Oct. 1984 to Aug 1990.*


The matter embodied in this thesis has not been submitted by me for the award of any other degree.

Date *Aug. 20, 1990*

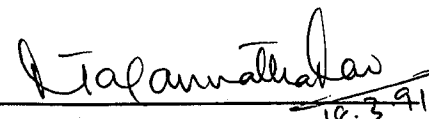

Surendra Pal Singh

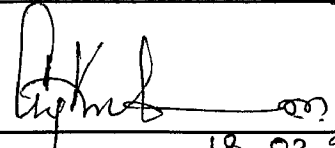
This is to certify that the above statement made by the candidate is correct to the best of our knowledge.

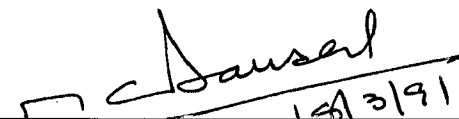

Dr. J. Anthony Bristow
Principal Research Advisor
Swedish Pulp and Paper
Research Institute (STFI)
Stockholm, SWEDEN


Dr. N. Jagannath Rao
Professor
Institute of Paper Technology
Saharanpur, INDIA

The Ph. D. Viva-voce examination of Shri Surendra Pal Singh, Research Scholar, has been held on 18th March 1991


18.3.91
Signature of Guide(s)


18.03.91
Signature of External Examiner


18/3/91
Signature of H. O. D.

AN APPRECIATION

The work for this thesis has been carried out at the Swedish Pulp and Paper Research Institute, Stockholm, Sweden and the Institute of Paper Technology (University of Roorkee), Saharanpur, India.

Thanks are due to the two collaborating institutions.

May such a collaboration continue in future.

PREFACE

The work presented in this thesis has been carried out at the Swedish Pulp and Paper Research Institute (STFI), Stockholm, Sweden. Most of the experimental work was completed during my visit to Sweden from October 1984 to December 1985 and the writing of the thesis was completed during my second visit from March to June 1990.

I express my sincere thanks and gratitude to my supervisor, Dr. J. Anthony Bristow, for his guidance, inspiration and encouragement throughout the course of this work. In spite of his busy schedules, he provided me the freedom to work with him at any time to discuss my problems and results, quite often beyond the normal working hours of the Institute. He showed his complete involvement in this work.

I am extremely thankful to Mr. Hilding Ekman and to Mr. Per-Åke Johansson with whom I worked in close cooperation during the experimental work and in the analysis of the results. Mr. Johansson provided guidance and help in the image analysis of the prints obtained in the partial coverage method, discussed in Chapter II, and of the microcontour ink stains, discussed in Chapter III. He has kindly written the Appendix A of this thesis describing the image analysis routines. I received guidance and help from Mr. Ekman during the work on surface characterization by the profilometry techniques, discussed in Chapter IV. Besides this academic help, Mr. Ekman also showed me much of the Swedish customs and cultural ways by inviting me to his home during most religious and social festivals.

I express my humble appreciation to Dr. Petter Kolseth for his critical comments, suggestions and help during the writing of this thesis.

I am indebted to my many friends at STFI, especially to Mr. Hans Bergenblad, Ms Eva Östlund, Ms Margareta Lind Kolseth and Ms Ann-Catrine Hagberg for their help in carrying out the experimental work and in the preparation of the figures in this thesis.

I thank the persons of the computer group of STFI, especially Mr. Luigi Masironi and Mr. Leopold Solis-Pinto, for their help in the computational work.

I am impressed by the high standard of research facilities at STFI and am grateful for the way in which they were made available to me.

I am grateful to the Svenska Institutet, Stockholm, for awarding me a scholarship to finance my first visit to Sweden and to Ms Ingrid Fineman, Head of the Paper Technology Department, STFI, for arranging financial assistance to enable me to complete the writing work. Acknowledgements are due to the Government of India for bearing the cost of travel for my first visit to Sweden and to STFI for bearing the travel costs for my second visit to Sweden.

I am extremely thankful to the personnel in the STFI lunchroom for kindly agreeing to prepare a daily vegetarian diet for me.

I gratefully appreciate the help of Ms Inga-Lisa Strömberg in typing many drafts of the manuscript with concern to see that the work was completed within the short period of my stay in Sweden.

Back home in India, I am grateful to my other supervisor, Dr. N. Jagannath Rao, for providing me with the encouragement and the will to complete the work. I am also thankful to my employer, the University of Roorkee, who granted me leave of absence from the University to work at STFI and permission to submit this thesis for the award of the Ph.D. degree.

Last but not least I am indebted to all my friends and relatives in India for their encouragement so that I could maintain my hope during the period of more than four years which elapsed between my two visits to STFI.

Stockholm, June 1990

Surendra Pal Singh

CONTENTS

	Page No
PREFACE .	3
CONTENTS	5
SUMMARY	9
Chapter I METHODS OF SURFACE CHARACTERIZATION	
- A literature review	13
1. INTRODUCTION	13
1.1 Importance of Surface Smoothness for Printing Papers	13
1.2 Definition of Smoothness	13
1.3 Surface Compressibility	15
1.4 Measurements of Smoothness	16
2. AIR-LEAK METHOD	16
2.1 Bekk Tester	17
2.2 Gurley-Hill Tester	18
2.3 Bendtsen Tester	18
2.4 Sheffield Tester	19
2.5 Parker-Print-Surf Tester	19
2.6 Application of Air Leak Testers in Printability Studies	20
3. OPTICAL METHODS	25
3.1 Viewing the Surface under Oblique Illumination	25
3.2 Optical Contact Area Measurement	26
3.2.1 Davis tester	26
3.2.2 Chapman tester	27
3.2.3 FOGRA-KAM	29
3.3 Optical Contact Area Measurement under Dynamic Pressure	31
3.4 Contact Area Measurement with Varying Wavelength of Incident Light	33
3.5 Measuring Scatter in the Reflected Light (K-L Smoothness Tester)	34
4. METHODS BASED ON TEST PRINTING	36
4.1 Minimum Ink Demand for Complete Coverage	36
4.2 Coefficients in Ink-Transfer Equations	38
4.3 Ink-Transfer Data as a Print Density Curve	39
4.4 Distribution of Depressions in Paper Surface	40

5.	SURFACE EVALUATION BASED ON APPLICATION OF LIQUID FILMS	42
5.1	Drawdown Tests	42
5.2	Wipe Tests	43
5.3	Drawdown using Magnetic Ink	44
5.4	Spreading of Liquid	45
6.	SURFACE PROFILOMETRY	49
6.1	Recording of Surface Profiles	49
6.2	Experimental Considerations	51
6.3	Visual Assessment	52
6.4	Quantitative Analysis	53
6.4.1	Amplitude parameters	53
6.4.2	Spatial parameters	55
6.4.3	Autocorrelation function	57
6.4.4	Power spectrum	57
Chapter II PARTIAL-COVERAGE PRINTING AND IMAGE ANALYSIS		59
1.	INTRODUCTION	59
2.	EXPERIMENTAL	61
2.1	Paper Samples	61
2.2	Printing Conditions	61
2.3	Elrepho Reflectometer Measurements	65
2.4	IBAS Image Analysis	66
3.	VISUAL OBSERVATIONS ON THE PRINTS	67
4.	MEASUREMENTS OF AREA OF COVERAGE	68
4.1	Comparison between Elrepho and IBAS Measurements	68
4.2	Relationship between Coverage Area and Ink on Forme	71
4.3	Mathematical Relationship between A and x	76
4.4	Spatial Distribution of Covered Regions	84
4.4.1	Chord length analysis	85
4.4.2	Wavelength analysis	86
5.	CONCLUSIONS	87

Chapter III SURFACE EVALUATION BY ANALYSIS OF MICROCONTOUR INK STAINS	89
1. SCOPE	89
2. EXPERIMENTAL	89
3. RESULTS AND DISCUSSIONS	91
3.1 Microcontour Values (Elrepho)	91
3.2 IBAS Image Analysis	93
4. CONCLUSIONS	94
Chapter IV ANALYSIS OF PROFILES	99
1. INTRODUCTION	99
1.1 General Characteristics of Profiling Technique	99
2. EXPERIMENTAL	101
3. ANALYSIS	104
3.1 Basic Definitions and Notations	104
3.2 Analysis of Variance	106
3.2.1 Band pass filtration by moving averages	107
3.2.2 Autocorrelation function	114
3.2.3 Autospectrum	115
3.2.4 Wavelength spectrum	118
3.3 Probability Density Function	119
4. ANALYSIS OF SURFACE PROFILES USING AUTOSPECTRA	120
4.1 Comparison of a Paper Surface Profile with a Random Profile	121
4.2 Development of Synthetic Profiles	124
4.3 Decomposition of the Profile by Bandpass Filtration	128
4.4 Conclusions	132

5.	EFFECT OF COATING METHODS ON THE SURFACE STRUCTURE OF BOARDS	133
5.1	Scope	133
5.2	Experimental	133
5.3	Results and Discussion	135
6.	PROBABILITY DENSITY FUNCTION OF SURFACE PROFILES	143
6.1	Scope	143
6.2	Determination of Probability Density Functions	143
6.3	Results and Discussion	143
Chapter V EFFECT OF TYPE OF MECHANICAL PULP ON SURFACE PROPERTIES OF HANDSHEETS		145
1.	SCOPE	145
2.	EXPERIMENTAL	145
2.1	Pulps	145
2.2	Sheet Formation	146
2.3	Wet Pressing, Calendering	146
2.4	Determination of Sheet Properties	147
3.	RESULTS AND DISCUSSIONS	147
3.1	Parker-Print-Surf Measurements	147
3.2	FOGRA-KAM Contact Area Measurements	150
3.3	Partial Coverage Printing	153
3.4	Microcontour Ink Stains	153
3.5	Autospectra of Surface Profiles	154
4.	CONCLUSIONS	156
REFERENCES		157
Appendix A - IMAGE ANALYSIS ROUTINES		169
Appendix B - SYNTHESIS OF PAPER PROFILE USING IDPAC		177

SUMMARY

Almost ninety per cent of the paper produced today is printed by one method or the other. The printer's primary task is to make a true reproduction on the paper surface of the original image given to him and to do so economically. To control the quality of the final printed matter he has a number of variables at his disposal in the printing press, the ink and the paper. In spite of the great flexibility a printer has, he nevertheless sometimes fails in his efforts to meet the present day customer's/reader's expectations. The printing press, the ink and the paper must then all be studied to find the reasons for the poor performance.

When paper is at fault, the defects in printing can frequently be attributed to a lack of smoothness. In a printing process the paper is, for a fraction of a second, pressed against a printing forme which bears a thin layer of ink. When the paper separates from the forme, ink transfers to the paper resulting in a print. It is expected that the paper makes complete contact with the inked regions on the printing forme which in the case of halftone images may be millions of tiny dots per square metre of surface.

The requirement is more stringent in gravure printing where the transfer of ink takes place from a number of tiny cup-like cells (about 100 μm diameter). It is required that each cell must make contact with the paper to enable the ink to be withdrawn from it during printing. Missing of even a few cells can be detrimental to the quality of the final print. The requirement of smoothness of the paper surface is only comparatively less important in off-set printing due to the presence of a deformable transfer roll.

Much emphasis during the manufacture of paper is placed on improving its surface smoothness without too greatly adversely affecting its other properties, the most important of which is its bulk. An important requirement is to be able to measure the smoothness of the paper surface as a means of controlling the papermaking process. A similar measure is required by the printer to control his operations. The preferred method would be one which can be used by both the papermaker and the printer, the values obtained being standardized to facilitate intercommunication.

The smoothness can be simply defined as the closeness of the paper surface to a plane surface, but it is not easy to measure this in quantitative terms. Nevertheless there are several ways to express the deviation of paper surface from a plane surface such

as mean separation, surface void volume, widths of the cavities etc. and this has led to the development of a large number of instruments.

These methods can be broadly classified as (I) Air-leak methods, (II) Optical methods, (III) Methods based on test printing and liquid film application and (IV) Surface profilometry.

The air-leak methods are based on the measurement of the air flow between a plane and the paper surface. The smoother the surface of the paper, the better will it conform to the plane surface and the slower will air pass through the intermediate gap. Instruments based on this principle are the most widely used ones. These instruments are very easy and quick in their operation and yield quantitative values which are fairly reproducible and free from operator error.

In optical methods the measurement of smoothness is based on the interaction of light and the paper surface. One group of instruments in this category involves pressing a smooth glass prism against a paper surface and determining the area of the surface which is in optical contact with the prism at a given pressure. The smoother the paper, the larger is the portion of the surface in contact with the prism. Another group of instruments is based on the measurement of the scatter in reflected light due to the roughness of the surface. The rougher the surface, the larger is the scatter. The latter methods can be employed without contact between the paper and the measuring probe and they thus have a potential for on line application.

In an actual printing process, the paper surface is required to make contact with a fluid ink layer rather than with the solid reference plane used in most laboratory smoothness measuring methods. Moreover, the ink layer and the paper surface are contacted by the application of a dynamic pressure. A number of techniques for surface evaluation have been reported where paper is actually printed in the laboratory under conditions similar to those in a printing press. The ink transfer data have been analysed to yield roughness and absorption characteristics of paper. A number of other methods which involve the application of liquid films on paper surface, although developed to study absorption and other liquid-paper interactions, also provide a measure of surface roughness.

The technique which provides the most exhaustive description of the surface topography involves recording surface profiles by a fine point stylus traversing the surface. A large number of statistical parameters can be derived from these profile records.

A difficulty arises in the evaluation of the surface of papers having very close differences in their smoothness, especially papers made by different processes and from different furnishes. The air-leak and optical methods lack resolution in such cases and quite often the measurements do not relate to the printing performance of the papers. In such cases, it is necessary to obtain more detailed information about those features of the surface structure which are also related to the behaviour of paper in a printing process. The methods of surface evaluation based on test printing resemble most closely the actual printing of paper, and surface profilometry provides the most exhaustive description of the surface.

The main objective of the present work has been to study these methods in detail. The contents of this thesis are summarized as follows:

Chapter I presents a review of available methods of smoothness evaluation. The available literature is large and diverse, and this short review is far from complete and covers only fundamentals involved in those methods which have been frequently cited in the literature. Quite often claims have been made that a particular method predicts printability of paper better than others. It is however difficult to establish the superiority of any one method over the others since smoothness is such a complex quantity that all the methods developed so far measure it to only a limited extent. They provide complementary information about the surface structure and it is unfair to compare them with each other.

Chapter II presents a method of surface characterization based on test printing of paper. The paper sample is printed in an IGT printability tester with a small amount of ink on a smooth metallic printing disc and at a low printing pressure to allow only a partial coverage of the paper surface by the ink. The peaks in the paper surface receive most ink while the deeper valleys remain unprinted. These black and white patterns show the contour structure of the paper surface for a visual assessment of the finger print of the paper. These prints were analysed on the Kontron IBAS image analyser. A number of ways to describe the paper surface quantitatively on the basis of the image analysis results are presented. The amount of ink required on the printing disc under specified printing conditions for 50 per cent coverage of the paper surface is suggested as a roughness index for paper. The slope at 50 % coverage of the curve relating area covered to amount of ink on disc is found to represent the shallowness of the

surface cavities. A typical wavelength describing the pattern of the surface can also be calculated.

Chapter III discusses microcontour ink stain tests, which are used for a qualitative evaluation of the surface roughness of coated papers and boards. In the present work the microcontour ink stains on a number of paper grades were analysed by the image analyser. The information obtained from the image analyser is more or less the same as that obtained from an Elrepho measurement except that the image analyser provides a coefficient of variation which quantifies the degree of mottle in the pigment stain and provides an additional measure of surface roughness.

Chapter IV deals with surface profilometry. Surface profiles of paper have been recorded with a Perthometer profile instrument. Since the profile data are stochastic in nature they can be described only by statistical laws. A number of ways to analyse these profile data are presented. The power spectra of profiles show the amplitude distribution as well as the spatial distribution of surface irregularities. A simple moving average bandpass filtration technique is used to sub-divide the variance of profile into four wavelength bands. Only the variations associated with wavelengths less than 1 mm are found to be related to the surface roughness and those beyond 1 mm are considered to be the waviness of the surface.

A comparison of actual paper profiles with purely random profiles simulated on a computer is presented. The actual profiles differ from the random profiles in that they have less shortwave and more longwave variations. Moreover, the analysis of an actual surface profile indicates variations at a specific wavelength which suggests the presence of a characteristic size of the surface irregularities.

The effects of various coating and calendering processes on the surface smoothness of paper and board have been studied using these profilometry techniques.

Chapter V presents data for the surface characterization of handsheets of mechanical pulps. Different methods of surface evaluation grade these pulps differently confirming the multidimensional nature of the surface structure and that no single method is sufficient to describe it completely.

CHAPTER I**METHODS OF SURFACE CHARACTERIZATION**
A literature review**1. INTRODUCTION****1.1 Importance of Surface Smoothness for Printing Papers**

Smoothness is the most important property of paper and paper board affecting printability. In a printing process, a printing forme bearing ink on its image portions is pressed against the paper surface for a few milliseconds. When the forme is separated from the paper, the ink transfers to the paper and a print is created. The smoothness of the surface controls the ease and the uniformity with which ink transfers to the paper and thus determines the final print quality. It determines how well the paper surface contacts the ink film making printing possible with low ink quantity and low pressure. Although there are many factors which affect the print quality such as the type of ink and the type of printing press, the amount of ink on the forme, the printing pressure, the softness of printing forme and backing, the absorbency of the paper etc., it is generally agreed that the smoothness of paper has the greatest effect. Considerable research effort has been devoted to acquiring the ability to predict the printability of paper by measuring its surface smoothness and compressibility.

1.2 Definition of Smoothness

An ideally smooth surface is one in which all the surface elements lie in one plane. The smoothness of a real surface such as that of paper can thus be easily defined as the closeness of its surface to the ideally smooth surface. Roughness, on the other hand, is an inversely related term which implies a deviation from the ideal surface.

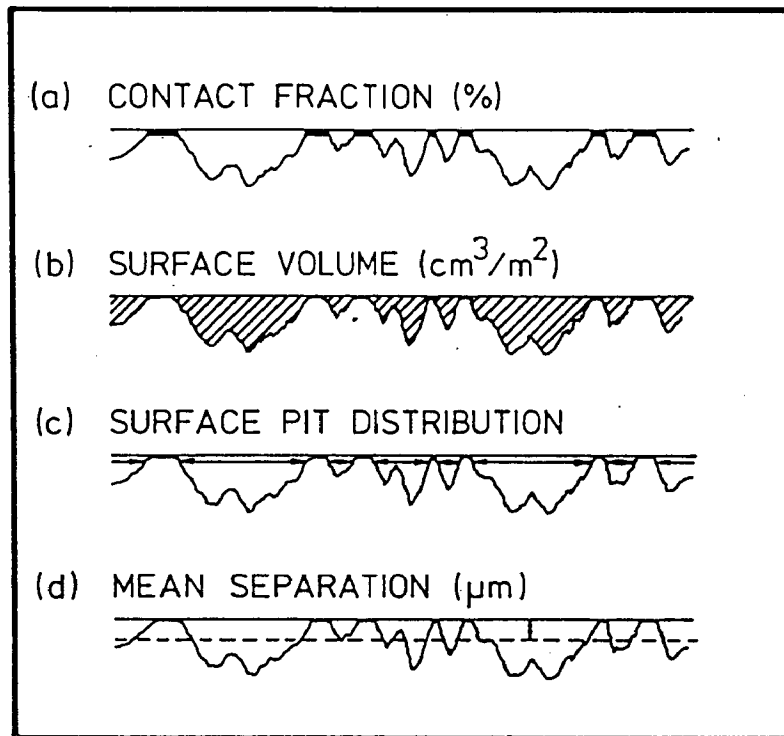


Figure 1.1 Various ways of defining roughness (Bristow, 1986)

Bristow (1986) has pointed out that to measure roughness is, however, not as easy as to visualize it as a deviation from a plane surface. Figure 1.1 shows profiles of a paper surface in relation to a plane reference surface, and various parameters which may be chosen to describe quantitatively the deviation between the surface and the reference plane. Bristow has listed some of the possible quantities as

1. volume of the voids between the two surfaces
2. fraction of the paper surface which comes in contact with the plane surface
3. mean width of surface pits
4. mean separation between the two surfaces

Many other parameters can be defined. Further, since the measured quantities show a spatial variation, it is necessary to give their distribution functions in order to describe the surface more completely.

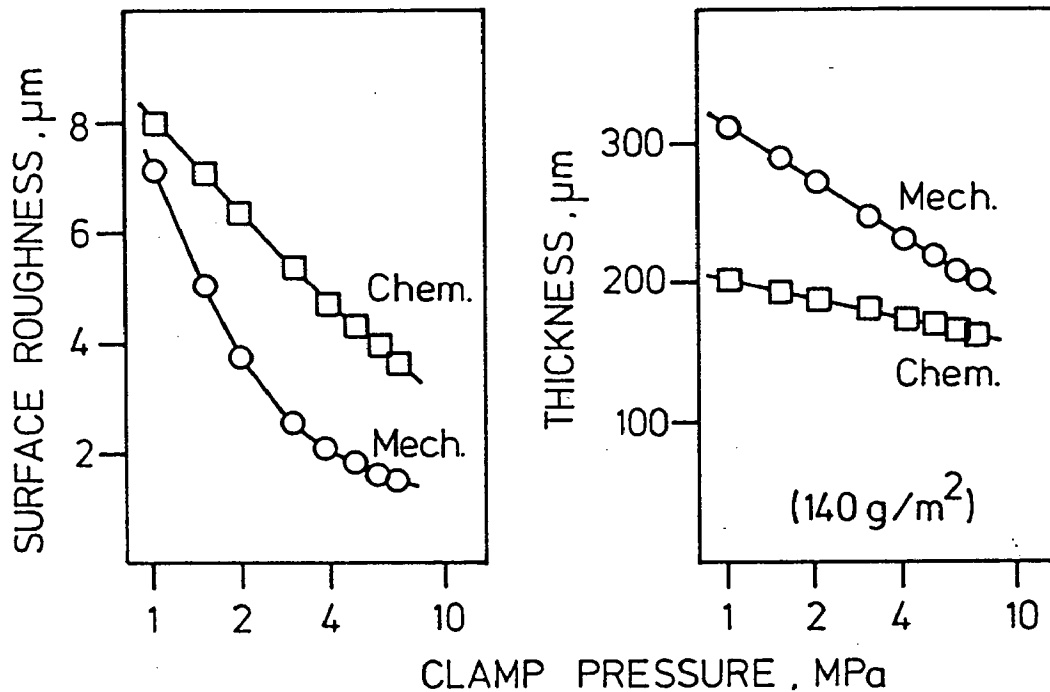


Figure 1.2 Effect of surface compressibility on the roughness (Bristow, 1986)

1.3 Surface Compressibility

An essential feature of paper is that both the paper itself and its surface are compressible so that the surface becomes smoother under the pressure applied in a printing process. Bristow (1986) has shown that two sheets of paper can assume entirely different roughness values under a given pressure even though they have nearly the same initial roughness (Figure 1.2). Those techniques which measure surface smoothness under pressure conditions similar to that in a printing nip should therefore correlate with the printability better than those which measure a free surface.

1.4 Measurements of Smoothness

Because of the lack of a single parameter which can completely characterize a surface, a large number of methods and instruments have been developed to measure smoothness to meet specific needs. Some of the instruments, due to their ease of operation, have become methods of routine measurement, whereas others, though yielding more useful information, are not greatly in use today.

The available methods of surface evaluation can be divided into the following groups:

1. Air-leak methods
2. Optical methods
3. Surface evaluation by ink-transfer
4. Surface evaluation based on liquid film application
5. Surface profilometry

The principles involved in most of these methods are presented briefly in the following paragraphs.

2 AIR-LEAK METHOD

In this method, the volume of voids between a paper and a plane surface is assessed by measuring the rate of air flow between the two surfaces. Air flow techniques generally involve pressing the test sheet against a flat surface and measuring either the time required for a given quantity of air to flow between them or the volumetric rate of flow of air leaking between them. The smoother the sheet of paper the better will it conform to the surface and the slower will the air pass through the intermediate gap. Hence the measurement of time is said to be a measure of smoothness. On the other hand the air flow rate will increase with decreasing smoothness; hence such instruments are referred to as roughness testers.

Several air leak instruments have been developed over the years. All these instruments have the following essential components:

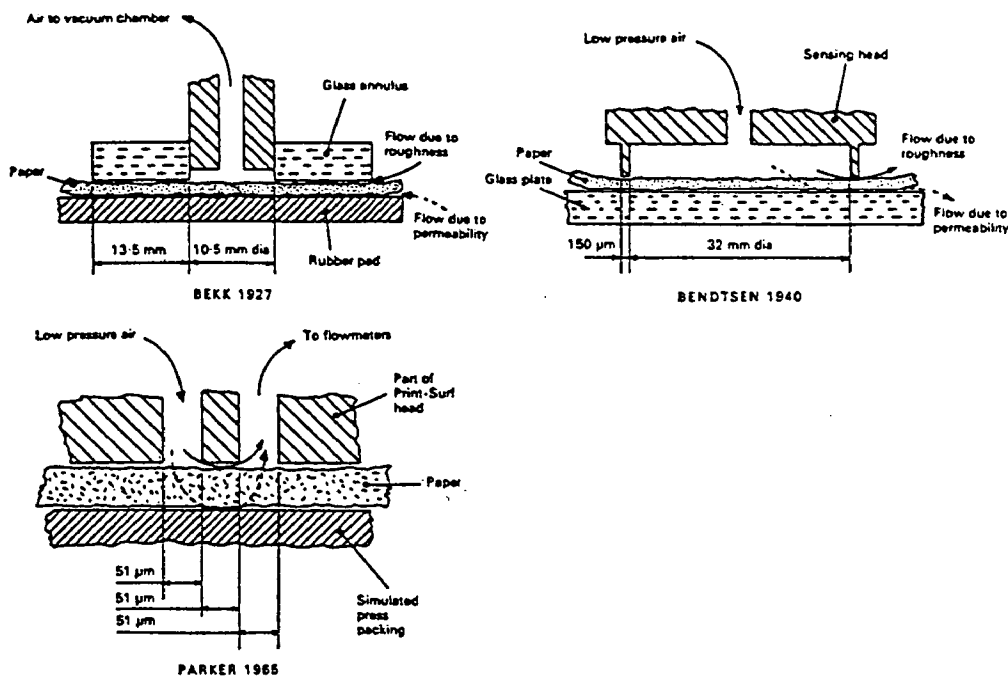


Figure 1.3 Schematic diagrams of the measuring heads of some of the air leak instruments

1. A measuring head - which includes a reference plane surface
2. Arrangement for a controlled low pressure air supply
3. Arrangement for measuring air flow
4. Arrangement for applying a known pressure between the measuring head and the paper sample

Measuring heads of some of these instruments are shown in Figure 1.3.

2.1 Bekk Tester

In the Bekk tester (TAPPI T479 om.86) the specimen is clamped with a pressure of 100 kPa between a plane, circular anvil having a small hole in its centre and a soft rubber pad. The time required to draw 10 ml of air radially between the anvil and the specimen is measured when a suction averaging 370 mm Hg (49.3 kPa) is applied at the hole.

The anvil surface has an effective area of $10 \pm 0.05 \text{ cm}^2$. The capillary connected to the suction chamber has such a volume that the addition of 10 ml of air at 23 °C and normal pressure causes its negative pressure to fall from 380 mm Hg to 360 mm Hg averaging 370 mm Hg suction. A 4 mm thick pad of soft rubber with smooth surfaces is used to contact the reverse side of the paper surface to check any flow of air through the sheet. A platen with a means of applying a load of $100 \pm 5 \text{ N}$, including the disk and rubber pad is used to clamp the sample against the anvil.

2.2 Gurley-Hill Tester

In the Gurley-Hill tester (Casey, 1981) a known volume of air is allowed to leak between two surfaces of paper and the time of leakage is measured. The paper is clamped between two optically flat metal surfaces that have an effective area of 1 in^2 (6.45 cm^2). A pressure of 3 psi ($\approx 20 \text{ kPa}$) is applied by a weighted lever arm. Ordinarily, 8 sheets are tested at a time and an average reading for 16 surfaces is obtained in one reading. The time required in seconds for 50 ml of the air to pass between the test surfaces is usually reported as the smoothness.

2.3 Bendtsen Tester

The measuring head of the Bendtsen roughness tester (SCAN:P21-67) consists essentially of a flat steel ring with a thickness of $150 \mu\text{m} \pm 2 \mu\text{m}$ and an inner diameter of $31.5 \text{ mm} \pm 0.2 \text{ mm}$. The rate of air flow through the measuring head is measured by one of a set of rotameters. A pressure governor controls the pressure of the air at the inlet of the rotameter tube at 150 mm water gauge. A small compressor is used to supply air at 1.25 atm before the pressure governor.

During the measurement, the test piece is placed on a plane ground glass plate and the measuring head is then placed on the test piece. The air flow rate is then read off in the appropriate rotameter tube. The dimensions and the mass of the measuring head are so chosen that the contact pressure between the paper and the ring is 1 kgf/cm^2 ($\approx 100 \text{ kPa}$). The contact pressure can be increased to 5 kgf/cm^2 by placing an additional weight over the

measuring head. The ratio between roughness values at 1 kgf/cm² and 5 kgf/cm² is said to give a measure of the softness or compressibility of paper surface.

2.4 Sheffield Tester

The principle of the Sheffield instrument (Sankey and White, 1948) is very similar to that of the Bendtsen instrument. The Sheffield smoothness head weighs 1640 ± 1 g and has two concentric circular lands with a total area of 0.150 ± 0.005 in² ($93.75 \pm .25$ mm²) and with each land 0.015 ± 0.0005 in (375 ± 12.5 μ m) wide. The air enters through an orifice in the head so as to fill the annular groove between the lands and escape across the surface of the paper under the lands with a smooth glass plate backing the paper. The pressure at the inlet of the rotameter is regulated at 1.5 psi (10 kPa) and is read on a mercury manometer.

2.5 Parker Print-Surf Tester

The measuring head of a Parker Print-Surf roughness tester (Parker, 1971) contains a hard steel shim 51 μ m thick and 100 mm long formed into a cylinder and sealed into place between a central plug and outer ring.

The lower edge of the shim forms the metering land on either side of which is a 1.26 mm side guard land formed by the ring or plug. The narrow gaps, also 51 μ m wide, between the metering land and guard lands serve as air ways. One communicates with a regulated low pressure air supply at 0.63 or 2.0 m wg and the other leads to a set of 4 rotameters. The central cavity is vented to the atmosphere.

During measurement, paper samples are pressed against the measuring head by a resilient backing which is carried on a moving platen. The flowmeters are calibrated to read roughness directly in micrometers, the roughness being calculated using the expression:

$$R = K (Q)^{1/3} \quad [1.1]$$

where R = roughness of the surface
 Q = volumetric flow rate of air
 K = constant for the instrument

In fact, the absolute roughness defined in this way is equivalent to the cube root of the mean cube gap between the metering land and the paper surface. By using the two standard supply pressures, results can be obtained over the range 0.7 to 9.6 μm .

The clamping pressures are high, 1 or 2 MPa, to correspond approximately to those in printing presses. The guard land also flattens the paper surface in the immediate vicinity of the metering land to eliminate the effects of waviness of paper.

2.6 Application of Air Leak Testers in Printability Studies

Instruments based on the principle of air leakage are the most widely used ones for the determination of paper roughness. The most important feature of these testers is their speed and simplicity in operation. They yield quantitative values which are reasonably reproducible and free from operator error, they have high resolution, and they can be used for different grades of paper and paperboard.

Since paper is a viscoelastic material, it deforms slowly under the pressure of the measuring head. The instruments based on the total time required for leakage of a given volume of air average out this variation in the surface of the paper over the period of measurement, whereas in instruments based on airflow the instrument readings vary with time; the instrument must be read after a fixed time so that comparative results are obtained.

Figure 1.4 shows a typical relationship between Bekk smoothness and Bendtsen roughness. It can be noted that the two instruments have opposite scales and that the two values are not easily interconvertible. Another important difference is that the instruments measuring flow rate are relatively much more rapid than those which measure time, particularly for very smooth papers.

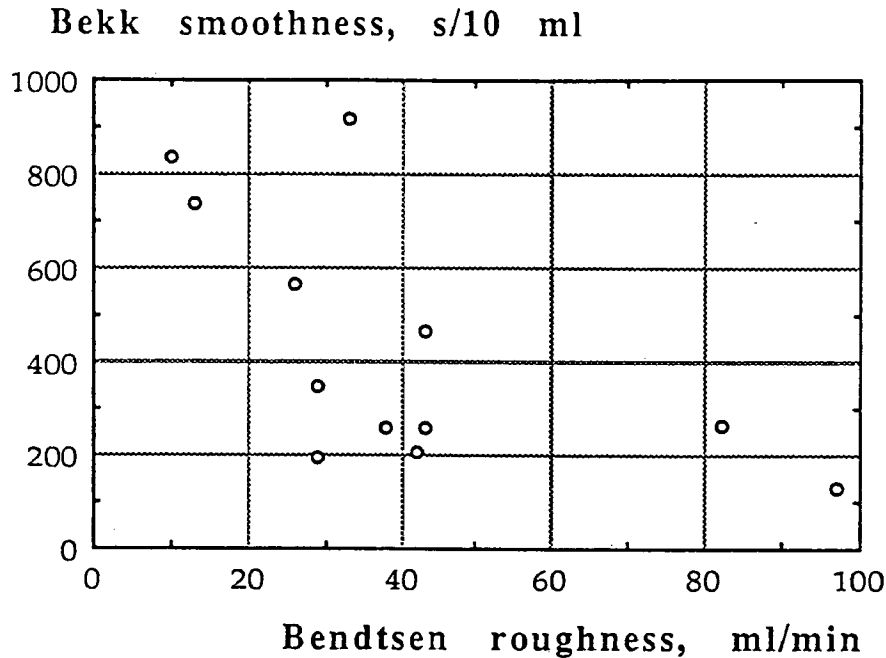


Figure 1.4 A typical relationship between Bekk smoothness and Bendtsen roughness (from data of Ginman, 1955)

An important characteristic of the air leak testers is that they give higher weights to deeper cavities. The air leakage rate is proportional to the cube of the depth of the cavities, i.e. if a cavity is twice as deep as the other cavities then the rate of air leakage through this cavity will be eight times the average leakage rate per cavity.

To obtain good print quality, almost complete contact between the ink and the paper surface must be achieved in image areas. It is easier to achieve such contact when the texture of the paper surface is uniform and free from pits of unusual depth. Thus the parameter chosen for the measurement of roughness should be one that is strongly affected by the presence of very deep pits, although the opposite view is also often expressed that the air-leak testers place inordinate emphasis on a few large imperfections and accidental particles that may be in contact with the flat surface of the instrument may introduce large errors.

A drawback with the air leak testers is that air leaking laterally through the sheet (permeance of paper) is also included in the measurement of roughness. A high degree of correlation

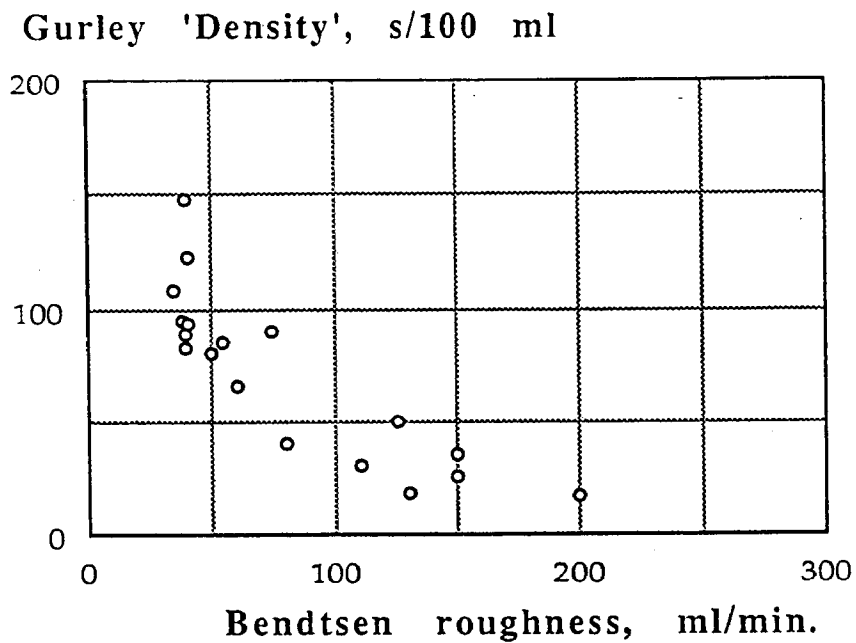


Figure 1.5 Relationship between air permeance and Bendtsen roughness (Redrawn from the data of Gunning, 1972)

between the Gurley density (air permeance) and the Bendtsen roughness as shown in Figure 1.5 is due to this error. The extent of error caused due to this leakage is dependent on the design of the measuring head, on the type of the material backing the paper sheet, and on the smoothness and porosity of the sheet.

Some important differences between various air leak instruments are given in Table 1.1.

Table 1.1 Difference between various Air-leak instruments

Instrument	Width of measuring land mm	Air Pressure difference kPa	Clamping pressure MPa	Backing	Quantity
Bekk	13.5	50	0.1	Soft Rubber pad	Time (s)
Gurley-Hill	5.9		0.02	Metal	Time (s)
Bendtsen	0.151	1.48	0.1 or 0.5	Glass	flow rate (ml/min)
Sheffield	0.375	10.34	0.1	Glass	flow rate (ml/min)
Print-Surf	0.051	6.17 (19.6)	0.5 1 or 2	Deformable	Mean roughness (μm)

In a study conducted to compare Sheffield roughness and Beck smoothness testers, Lashof et al (1956) observed that the two instruments give approximately the same performance over a large smoothness range, except for very smooth papers. For smooth papers there was some indication that Sheffield correlates better with ink transfer data.

The reason for the poor correlation is that the effect of leakage of air through the sheet of the paper increased in the case of smooth papers where leakage rate through surface voids becomes small. The Sheffield instrument should be less sensitive to horizontal porosity than the Bekk instrument for two reasons. Firstly, the air pressure difference in the Sheffield is only 1/5 of the average difference of that in the Bekk. Secondly, the path for surface leakage is much shorter, 0.375 mm in the Sheffield against 13.5 mm in the Bekk, so that a leakage path into and through the paper should be relatively less important in the Sheffield. On the other hand, the Sheffield instrument is more sensitive to specks of foreign material. Increased air leakage occurs when one of the lands of the Sheffield smoothness head rests on a speck. The Bekk instrument is less sensitive to specks and lumpiness because of the wide land, the greater test area and the rubber backing.

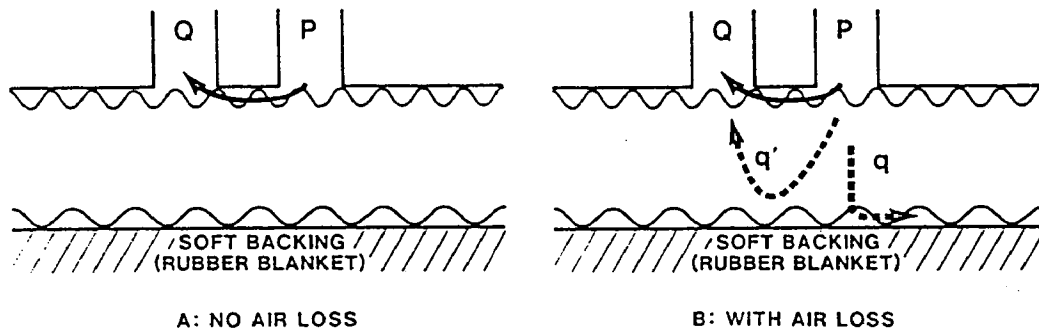


Figure 1.6 (A) the schematic drawing of the PPS tester with the assumption that no loss of air occurs through the bulk of the sheet. (B) the error introduced by leakage of air through the sheet. The leakage of air, q' , through some fiber layers is included in the measured flow Q . (Mangin and DeGrace, 1984).

The Parker Print-Surf (PPS) roughness tester attempts to reduce the errors further. The important features are

1. The metering land is narrow.
2. A deformable backing is used.
3. Guard rings limit the area of paper directly exposed to the upstream air supply to 5 mm^2 , about 1 per cent of the exposed area in some instruments. Thus air flow through the paper is minimized.

The usual assumption in the case of the PPS tester is that there is no loss of air through the bulk of the sheet due to the porosity of the paper. However, Mangin and De Grace (1984) have reported that in the case of porous papers such as newsprint a significant portion of the total air flow may escape the measure of the roughness as shown in Figure 1.6.

3. OPTICAL METHODS

In these methods the evaluation of paper surface smoothness is based on the interaction of light and the paper surface. These methods can be broadly classified into

1. Viewing the surface under oblique illumination.
2. Optical contact area measurement.
3. Measuring scatter in the reflected light.

3.1 Viewing the Surface under Oblique Illumination

When a rough surface is illuminated by a light beam at a high angle of incidence, 75 to 80°, a pattern of light and shadowed areas can be detected through a microscope with a magnification of roughly 20 to 30 times. The illumination may be oriented across the grains for greater detail and the roughest portion of the paper sample may be deliberately selected for examination. This method provides a quick qualitative evaluation of the surface. Photographs of these magnified surfaces give very good visual information about the topography of the surface, (Ragan, 1959; Andersen, 1959 and Janes, 1959), and they can also be used for grading a limited number of surfaces by a panel of judges. However, the area examined in these methods is often too small to be representative of the total sample. Moreover, the subjective evaluation is difficult to standardize. Skill and careful sample selection are needed to give a valid interpretation of results.

Scheid (1953) developed a tester for the quantitative determination of the smoothness of coated papers. Paper was illuminated by a grazing light beam and viewed normal to the paper surface through a microscope which was equipped to magnify 30 times. When the angle of incidence of the illumination is decreased, an increase in spectral reflectance occurs, and the sharpness and number of light and shadowed areas decreases. The angle where this change is most significant can be used to quantitatively determine the smoothness. In the normal range of coated paper surfaces, several different end points can be noted, all dependent on various optical illusions caused by these changes in light and shadow relationships. Two end points were found useful by Scheid, the first involving an optical illusion of loss of depth of surface irregularities and the second involving a sharp decrease in

the resolution of surface imperfections. These were referred to as Scheid 1 and Scheid 2 smoothness values. The larger the angle at which the change occurs, the smoother the surface. The Scheid results have however been found to be operator sensitive. One operator is capable of reproducing his own end points but not those of another operator.

Huynh and Peticca (1990) have recently presented a method of calculating a roughness index from the pictures of paper surface seen under grazing illumination and normal viewing. The technique is based on a digital image analyser. The image of the scattering pattern of the paper surface was focused onto a CCD camera. The analog signal from the camera was digitized by an imaging board into a matrix of 512 x 512 bixels and the intensity of shadows was resolved into 256 grey levels to yield a grey-level histogram. It was assumed that the distribution of the grey levels was Gaussian and the coefficient of variation was taken as a roughness index. The roughness index was found to show a high correlation with Sheffield roughness values.

The viewing of the surface under grazing angle illumination is a good and quick method for qualitative evaluation of paper surfaces for production control purposes. The quantitative determination is however not easy to standardize due to complicated optical effects.

The translucency of the paper surface tends to hide some of the contour differences, and variations in translucency of the paper can give the impression of being contour differences (Hull and Rogers, 1955).

3.2 Optical Contact Area Measurement

Due to its porous nature, paper is a compressible substance and the paper surface smoothens out to some extent under high printing pressures. A good measure of the smoothness of a paper surface can thus be the fraction of contact between a level reference surface and the paper surface under pressures equivalent to those expected during the real printing of paper.

3.2.1 Davis tester

Davis (1936) developed a tester in which the sample was pressed against a glass prism by means of a hydraulic press. The inside

lower prism face was illuminated by a beam of light at such an angle that total internal reflection occurred if the prism was in contact with air. This angle is dependent on the refractive index of the glass according to the equation:

$$\sin\theta/\sin\phi = n \quad [1.2]$$

where

θ is the angle of incidence
 ϕ is the angle of refraction
 n is the refractive index

This gives a critical angle of $41^{\circ}8'$ for a refractive index of 1.52.

The totally reflected beam passes out on the other side of the prism and is intercepted by a photocell placed at an angle equal to the incident angle. Wherever the paper sample makes optical contact with the lower face of the prism, the light is no longer totally reflected but enters the paper because the paper has a reflective index nearly equal to that of glass. Upon entering the paper it is partly absorbed and partly diffusely reflected, thus decreasing the amount of totally reflected light leaving the prism in the direction of specular reflection.

The higher the smoothness the greater the contact with the prism and the less the amount of totally reflected light. The photocell reading is an inverse measure of smoothness under pressure.

3.2.2 Chapman tester

Chapman (1947) developed, independently, a similar tester where the fraction of the paper surface which came into contact with the prism was determined. In Chapman's tester, the sample is illuminated through the prism by a parallel beam of light at an angle normal to the paper surface. This incident light is scattered by the paper and reflected back to reenter the prism from all directions.

Light reflected by the portions of paper in contact with the prism can pass directly into it with little or no bending since the refractive indices of glass and paper are nearly the same. Light coming from non contact areas passes through an air film

before entering the prism, and must pass into the glass within the critical angle.

Thus all light rays passing the prism at an angle to the normal greater than the critical angle must come from areas of the sample in contact with the glass since they cannot have come from air. Two photocells are used to pick up the reflected light, one at an angle greater than the critical angle and the other at an angle less than the critical angle.

The former (A) receives light only from the contact areas whereas the latter (B) receives light from both contact and non-contact areas and the fractional contact area can be calculated according to:

$$F = \frac{A C_a}{C_b + B C_a} \quad [1.3]$$

where

- F = fractional contact area or smoothness
- C_a = current from the cell A
- C_b = current from the cell B
- A, B = constants for the instrument

A standard piece of opal glass ground flat and with oil on the surface was used to define A and B. The principal of the Chapman device is shown in Figure 1.7.

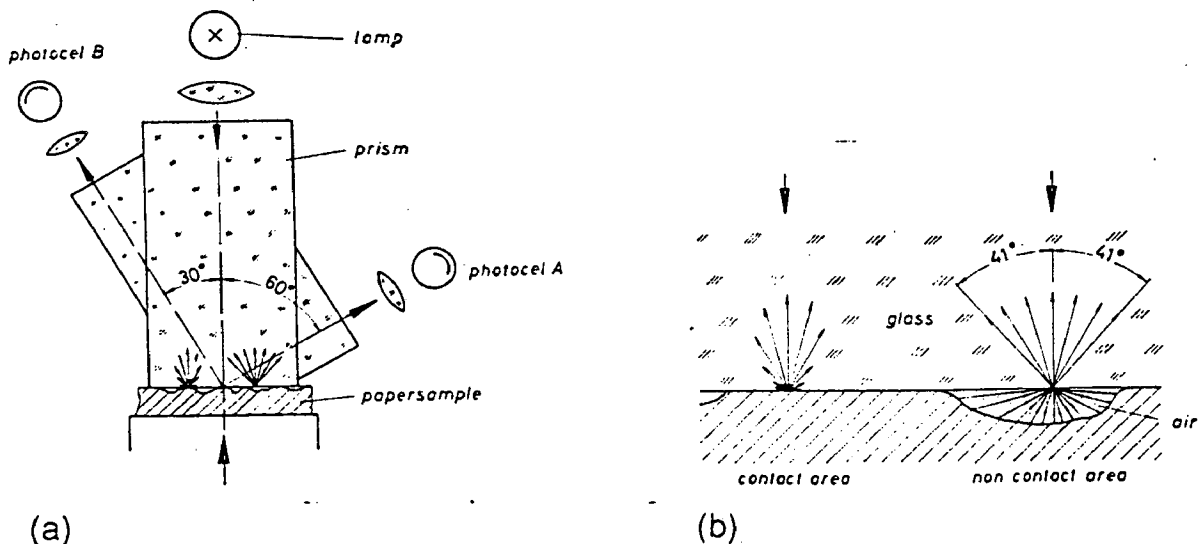


Figure 1.7 Principle of Chapman smoothness tester (a), optical arrangement, (b) light distribution at contact and non-contact areas (Albrecht and Brune, 1971)

From a study on 10 different newsprint samples Chapman found that the printing smoothness measured as percentage contact area at 400 psi (= 2.7 MPa) pressure matched the printing tests on a Vandercook proof press whereas the Bekk tester showed no relation with the printing performance.

The drawback of Chapman's concept is that the accurate determination of contact area from two reflectance values is difficult. The portions of light being measured under different angles are strongly dependent on the spatial light distribution (indicatrix). Different papers normally have different indicatrices. The Chapman equation contains two correction factors A and B. With different standards, different values of A and B are obtained. Studies made in Japan (Kittaka and Inamoto, 1965) using different standards with just one device, found values for A between 3.95 and 3.04 and for B between 1.78 and 1.11. Consequently for each type of paper appropriate corrective factors should be used.

3.2.3 FOGRA-KAM

A modified version of the Chapman tester incorporating ideas closer to those presented by Davis was developed at the German Research Association for the Printing and Reproduction Techniques (FOGRA) with the name FOGRA-KAM. (Albrecht and Brune, 1971).

The bottom surface of the prism is illuminated at an angle greater than the angle of total reflection, about 50°. The light is totally reflected by the prism if the bottom surface is in contact with air. This totally reflected light is measured by a photocell positioned at an angle equal to the angle of the incident light. On the other hand, when a paper surface is in contact with the prism the light enters into the paper and is diffusely reflected at all angles into the prism. The distribution of light from contact and non-contact areas is shown in Figure 1.8.

The amount of diffusely reflected light reaching the photocell from the contact area of the paper sample is very small. Thus the light reaching the photocell indicates primarily the regions of non-contact. The ratio of the intensity of the light reaching the photocell to that of the incident light gives the fractional non-contact area. This type of measurement requires no calibration and is free from disturbances due to optical characteristics of paper such as colour, gloss, indicatrices etc.

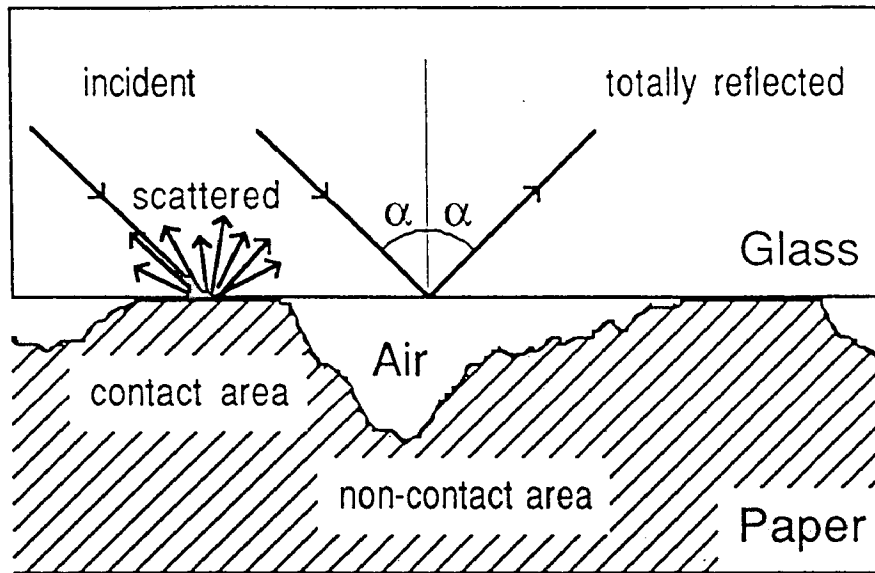


Figure 1.8 Light distribution at contact and non-contact areas in the FOGRA tester

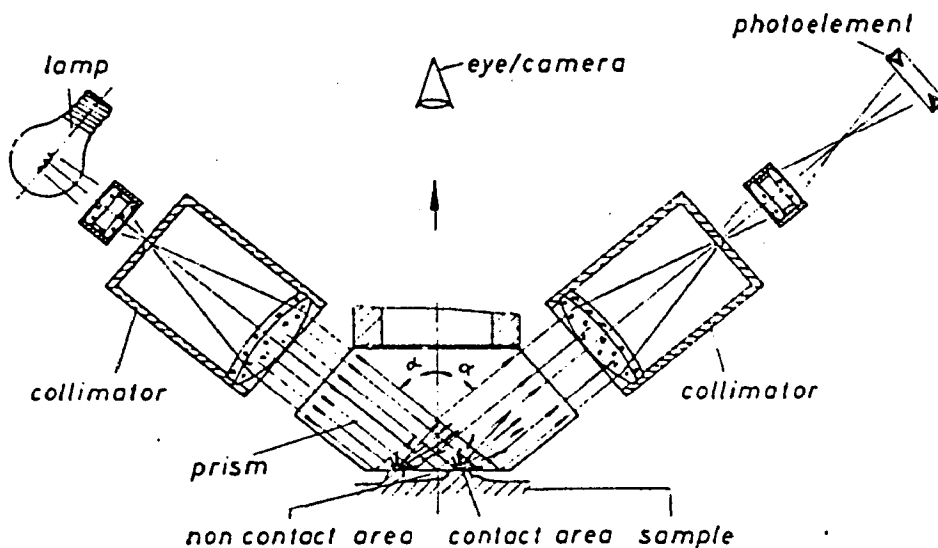


Figure 1.9 Optical arrangement in the FOGRA tester (Albrecht and Brune, 1971)

When viewed normal to the paper surface, only the scattered light coming from the paper surface reaches the eye, and the portions of the paper surface not in contact with the prism appear black. An image of the contact distribution is obtained. Photographs can be taken and these can be evaluated on an image analyser to obtain more information about the structure of the paper surface. The instrument is shown diagrammatically in Figure 1.9.

Albrecht & Brune (1971) found in a study on 16 coated papers of comparable quality that FOGRA values had a strong correlation with the FOGRA inking monitor results on solid letterpress printing. No relation with the subjective evaluation of halftones could be clearly established.

Leekley (1971) pointed out in a discussion of this paper that a better correlation was expected between optical contact measurement and gravure printability than with letterpress printability because this method did not indicate whether the non-contact area will be reached by the rather thicker ink film. Surprisingly a good correlation with letterpress solid tones was obtained in the work of Albrecht and Brune and not with halftones.

3.3 Optical Contact Area Measurement under Dynamic Pressure

In the Chapman or FOGRA testers the smoothness is measured under a static pressure whereas printing is carried out under dynamic conditions. Due to the viscoelastic nature of paper, the smoothness is undoubtedly different in the two cases.

The Chapman tester was modified by Bliesner (1970) to give smoothness under dynamic conditions, the contact area being measured under a pressure pulse rather than a static load. A compressive stress up to 1000 psi (7 MPa) could be applied in a time of 40 - 160 ms and then released to zero value in a comparable period of time. The contact surface was photographed at maximum pressure using a 2 ms high intensity Xenon flash. The photographs were then analysed to determine fractional contact area.

Another dynamic smoothness tester was developed by Blockhius and Kalff (1976). This determines the contact between glass and paper under rolling conditions rather than with the flat-flat geometry used by Bliesner. The paper is pressed against a glass cylinder by a sector in the same way as in the IGT printability tester. The compressive force can be varied between 0 and 80 kg over the 2 cm wide sector (Figure 1.10).

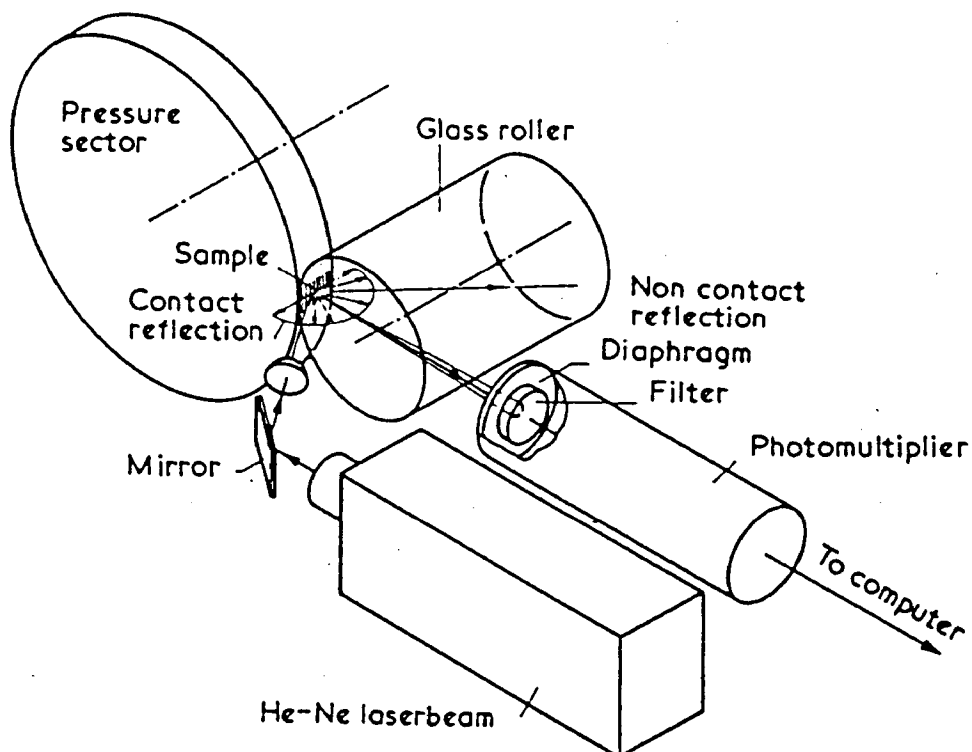


Figure 1.10 The IGT dynamic smoothness tester (Blokhuis and Blogg, 1974)

A He-Ne laser (632.8 nm) beam is directed to the glass roller via a mirror. This parallel beam is converged in an oval spot about $50\ \mu\text{m} \times 25\ \mu\text{m}$ by a lens system onto the middle of the nip. The laser beam strikes the surface of the glass at an angle of about 70° to the normal (more than critical angle). When a sample of paper is pressed against the glass roller, light is reflected diffusely from the contact areas and is detected by the photomultiplier located at an angle normal to the contact surface.

The sector rolls over the glass cylinder with a circumferential velocity of 25 cm/s. The amount of reflected light is recorded on a computer at close intervals, and an average value or a frequency distribution can be determined.

It should be noted that the Chapman and FOGRA testers measure smoothness over a larger area whereas the IGT dynamic tester scans a line about $50\ \mu\text{m}$ wide and 20 cm long over the paper surface.

Bruce Lyne (1976) used a similar principle to measure the distribution of surface void sizes in paper. The signal from a scanned area $5\ \mu\text{m}$ in diameter was fed to a spectrum analyser and a computer to display the variance distribution of the lengths of voids lying along the scan line. The time average amplitude of the signal gave the dynamic contact fraction of the surface.

3.4 Contact Area Measurement with Varying Wavelength of Incident Light

The Chapman or FOGRA testers determine the fraction of the paper surface which comes in optical contact with the prism, but give no measure of the depths of surface cavities which are not able to contact the prism. In the case of actual printing, the ink film is flexible and can even contact portions of the surface which do not come into optical contact with the prism. Information about the depths of the gaps between the prism surface and the paper can be obtained by varying the wavelength of the incident light.

When internal reflection occurs, the light waves penetrate slightly into the air beyond the prism boundary before being reflected, the depth of penetration being proportional to the wavelength of the light. The phenomenon is called Frustrated Total Reflection (FTR) and it influences what is registered as optical contact. A surface region not in physical contact with the prism may thus be interpreted as being in contact by light of wavelength λ_2 but not by light of wavelength λ_1 , as shown in Figure 1.11. If the optical contact area is determined with light of different wavelengths, the fractional area of paper within a depth from the

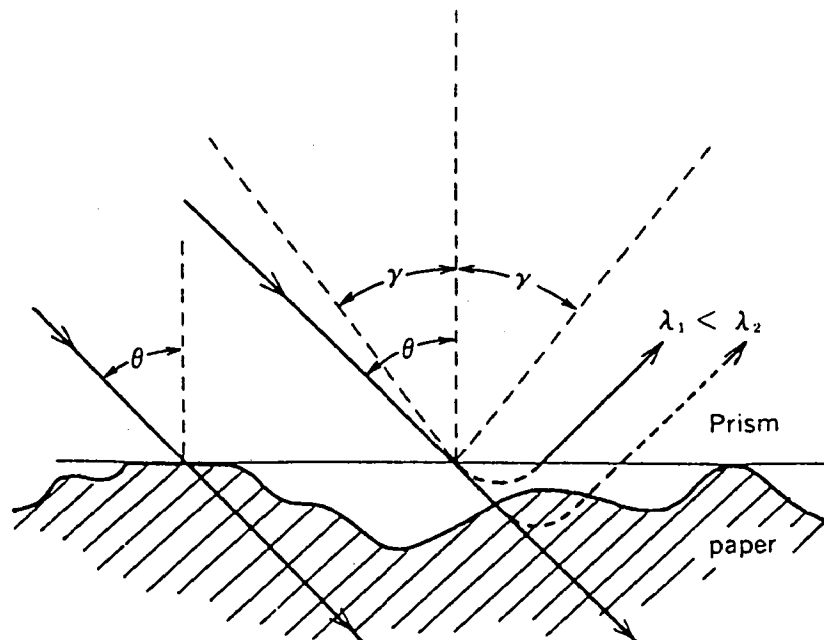


Figure 1.11 Effect of wavelength of light in discriminating contact and non-contact areas

surface of the prism corresponding to each wavelength can be calculated and hence the topographical structure of the paper surface can be estimated.

A dynamic smoothness tester based on this principle has been developed in Japan (Toyo Seiki Bulletin 1984).

A parallel beam of light is incident at an angle of 45° and the specularly reflected light is separated into four components of wavelength of 500, 900, 1300 and 1700 nm which are received by four separate photodiodes.

Arrangements are provided for applying pressure between the prism and paper surfaces under dynamic conditions.

A schematic diagram of the Toyo Seiki tester is shown in Figure 1.12.

3.5 Measuring Scatter in the Reflected Light

The K-L smoothness tester (Schmidt, 1982; Hartig, 1985) was developed mainly for on-line smoothness measurement but the tester can also be used in laboratories. An infrared light (900 nm) beam

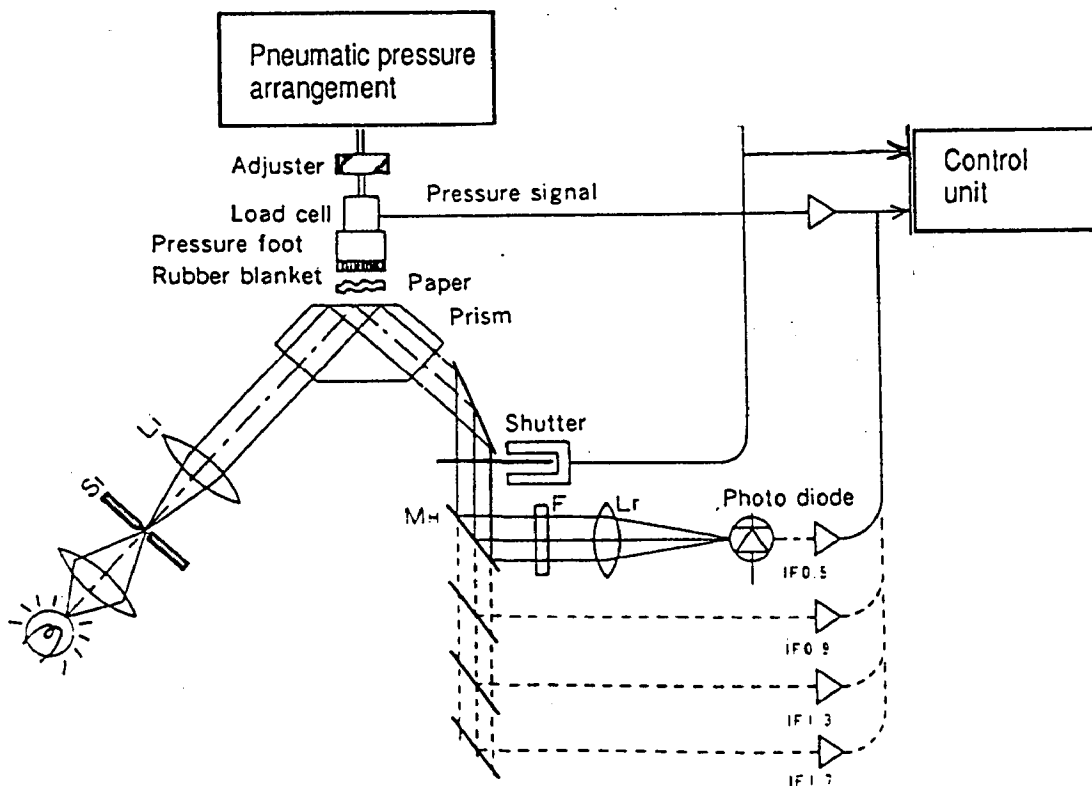


Figure 1.12 Toyo Seiki Dynamic Smoothness Tester

strikes the surface of the specimen at a high incident angle. Due to surface roughness, the reflected light is scattered as a cone of light, the diameter of which in a plane perpendicular to the surface of paper is dependent on the surface roughness. This diameter is measured by a diode array, and is expressed as the percentage of the number of diodes receiving illumination above a set threshold value (Figure 1.13).

Since no physical contact is required between the instrument and the test surface, the instrument is suitable for use on-line on a paper machine. The measurement is very fast and an arithmetic mean of a number of observations can be obtained in less than one second. The instrument has no absolute smoothness scale; it can be calibrated against any reference surface. The K-L smoothness tester has been reported to be successfully employed on a number of paper machines and coating machines for comparison within the same grade of paper or board.

In a study conducted by Singh and Ekman (1985) it was, however, observed that the optical smoothness as measured by the tester is different from the geometrical notion of smoothness. Some rough handsheets made from mechanical pulp showed unexpectedly high K-L smoothness which was gradually reduced by calendering. This strange response suggests that this instrument is not suitable for the measurement of the smoothness of some grades of paper.

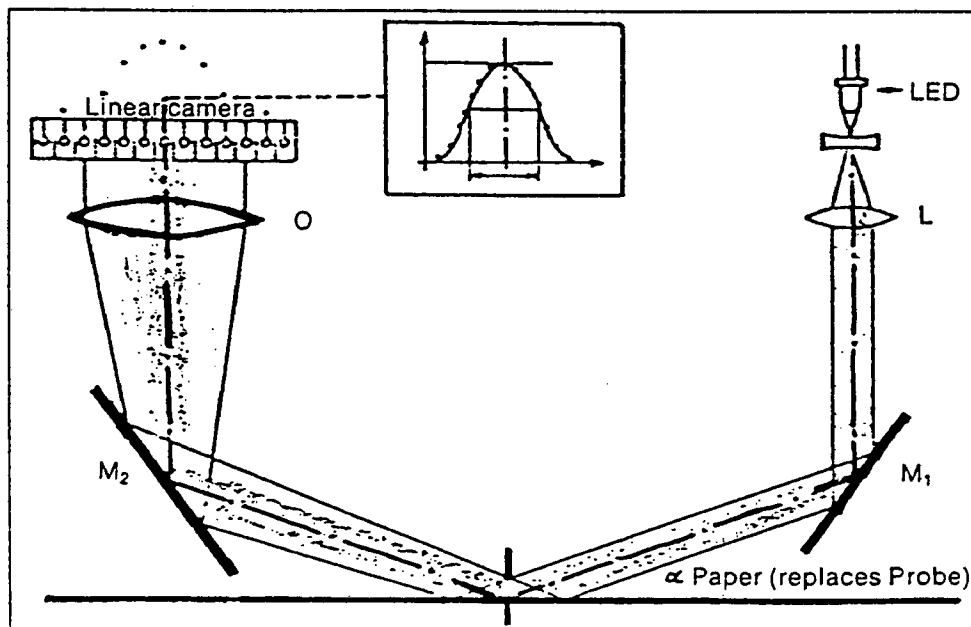


Figure 1.13 The optical arrangement in the KL smoothness tester

4. METHODS BASED ON TEST PRINTING

Most laboratory smoothness measuring methods differ from actual printing conditions. The important differences are:

1. Printing occurs under dynamic forces. The forces involved vary considerably for various printing processes, being largest in letterpress and decreasing in gravure and offset processes. The duration varies between 1/25 and 1/150 sec.
2. The paper surface is required to contact a flexible ink film on the printing forme rather than a hard surface.
3. The entire paper surface should achieve perfect contact with the ink layer on the forme. Methods giving average values may often not give enough weight to those surface defects in the paper which are detrimental to its printability. Poor prints are obtained at defective positions notwithstanding what the average values are.

Obviously, the evaluation of paper surface smoothness should be more relevant from the printability viewpoint if it is based on method in which the paper is actually printed under conditions similar to those encountered in real printing. A number of such studies have been reported in the literature. In most of these methods the paper is printed on a laboratory printability tester under controlled conditions of ink film thickness, pressure and speed of printing, a series being printed with increasing amount of ink on the printing forme. A number of ways have been reported to analyse these data.

4.1 Minimum Ink Demand for Complete Coverage

When the paper is printed with a small amount of ink, the paper surface does not establish complete contact with the ink layer on the printing forme. The ink from the forme is transferred to those portions of the paper which make contact and results in a discontinuous print on the paper. As the amount of ink is increased on the forme, more and more of the paper surface receives ink during printing. The minimum amount of ink required to give continuous coverage is reported to be a good measure of printing smoothness,

but the point at which this occurred was determined subjectively (Fetsko, 1958; Luey, 1959, Trice et al, 1973, Broadway, 1979.)

Luey [1959] studied the letterpress printability of boxboard using a Vandercook proof press model No. 4. He used a step wedge printing plate which carried an ink layer of varying thickness from one end to the other.

An important observation was that the results were affected by the impression, i.e. the excess thickness of board plus packing over the nip gap, because this affected the effective printing pressure. The method is therefore not a pure measure of roughness independent of other material properties such as thickness and compressibility, but it may give valuable information concerning the effective surface roughness in this type of press.

Trice et al [1973] used the same method as that of Luey but stressed the need for rigid control of printing variables. Besides controlling the type of ink, printing speed, and ink film thickness, they pointed out that the printing pressure rather than the printing impression should be standardized since the pressure-impression relationship is altered by the compressibility of the packing and the paper. The values of printing smoothness have been reported to vary from about 3 μm for a very smooth coated paper to about 15 μm for a medium density coarse paper.

Since the term "ink film thickness" is not relevant in gravure printing, the number of dots per square inch which do not transfer from a half tone with a screen ruling of 100 lines/in. has been found to be a good roughness index (Bradway, 1979).

The Heliotest attachment to the IGT printability tester is based on a similar concept but uses an engraved cylinder with progressively increasing cell depth. This method can however be tedious and time-consuming.

George et al (1976) developed a gravure print smoothness tester to count the missing dots. The method involves scanning a printed tone area by means of a modified telephoto-transmitter. The scanner output is converted to optical density and passed through a bandpass filter centred on the dominant frequency of the skip signals. When the scan passes over a skip, the reduction in density produces a signal at the filter output. The number of signal pulses gives an index number related to the incidence of missing dots on the print.

4.2 Coefficients in Ink-Transfer Equations

From measurements of the amount of ink transferred to the paper, y , corresponding to the amount of ink on the forme, x , Walker and Fetsko (1955) showed that the data could be expressed as

$$y = b + f(x-b) \quad [1.4]$$

where b = amount of ink immobilized by the paper, and

f = fraction of the non-immobilized ink which transfers to the paper. (The value of f is close to 0.5).

For small values of x , when only partial coverage of the surface occurs, the experimental values do not obey the above equation. The ink transfer equation was therefore modified by Walker and Fetsko to

$$y = (1-e^{-kx}) [b(1-e^{-x/b}) + f(x - b(1-e^{-x/b}))] \quad [1.5]$$

The term $(1-e^{-kx})$ is postulated to represent the fractional area of the paper surface which comes in contact with the ink film of thickness, x , on the forme and approaches unity with increasing x .

The constant k accounts for how quickly the ink covers the total surface with increasing ink film thickness on the forme and represents the smoothness of the paper. Karttunen (1970) pointed out that the term $(1-e^{-kx})$ falls to zero as x approaches zero even though there will be some contact between the surface and the forme due to the applied pressure. He suggested that the Walker-Fetsko equation could be modified by replacing the term $(1-e^{-kx})$ with a new term

$$A(x) = 1-(1-A_0)e^{-kx} \quad [1.6]$$

where A_0 represents the limiting value of $A(x)$ as x approaches zero.

Both k and A_0 are characteristics of the paper surface. A_0 represents the flattened fraction of the surface due to the printing pressure.

4.3 Ink-Transfer Data as a Print Density Curve

Tollenaar et al (1966) proposed that the ink transfer data could be expressed by the equation

$$D = D_{\infty}(1 - e^{-mx}) \quad [1.7]$$

where D = optical density

D_{∞} = saturation density; the density approached by the theoretical curves if the ink film thickness is increased infinitely.

m = a constant for the paper.

Tollenaar and Ernst (1982) had found in earlier work that equation (1.7) fitted the experimental data better when the amount of ink transferred to the paper, y , was used in the equation in place of x . However for the evaluation of surface roughness the amount on the printing disc is more relevant and the equation is found to express the experimental data satisfactorily at the intermediate values of x found under practical conditions.

The constant m , the density smoothness, is closely related to the printing smoothness, k , introduced by Walker and Fetsko, and indicates how quickly the saturation density is obtained.

The constant k of the Walker-Fetsko equation and the constant m of the equation of Tollenaar et al should be equal if the prints with partial coverage were true black and white images, i.e. if the printed portions were printed to saturation density. In practice, the m value is somewhat lower than the k value. The values of m and D_{∞} are characteristics of the paper if the testing procedure is suitably standardized.

Tollenaar et al (1966) suggested that the values of m (and D_{∞}) can be obtained reasonably accurately by test printing at only two ink film thicknesses such that $x_2 = 2x_1$, in which case:

$$m = \frac{1}{x_1} \ln\left(\frac{D_2}{D_1} - 1\right) \quad [1.8]$$

The optimum accuracy is obtained if x_1 is chosen such that

$$\frac{D_1}{D_2} = \frac{e}{e+1} = 0.73$$

This means that the choice of x_1 is dependent on the roughness of the paper. Tollenaar et al suggested that the following values of x_1 could be taken as a rough guide:

$x_1 = 2.4 \mu\text{m}$ for a medium quality of paper

$x_1 = 3.2 \mu\text{m}$ for rough paper, and

$x_1 = 1.6 \mu\text{m}$ for smooth papers.

When comparisons were made on four machine-coated papers, the obtained values of m gave the same ranking as the visual examination. O'Neill (1959) used an IGT printability tester to determine the printing smoothness of paper. The initial ink film thickness was kept below that which provides complete coverage of the paper surface to accentuate the coverage differences. The different surface structures of the papers show up clearly on these prints. The average optical density of these prints was determined by scanning the print by a densitometer over a 300 mm length. The diameter of the illuminated area of the print was 4 mm. The mean value of the density on the prints obtained under standardized conditions was found to be a good measure of printing smoothness. He found that the method had a great power to discern differences in paper surfaces even when the Chapman tester completely failed to show differences.

4.4 Distribution of Depressions in Paper Surface

Hsu (1962, 1963) developed an elegant technique to derive expressions for the distribution of depressions in a paper surface using information obtained from printing experiments.

When a printing forme bearing an ink layer of thickness x is pressed against the paper surface, the ink layer will seek to conform to the shape of the surface and the area A to which ink is transferred provides information about the distribution of depressions.

Hsu postulated that the depth was given by:

$$\delta = \int_0^x dx/(1-A) \quad [1.9]$$

and the distribution function by:

$$\Phi(\delta) = \frac{1}{1-A} \cdot \frac{dA}{dx} \quad [1.10]$$

This was valid for flat-bed printing, but a slightly different expression was obtained for the case of printing under rolling pressure, where lateral flow of the ink is possible.

In this case:

$$\delta = x \quad [1.11]$$

and

$$\Phi(\delta) = \Phi(x) = \frac{dA}{dx} \quad [1.12]$$

The distribution curve passes through a maximum and the corresponding value of δ represents the depth of the most frequently occurring depression and may be taken as an index of surface roughness. It is not necessarily equal to the commonly used mean depth which is given by $\int_0^{\infty} \delta \Phi(\delta) d\delta$.

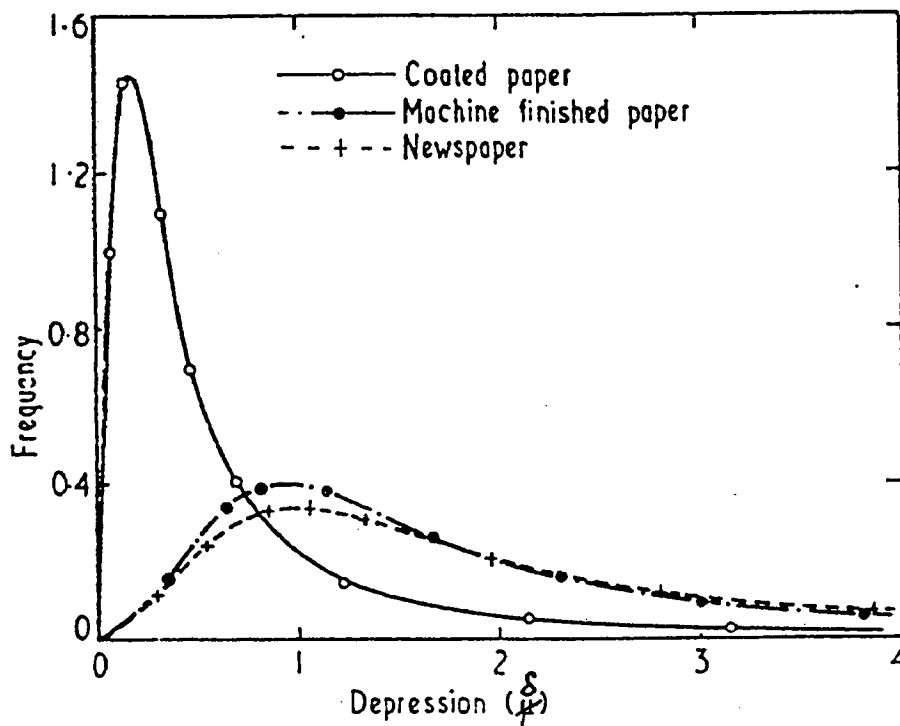


Figure 1.14 Frequency distribution of depressions (Hsu, 1962)

For papers, the mean depth is usually greater than the depth of the most frequently occurring depression.

To determine the distribution curve, the area covered by ink on each print has to be determined. Hsu suggested that it could be determined (a) planimetrically, (b) by taking the ratio of masses of printed and non-printed portions cut from a magnified photograph of a print or (c) from reflectance measurements.

From studies of a number of paper grades, Hsu observed that the frequency distribution may be assumed to be of the logarithmic normal type, i.e. the Gaussian function of the logarithm of δ .

The mean value of $\ln \delta$ gives the value of x for 50 % coverage, i.e. $x_{0.5}$ at $A = 0.5$.

And the most frequently occurring depression is given by

$$\delta = x_{0.5} \cdot e^{-\sigma^2} \quad [1.13]$$

Hsu showed that for paper surfaces the A vs x data could be fairly accurately expressed as

$$\frac{A}{1-A} = kx^n \quad (1.14)$$

where k and n are constants for a given paper. This equation allows analytical solutions to be rapidly derived from the data.

5 SURFACE EVALUATION BASED ON APPLICATION OF LIQUID FILMS

5.1 Drawdown Tests

Drawdown tests were initially devised for the inspection of inks. In these tests a small quantity of ink is drawn down on a sheet of bond paper with the help of a knife to a thin film suitable for colour comparison.

Hull and Rogers (1955) found that the technique was equally useful for the study of the texture of the paper surface under the ink film. They found that a number of paper characteristics could be studied by varying the design of drawdown blade and the type of ink used.

In a rigid-blade drawdown test the paper sample is placed on a flat glass plate and the drawdown is made with a thick blade with relatively blunt edge. A load equivalent to 0.5 - 2 MPa is applied

by putting a weight at the centre of the blade. A specially formulated or non drying, pigmented ink is used for these tests.

In flexible-blade drawdown tests, the paper sample is backed by a soft material like a pad of rubber or paper and the drawdown is made with a thin flexible blade similar to the doctor blade used in a gravure press. The load applied is of the order of 0.5 MPa. A relatively longer ink is more suitable for flexible blade drawdowns.

The patterns obtained on the paper surface from these drawdown tests vary in darkness with the weight on the blade, the speed of the blade and the angle at which the blade is held. These factors are not, however, found critical for showing the contour variations on the surface but they may need to be standardized for the purpose of comparison of different paper samples. A drawdown at 45° to the machine direction is optimum because it emphasizes marks in both machine and cross directions.

The pattern shown by the rigid-blade drawdown test indicates the variation in thickness and hardness of the paper examined. Thin spots are dark and thick spots are light. When drawdowns are made on opposite sides of the paper the pattern is roughly duplicated on both sides of the paper confirming that the variation is in the formation of the paper and not limited to the surface alone.

The flexible-blade drawdown test shows a much finer pattern with usually no relation to the large rigid-blade pattern. The pattern is not the same on both sides of the paper and is not caused by the absorption properties. The test essentially shows the surface characteristics of the paper. Holes in the coating, surface fiber structure, wire marks and other similar characteristics which can be identified under oblique illumination are made visible by these tests.

5.2 Wipe Tests

Wipe tests are a variation of the drawdown tests. The inks are spread in a thin layer on the paper sample by means of a spatula. The inks are allowed to remain there for a specified time (0-2 min) and the excess is then wiped off using cleaning tissues. Patterns produced by pigmented inks indicate surface contours and those produced by dye-base inks indicate a combination of roughness and absorption. The microcontour ink which contains a blue pigment suspended in a colourless oil is used particularly for surface evaluation. Upon application of such an ink, the solid

phase pigment stays in the surface cavities and the oil is absorbed in the paper. The intensity of the stain is almost independent of the time of application of the ink.

The rigid-blade drawdown, the flexible-blade drawdown and the wipe tests differ in the frequencies and sizes of the irregularities indicated. The rigid-blade drawdown tests indicate variations in the surface features in the wavelength range 2.5 mm to 25 mm which are mainly affected by formation and thickness variations in the paper. The flexible-blade drawdown test indicates a medium surface structure with a wavelength range of 0.25 to 2.5 mm and the wipe test³ show fine surface structures at wavelengths less than 0.25 mm. According to Hull and Rogers, the wipe tests indicate roughness of the same order as that which affects the gloss of the paper.

These tests are fairly easy and quick to perform, but they have the disadvantage that they do not yield numerical values, and experience and skill are required in interpreting these tests. The optical densities of these stains are sometimes measured by a reflectance densitometer or a photometer to obtain a quantitative measure of the stain intensity but this gives only an average value and the details of the pattern are neglected.

5.2 Drawdown using Magnetic Ink

Lyne and Copeland (1968) used the drawdown technique to obtain profiles of paper surfaces which could be analysed to measure the size and distribution of surface irregularities. In their technique, a magnetic ink was applied to the specimen with a drawdown blade which filled the surface voids of the paper.

The upper surface of the film of ink may be regarded to be a plane through the high spots of the sheet. After the ink had dried, a strip of the specimen was cut and used as a recording medium in a special recording apparatus. An AC-signal was recorded and played back in such a way that the amplitude of the pulse at any point was proportional to the thickness of the magnetic film at that point, and thus represented the surface profile of the paper. The width of the line scanned was about 300 μm and the data were recorded at a distance of 100 - 125 μm .

These profile records were analysed using techniques similar to those used by Roehr (1955).

Verseput and Mosher (1971) used a similar technique and divided the profile into 5 levels with depths from 0 to 5 μm . The

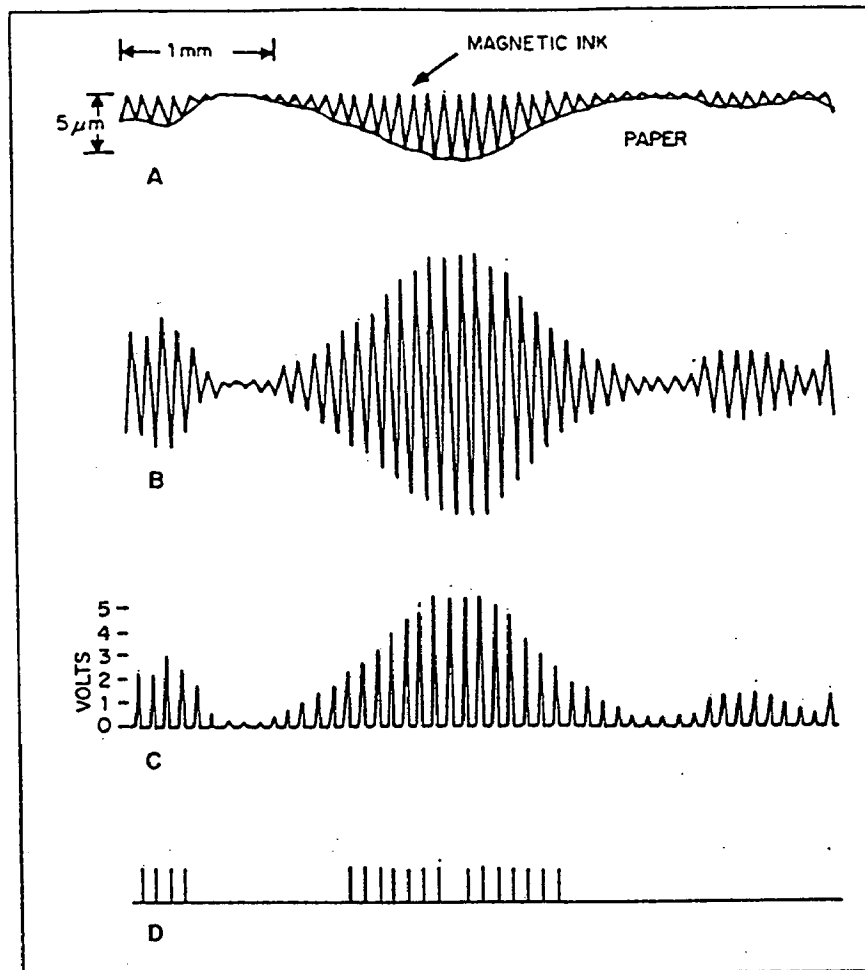


Figure 1.15 The surface profile recorded using magnetic ink to make adrawdown (Verseput and Mosher, 1971)

number of times the signal crossed a level was counted and the results were expressed in the form shown in Figure 1.15.

The more rapidly the count approaches zero as the depth increases, the better the printing smoothness of the paper. It may be possible to characterize the rapidity of this drop by a single number.

5.3 Spreading of Liquid

Several apparatuses have been developed in which a certain liquid film is spread over the paper surface. A part of the liquid applied penetrates into the paper depending on its absorptivity and a part of the liquid remains in the valleys of the paper sur-

face. This latter quantity is determined and is used to express the smoothness of the paper.

Wink and van den Akker (1957) developed a nip spreading apparatus where the liquid film could be applied under controlled conditions of nip load and speed. The apparatus consists essentially of a pair of soft rubber-covered rolls, driven in contact by means of a variable speed drive. The paper sample together with a glass plate is inserted between the two rolls and a known amount of liquid is pipetted into the nip between the paper and the glass plate. They derived expressions to determine a permeability pattern and a surface roughness index from an analysis of the liquid spread patterns.

Sweerman (1961) developed another apparatus for applying liquid to the paper, in which the calculation of roughness and porosity parameters of the paper is much simpler than the Wink and van den Akker technique.

The Sweerman apparatus is shown in Figure 1.16. The paper is drawn at a uniform velocity passed a rectangular slit filled with liquid. During this movement, the liquid fills in the valleys of the paper surface and at the same time penetrates into the paper. The total quantity transferred to the paper per unit area is expressed as

$$Y = R + K \left(\frac{\gamma t \cos \theta}{\eta} \right)^{\frac{1}{2}} \quad (1.15)$$

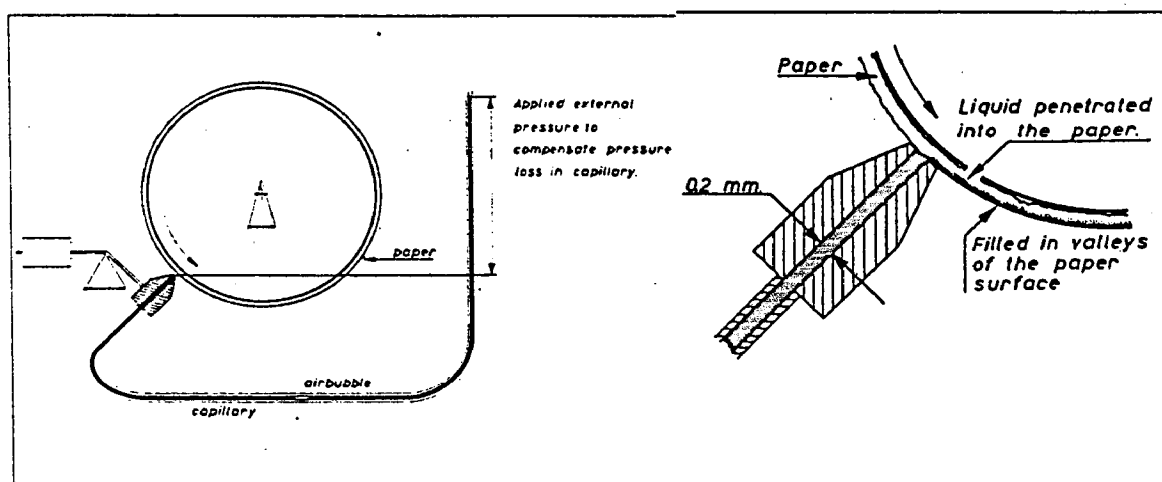


Figure 1.16 The Sweerman apparatus (Sweerman, 1967)

where R equals the liquid quantity that remains in the valleys of the paper surface and the second term represents the liquid that has penetrated into the paper. Here γ is the surface tension of the liquid, η is the viscosity of the liquid, t is the penetration time and θ is the contact angle of the liquid on the paper, K is a measure of the porosity of the paper.

Sweerman used paraffin oil as the testing liquid with $\gamma = 25 - 30$ mN/m, $\eta = 1.5$ to 60 mPas, $t = 0.04$ to 0.002 s and $\cos\theta = 1$. The pressure exerted on the paper by the edges of the slit was about 100 kPa.

A plot of y against \sqrt{t} should give a straight line and the intercept of the line with the y axis gives the roughness index.

The disadvantage of the Sweerman method is that it still requires a long time and great experience to get reliable results. The external pressure appropriate to each sample could only be found by trial and error and this was a time-consuming process.

Hawkes and Bedford (1963) developed the idea further in an apparatus in which a known quantity of liquid was placed in a small slider having a slot on the underside. The slider was drawn at a constant speed over the surface of a paper sample which was placed on a flat table. The length of the track left by the slider was measured. Repetition at different speeds enabled both the roughness of the paper and its absorption coefficient to be determined. The slider design eliminated the necessity of external pressure on the liquid and it was found that the absorption of liquid was mainly due to capillary action and was independent of the hydrostatic pressure in the slider.

A similar method was used by Bikerman and Whitney (1963), who employed inverted polyethylene cups. Rosen and Hemstock (1967) developed an apparatus designed to simulate a pond type trailing blade coater.

Bristow (1967) developed an apparatus which is more suitable for routine test purposes. He combined the Hawkes and Bedford design of liquid holder with Sweerman's wheel to support the paper sample and move it at constant speed under the stationary holder. The absorption time t is given by the ratio of the tangential width of the slot and the circumferential speed of the wheel. The values of the roughness index for a number of different liner and fluting grades of paper were compared with the Bendtsen roughness values and a good correlation was found. The principal of liquid spreading in the Bristow apparatus is shown in Figure 1.17.

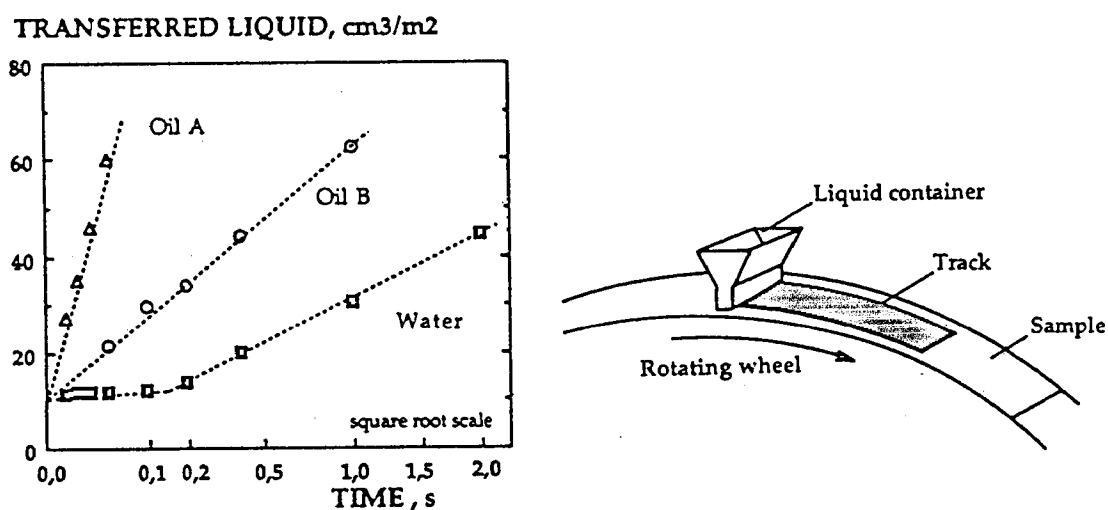


Figure 1.17 The Bristow absorption tester (Bristow, 1967)

Van der Vloodt (1964) applied the same principle in a simpler and more rapid way. A small, accurately determined, quantity of water is spread over the paper with the aid of the IGT tester. Two strips of paper are placed in the IGT printability tester with identical sides facing each other. One strip is mounted over the aluminium disc and the other over the rubber blanket on the sector. On the strip mounted over the aluminium disc, a metered quantity of distilled water stained with a dye is placed. The IGT is then operated so that the water is rolled between the two paper surfaces producing an oval spot. A drop of lacquer was placed over the paper before the water was applied to prevent water from penetrating into the paper before spreading.

The volume per unit surface area of the oval spot is calculated and represents the average depth of irregularities of the paper surface. Van der Vloodt found that when the water was applied very quickly it had no opportunity to penetrate into the capillary space of the paper and the second term in the Sweerman equation was negligible. The total water applied occupies the surface irregularities. Absorption within the body of the paper after the spot is formed has no influence on the subsequent measurement of the area of the spot. Van der Vloodt found that the roughness values determined by this method have a very high correlation (0.96) with the roughness parameter determined by Sweerman's apparatus.

6 SURFACE PROFILOMETRY

The technique which provides the most exhaustive description of the surface topography involves recording surface profiles by a fine point stylus traversing the surface.

The technique was originally developed for the evaluation of very smooth surfaces in the metal industry and was later adopted in many other fields including the topographical study of paper and paper-board surfaces. A number of workers have reported that the results obtained using the profiling methods show high correlations with the performance of paper in actual printing operation. Most other methods of measuring smoothness lack resolution for very smooth papers whereas the profiling instruments are fairly sensitive to surface imperfections in such papers. Moreover, the technique provides information of a fundamental nature not readily obtainable by other methods.

The technique is useful because:

1. the profile of the surface can be drawn with different magnifications on the vertical and horizontal axes allowing a clearer visual assessment of the surface,
2. the actual size and shape of the surface irregularities are measured rather than merely a single average value,
3. a distinction is made between periodic and irregular surface features.

6.1 Recording of Surface Profiles

The paper surface is scanned by a fine point stylus which moves over the surface at a constant speed. The vertical motion of the stylus is measured by means of a positional transducer which generates a voltage proportional to its vertical displacement. In early instruments, the voltage generated was magnified by a calibrated amplifier and fed to a direct linking oscillograph. Analogue techniques used to analyse the output required complex instrumentation and allowed little flexibility. In modern instruments the output is digitized at close time intervals and the data are stored in a computer. This has the advantage of avoiding errors due to mechanical inertia which may arise in a real time

recorder. Moreover, the data can be treated to yield a number of statistical quantities. With modern computation facilities the profiling methods are quite fast and easy to use.

A number of profiling instruments with different proprietary names have been used for the topographical studies of paper surfaces. Table 1.3 presents the important differences among the various instruments used.

Table 1.3 Some important parameters of profiling instruments used to study paper surface structure.

Reference	Name of the Instrument	Radius of tip μm	Mass of stylus mg	Scan length mm	Scanning interval μm
Roehr(1955) Fetsko et al (1971)	Brush Surface analyser	12.5		12.5	
Hendry (1961)	Talysurf.	3.5-5	200-400	3.5	
Climpson (1984) Kent (1984)	Talystep	13		2	4.17
Gate et al. (1973)	Talystep	13	1		
Nordman, Aschan (1980) Ginman et al (1974) Aschan et al (1986)	FPPRI Profiling instrument	4	400	1000 2000	8
Kapoor (1977)	Talysurf	5	50-100	100	88
STFI	Perthometer	3	80	20.25	4.5-13.5



245685.

6.2 Experimental Considerations

A stylus has a finite mass and size, and it records the surface heights in a fixed frame of reference. Both these factors significantly affect the recorded profile data. It is therefore important that the methods by which surface profile records are obtained should be fully understood together with their scope and limitations.

When the mass of the stylus is considered to be concentrated over a relatively small tip area, it ought to exert quite a high pressure on the surface being measured. Styluses are known to scratch the surfaces of soft materials [Gate et al, 1973]. However, the load per unit area is regarded as being less important in the case of paper surfaces since the paper is a resilient material and large edge effects are involved.

The size of the stylus obviously causes some filtering out of the very fine details. The stylus cannot enter deep valleys narrower than its cone angle, which has the effect of reducing the measured roughness obtained from a surface. Similarly the peak shape is distorted when a spherical stylus passes over a sharp peak because the contact point moves across the stylus. This makes the peak appear more rounded. But such fine details are considered to be of no consequence to the printing performance of the paper. In recording surface profiles the stylus moves on the surface relative to a reference plane and the profile values are read with respect to this reference datum. Two types of datum are used: one independent datum not related to the surface and another a skid which carries the stylus and moves over the surface. A skid is the most convenient and most commonly used reference. The skid travels across the surface riding on the peaks of the profile. It follows the long wave variations of the surface and eliminates these from the data recorded, but at the same time allows the stylus to discriminate the variations in the surface at narrow wavelengths. Ideally, the skid and the stylus should be coincident, but this is not possible for practical reasons. The offset between the skid and stylus can give rise to some errors of assessment. The effect of the size and shape of the skid on the recorded profile is quite difficult to estimate and it is not known exactly how it distorts the profile. However, the surface profiles recorded with such instruments correspond qualitatively with the surface structure seen with a scanning electron microscope [Gate et al, 1973].

An independent datum is likely to give more complete information including that of waviness of the surface, but such references are practically more difficult to cope with than the skid type. Moreover the variation in the thickness of the paper sheet may be included in the surface profile records. For all the designs it is important to keep the paper flat so that as far as possible only surface variations are recorded.

6.3 ~~A~~ Visual assessment

Kent (1984) and Climpson (1984) have shown that, by plotting a number of profiles together, a perspective view of the surface structure can be obtained, Figure 1.18. The pictures thus obtained present the surface structure more accurately than those presented by photographs of the magnified surface under oblique illumination since they are free from complicated optical effects. Any irregularity in the paper surface is clearly visible in these plots. But the drawback of this technique is that it is very time-consuming, the area examined is small, and it yields no quantitative information. This type of study has been restricted to the presentation of qualitative visual representations.

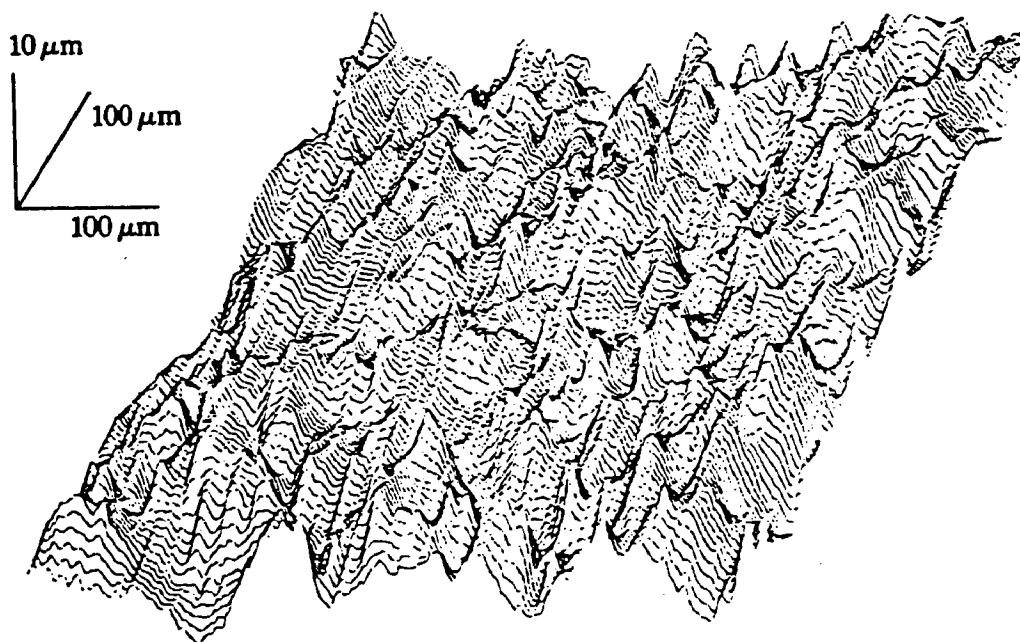


Figure 1.18 A perspective view of the surface structure obtained by plotting a number of parallel profiles (Kent, 1984)

6.4 Quantitative Analysis

A large number of statistical properties of the recorded profiles have been reported in the literature. Both analogue and digital techniques have been used. The statistical procedures applied have ranged from simple calculation of variance of profile data to more involved time series analysis techniques. In the following brief review, the various parameters used to characterize paper surfaces are only broadly discussed leaving out the involved mathematics.

A typical profile record contains variations ranging from very short wavelengths to fairly long wavelengths. The short wavelength variations can be considered to account for the roughness of the surface and the longwave variations indicate waviness of the paper. In most analyses of paper surfaces, the wavy part of the profile is filtered off by some method before any properties of the profiles are determined. There is no unanimous agreement, however, as to the wavelength which discriminates waviness from roughness.

The profiles of paper surfaces are stochastic in nature, i.e. the profile data cannot be described by an explicit mathematical expression. Such data can be described only by their average statistical properties. Both amplitude parameters and spatial parameters have been used to characterize paper surface profiles.

6.4.1 Amplitude parameters

A number of parameters can be defined to describe the nature and magnitude of the variation of the heights and depths of the surface features. Some of the more commonly used parameters are given here and illustrated in Figure 1.19 (Stout, 1981) for a profile record $z(n)$, $n = 1, 2, \dots, N$.

1. The arithmetic mean of the departure of the profile from the mean line $R(R_a)$

$$R_a = \frac{1}{N} \sum_{1}^N |z(n) - \bar{z}| \quad [1.16]$$

2. The root mean square roughness (R_q)

$$R_q = \left[\frac{1}{N} \sum_{1}^N (z(n) - \bar{z})^2 \right]^{1/2} \quad [1.17]$$

cavity width at that depth and calculated the percentage of the total surface area of the sample falling below that level. This value was found to correlate well with actual printing observations on coated papers.

Ginman et al (1973) defined surface roughness in relation to a moving average. The profile roughness is then defined as the cumulative width of depressions at a level at a given distance below the centre line expressed as a percentage of half the total length of the profile. The half length of the profile was selected because it was assumed that about half the total length fell above the centre line. Measurements at two different levels for each sample were suggested. The choice of the levels was however, arbitrary depending on the grade of paper. The levels used were 3 and 6 μm for newsprint and 1.5 and 3 μm for magazine paper

Paper surfaces contain peaks and cavities of different widths, heights and depths. A fuller description of these surface features requires the distribution of the amplitude parameters rather than their mean values. A number of ways of expressing these distributions have been reported.

Ginman et al determined three amplitude distributions, namely, total profile variation, variation from centre line to top of the peaks, and variation from centre line to bottom of depressions. When tested to predict unevenness of solid areas printed on the wire side of newsprint, none of the above parameters gave any improvement on the simpler and more rapidly determined Bendtsen roughness. However, the profile roughness parameters explain about 40 % of the variation in unevenness of light grey areas printed in gravure on the wire side compared with about 20 % in the case of the Bendtsen tester.

Fetsko et al (1974) using a Brush surface analyser, counted the number of peaks and troughs of various heights and depths and determined frequency distribution and cumulative distribution functions. An index of roughness was defined as the total number of peaks and troughs per equivalent length of scan. They found that the specular gloss at the grazing angle of 85° is directly related to the surface smoothness of the paperboard substrate and printed ink films.

Hendry (1961), using the talysurf, calculated the average distance of the irregularities from a moving average calculated over a length of surface of 0.75 mm. The numerical quantity obtained was found useful and adopted for the routine quality control of art paper.

Aschan et al (1986) have used a number of depression width

distribution functions to describe profile characteristics in a study of paperboard surface structure and its effect on gravure printability.

They determined the depression width distributions at a depth of $1\ \mu\text{m}$ from the centre line. The number of voids with depression widths between 75 and $175\ \mu\text{m}$, called the cumulative number, CN, has been found to have a pronounced effect on gravure printability of boards, a large number of voids being a disadvantage.

6.4.3 Autocorrelation function

The statistical properties of profile records relating to spatial features are probably best described by the autocorrelation function and power spectrum. These methods are only briefly reviewed here as they are discussed in detail in Chapter 4.

The variance of a series of data is obtained by averaging the squares of the data points over the entire profile length. In the case of two series, the average of the product of the corresponding data points is called covariance. Autocovariance is obtained by shifting the series relative to itself by a few data points, then determining the covariance over the common length of the series. The autocovariance calculated several times with different shifts gives an autocovariance function. The shift or displacement is called the lag. The autocovariance function normalized by dividing by the variance of the series is called the autocorrelation function.

When the lag is zero, the correlation coefficient is unity. As the lag increases, the correlation between the corresponding data decreases. If a periodicity is present in a profile the autocorrelation coefficient rises as the lag approaches the periodicity length or an integral multiple thereof.

Two items of information are readily available from the autocorrelation function. Firstly the peaks which represent the oscillatory or periodic components in the profile record and secondly the rate of decay of the function which is an indication of the random nature of the profile data.

6.4.4 Power spectrum

The power spectrum is a fourier transform of the autocovariance function, and it presents the distribution of the variance in the profile data at different frequencies. Since the profile record is

of finite size, the true power spectrum of the surface cannot be determined. It is only possible to determine a statistical estimate of the power spectrum. Another important consideration is that the digital record of a profile is a discrete series of data and the maximum frequency is limited by the sampling interval at the time of recording the profile.

Kapoor (1977) first applied this technique to profile records to derive various indices which he showed were able to predict printability of various types of coated papers in different printing processes.

A number of profile characteristics were derived from its power spectrum. For example, the zero order moment

$$m_0 = 2 \int_0^{f_{\max}} P(f) df \quad [1.20]$$

which is the area under the distribution curve and is equal to the variance of the profile heights, a second order moment,

$$m_2 = 2 \int_0^{f_{\max}} f^2 P(f) df \quad [1.21]$$

which denotes the variance of profile slopes, and a fourth order moment

$$m_4 = 2 \int_0^{f_{\max}} f^4 P(f) df \quad [1.22]$$

which denotes profile curvature. The values of m_0 , m_2 and m_4 will be small for a smooth surface.

Further, a number of printability indices have been defined as functions of these spectral moments to characterize letterpress, gravure, light and heavy coated papers. Quantities such as the density of peaks in contact at a given depression, percentage of non-contact area at a specific level of separation, pattern size, pattern depth, acuteness, summit density, mean contour length etc have been determined.

Unfortunately the number of indices defined is too large and different criteria are required for different grades of paper. Moreover, the assumptions made while analysing the data need further confirmation from more experimental work.

6.4 Quantitative Analysis

A large number of statistical properties of the recorded profiles have been reported in the literature. Both analogue and digital techniques have been used. The statistical procedures applied have ranged from simple calculation of variance of profile data to more involved time series analysis techniques. In the following brief review, the various parameters used to characterize paper surfaces are only broadly discussed leaving out the involved mathematics.

A typical profile record contains variations ranging from very short wavelengths to fairly long wavelengths. The short wavelength variations can be considered to account for the roughness of the surface and the longwave variations indicate waviness of the paper. In most analyses of paper surfaces, the wavy part of the profile is filtered off by some method before any properties of the profiles are determined. There is no unanimous agreement, however, as to the wavelength which discriminates waviness from roughness.

The profiles of paper surfaces are stochastic in nature, i.e. the profile data cannot be described by an explicit mathematical expression. Such data can be described only by their average statistical properties. Both amplitude parameters and spatial parameters have been used to characterize paper surface profiles.

6.4.1 Amplitude parameters

A number of parameters can be defined to describe the nature and magnitude of the variation of the heights and depths of the surface features. Some of the more commonly used parameters are given here and illustrated in Figure 1.19 (Stout, 1981) for a profile record $z(n)$, $n = 1, 2, \dots, N$.

1. The arithmetic mean of the departure of the profile from the mean line $R(R_a)$

$$R_a = \frac{1}{N} \sum_{1}^N |z(n) - \bar{z}| \quad [1.16]$$

2. The root mean square roughness (R_q)

$$R_q = \left[\frac{1}{N} \sum_{1}^N (z(n) - \bar{z})^2 \right]^{1/2} \quad [1.17]$$

3. The maximum profile depth, i.e. the vertical distance between the highest point and the lowest point (R_t)

$$R_t = z_{\max} - z_{\min} \quad [1.18]$$

The above quantities are defined over the entire assessment length of the profile. Further quantities are defined based on calculations for a number of sections of the profile length called sampling lengths.

4. Average value of the individual roughness depths in 5 sampling lengths

$$R_z = (R_{z1} + R_{z2} + R_{z3} + R_{z4} + R_{z5}) / 5 \quad [1.19]$$

5. Ten-point height parameter (introduced by Rank Taylor Hobson and also called R_z) is the average height difference between the five highest peaks and the five lowest valleys within the sampling length.
6. The individual roughness depth determined as the vertical distance between the third highest peak and the third deepest valley in each sample length. This eliminates the effect of extreme peaks and valleys. The average of this value for 5 sample lengths is R_{3z} .
7. The profile height from the mean line within a sample length (R_p).
8. Mean value of R_p over 5 sampling length (R_{pm}).
9. The so-called Swedish height parameter which is similar to R_t but which excludes extreme values by evaluating the surface between two reference lines positioned to exclude the top 5 per cent of the plane length provided by the extreme peaks and the bottom 10 per cent of the plane length provided by the extreme valleys. The height parameter is the vertical distance between the two lines.

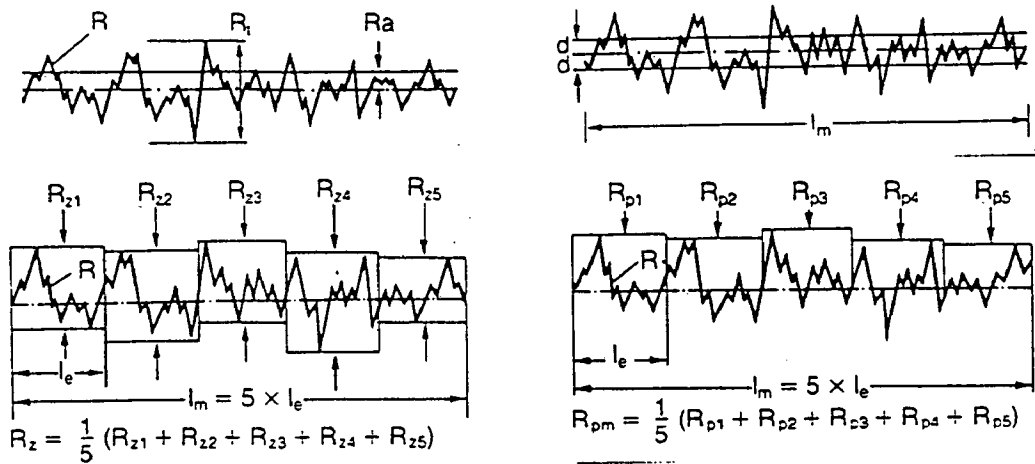


Figure 1.19 Definition of amplitude roughness parameters (a) R_a and R_z (b) the Swedish height parameter (c) R_z and (d) R_{pm}

6.4.2 Spatial parameters

The amplitude parameters provide information on the depths of cavities but give very little information about their shape. Surfaces of entirely different appearances may yield similar values for the standard deviation or mean deviation. To provide information about both the height and width of surface features, the Bearing Ratio Curve was devised in the study of metal surfaces. A similar quantity appropriate to the characterization of paper surfaces is defined as the sum of the width of cavities at a certain distance from the mean as a proportion of the assessment length. The determination of this quantity at different distances from the mean gives a cavity width distribution (Nordman and Aschan 1980).

When surface profiles of paper are evaluated from a printability viewpoint the entire bearing ratio curve may not be necessary. Since in a printing process the paper surface is required to contact a fluid ink film, only those cavities which are deeper than a certain fixed depth, dependent on the amount of ink on the printing forme and the nip pressure, will miss contact with ink and cause a poor print. The cavities shallower than this do not affect print quality. Thinking in these terms, Roehr (1955) counted the number of depressions deeper than a given depth ($5.7 \mu\text{m}$) in a unit length of profile. He also measured the average

cavity width at that depth and calculated the percentage of the total surface area of the sample falling below that level. This value was found to correlate well with actual printing observations on coated papers.

Ginman et al (1973) defined surface roughness in relation to a moving average. The profile roughness is then defined as the cumulative width of depressions at a level at a given distance below the centre line expressed as a percentage of half the total length of the profile. The half length of the profile was selected because it was assumed that about half the total length fell above the centre line. Measurements at two different levels for each sample were suggested. The choice of the levels was however, arbitrary depending on the grade of paper. The levels used were 3 and 6 μm for newsprint and 1.5 and 3 μm for magazine paper

Paper surfaces contain peaks and cavities of different widths, heights and depths. A fuller description of these surface features requires the distribution of the amplitude parameters rather than their mean values. A number of ways of expressing these distributions have been reported.

Ginman et al determined three amplitude distributions, namely, total profile variation, variation from centre line to top of the peaks, and variation from centre line to bottom of depressions. When tested to predict unevenness of solid areas printed on the wire side of newsprint, none of the above parameters gave any improvement on the simpler and more rapidly determined Bendtsen roughness. However, the profile roughness parameters explain about 40 % of the variation in unevenness of light grey areas printed in gravure on the wire side compared with about 20 % in the case of the Bendtsen tester.

Fetsko et al (1974) using a Brush surface analyser, counted the number of peaks and troughs of various heights and depths and determined frequency distribution and cumulative distribution functions. An index of roughness was defined as the total number of peaks and troughs per equivalent length of scan. They found that the specular gloss at the grazing angle of 85° is directly related to the surface smoothness of the paperboard substrate and printed ink films.

Hendry (1961), using the talysurf, calculated the average distance of the irregularities from a moving average calculated over a length of surface of 0.75 mm. The numerical quantity obtained was found useful and adopted for the routine quality control of art paper.

Aschan et al (1986) have used a number of depression width

distribution functions to describe profile characteristics in a study of paperboard surface structure and its effect on gravure printability.

They determined the depression width distributions at a depth of $1\ \mu\text{m}$ from the centre line. The number of voids with depression widths between 75 and $175\ \mu\text{m}$, called the cumulative number, CN, has been found to have a pronounced effect on gravure printability of boards, a large number of voids being a disadvantage.

6.4.3 Autocorrelation function

The statistical properties of profile records relating to spatial features are probably best described by the autocorrelation function and power spectrum. These methods are only briefly reviewed here as they are discussed in detail in Chapter 4.

The variance of a series of data is obtained by averaging the squares of the data points over the entire profile length. In the case of two series, the average of the product of the corresponding data points is called covariance. Autocovariance is obtained by shifting the series relative to itself by a few data points, then determining the covariance over the common length of the series. The autocovariance calculated several times with different shifts gives an autocovariance function. The shift or displacement is called the lag. The autocovariance function normalized by dividing by the variance of the series is called the autocorrelation function.

When the lag is zero, the correlation coefficient is unity. As the lag increases, the correlation between the corresponding data decreases. If a periodicity is present in a profile the autocorrelation coefficient rises as the lag approaches the periodicity length or an integral multiple thereof.

Two items of information are readily available from the autocorrelation function. Firstly the peaks which represent the oscillatory or periodic components in the profile record and secondly the rate of decay of the function which is an indication of the random nature of the profile data.

6.4.4 Power spectrum

The power spectrum is a fourier transform of the autocovariance function, and it presents the distribution of the variance in the profile data at different frequencies. Since the profile record is

of finite size, the true power spectrum of the surface cannot be determined. It is only possible to determine a statistical estimate of the power spectrum. Another important consideration is that the digital record of a profile is a discrete series of data and the maximum frequency is limited by the sampling interval at the time of recording the profile.

Kapoor (1977) first applied this technique to profile records to derive various indices which he showed were able to predict printability of various types of coated papers in different printing processes.

A number of profile characteristics were derived from its power spectrum. For example, the zero order moment

$$m_0 = 2 \int_0^{f_{\max}} P(f) df \quad [1.20]$$

which is the area under the distribution curve and is equal to the variance of the profile heights, a second order moment,

$$m_2 = 2 \int_0^{f_{\max}} f^2 P(f) df \quad [1.21]$$

which denotes the variance of profile slopes, and a fourth order moment

$$m_4 = 2 \int_0^{f_{\max}} f^4 P(f) df \quad [1.22]$$

which denotes profile curvature. The values of m_0 , m_2 and m_4 will be small for a smooth surface.

Further, a number of printability indices have been defined as functions of these spectral moments to characterize letterpress, gravure, light and heavy coated papers. Quantities such as the density of peaks in contact at a given depression, percentage of non-contact area at a specific level of separation, pattern size, pattern depth, acuteness, summit density, mean contour length etc have been determined.

Unfortunately the number of indices defined is too large and different criteria are required for different grades of paper. Moreover, the assumptions made while analysing the data need further confirmation from more experimental work.

CHAPTER II

PARTIAL-COVERAGE PRINTING AND IMAGE ANALYSIS

1. INTRODUCTION

In the printing operation, a paper surface is brought into contact with an ink-bearing printing forme, and the degree to which a uniform transfer of ink takes place depends primarily on the smoothness of the paper. It is, therefore, natural to suppose that the best way to characterize the surface from the printer's point of view would be to determine the efficiency of contact between a paper surface and a smooth surface under appropriate conditions.

Two approaches have generally been used to measure this contact efficiency. In one of them, the paper surface is pressed against a smooth glass prism and the fractional area of contact between them is measured optically, for example in the Chapman and FOGRA testers.-Blokhuis and Blogg (1974), Blokhuis and Kalff (1976) and Lyne (1976) have further modified these instruments to measure optical contact under dynamic pressures similar to those in a printing nip. Data obtained by these methods fail however to correlate well with the printability and are therefore not widely used. The optical contact area measured by these methods is perhaps not relevant to actual printing where the contact required is that between paper and a free ink layer. Due to its fluid nature, the ink can contact portions of the surface which do not come into optical contact with the prism.

The other more direct approach is to print the paper in the laboratory under conditions similar to those encountered in actual printing.

In the Walker-Fetsko (1955) equation for ink transfer, a term $(1 - e^{-kx})$ is introduced to represent the fraction of the paper surface which comes in contact with the ink layer. In this equation, x is the amount of ink on the forme and k is a constant which is characteristic of the printing smoothness of the paper surface.

Tollenaar et al. (1966) related the ink transfer data to the optical density of the prints using the expression

$$D = D_{\infty} (1 - e^{-mx}) \quad [2.1]$$

where x is ink film quantity on the disk, D_{∞} is the optical density of the ink film of infinite thickness and m is a constant. They found that the constant m is closely related to the printing smoothness k defined by Walker and Fetsko.

While the equations of both Walker-Fetsko and Tollenaar et al. are primarily intended to represent ink transfer data under conditions of near complete coverage, O'Neill (1959) used a low amount of ink and low printing pressure to accentuate the effect of roughness. He suggested that the average print density on the partially covered print is a good measure of printing smoothness if the printing conditions can be suitably standardized.

Hsu (1962, 1963) suggested that the area of the portions covered by ink on the test prints could be directly measured either planimetrically on magnified photographs or by determining the weight fractions of the covered and non-covered parts of the photographs. He also suggested that the area could be determined by measuring the reflectance of the prints. From these experiments he derived a distribution function for the depressions in the paper surface. In a printing operation under rolling pressure the frequency of occurrence of depression x in the surface measured from the printing forme is given by

$$\Phi(x) = \frac{dA}{dx} \quad [2.2]$$

where A = fraction of the surface covered by ink, and
 x = thickness of ink film on the printing forme

Equation [2.2] may be analytically solved if A can be expressed as a function of x . Hsu suggested that A and x can be related by the equation

$$\frac{A}{1-A} = k x^n \quad [2.3]$$

where k and n are constants for a given paper.

Another interesting observation made by Hsu was that the frequency distribution of depressions in a paper surface is of the log normal type. He suggested that the size of the most frequently occurring depression could be a good measure of surface roughness.

The present work describes an approach similar to that of Hsu in which the paper to be studied is printed with a small quantity of ink under a light pressure in order to provide a print with only partial coverage. The printed area is analysed by an image analyser which is more accurate and quicker than the methods used by Hsu. Besides measuring the coverage area, image analysis techniques provide means to further analyse the printed patterns and to derive parameters related to the appearance of the surface. The number and mean length of chords of inked regions determined by repeated parallel scanning over the printed area are characteristics of surface structure. The spatial distribution of the variance of the greytone values gives a measure of the surface roughness and also a surface structure wavelength characteristic of the surface.

2. EXPERIMENTAL

2.1 Paper Samples

A number of different types of papers were used for the present study, including commercial coated papers, newsprint, uncoated fine papers and papers made on experimental machines. Relevant properties of the papers are given in Table 2.1. Besides the paper grades mentioned in this table, seven additional uncoated fine papers were included in this study. The optical properties of these papers were not measured. The PPS roughness values of these additional papers are given in Table 2.2. Some of these samples were calendered to different extents in the laboratory.

2.2 Printing Conditions

A series of samples was printed in an IGT-AC2 laboratory printing press using the IGT offset ink supplied by the instrument manufacturer. A metal disc with a ground and polished surface was used for printing to ensure that no pattern or irregularity in the surface of the disc disturbed the print. A rubber blanket was used as backing. The samples were printed at a speed of 1 m/s with different amounts of ink on the disc and, except in an initial test series, with a printing force of 100 N on a 31.5 mm side strip. The amount of ink on the printed disc and the amount of ink transferred to the paper were determined by weighing the disc before and after printing. The size of the prints was 31.5 mm x 182 mm.

Table 2.1 Properties of paper samples used

Sample code	Type of paper	PPS(10) ⁽¹⁾ μm	Y-value ⁽²⁾ %	Opacity ⁽³⁾ %
Coat 1	Coated	2.2	86.9	93.2
Coat 2	Coated	2.1	84.5	93.2
Coat 3	Coated	1.6	81.6	93.5
Coat 4	Matt coated	5.0	84.9	96.2
Mag	Magazine	1.5	69.9	95.5
News1	Newsprint	4.8	76.3	95.8
News2	Newsprint	7.4	81.2	-
F	Uncoated fine	5.5	85.2	92.5
G	Uncoated	6.2	86.4	95.0

- (1) Parker Print-Surf roughness at a clamping pressure of 1 MPa
(2) Intrinsic reflectance factor (FMY/C) filter
(3) Ratio of reflectance factor of paper with a black backing to the intrinsic reflectance factor (FMY/C filter).

Table 2.2 Parker Print-Surf roughness of the paper samples

Sample code	Calendering load kN/m				
	0	10	35	60	60(Super)
Q0	6.5				
Q3	6.55				
C	6.3				
P	5.1				
SD1	6.5				
SD2	6.5	4.6	3.5	3.2	3.3
S	6.6	5.1	3.75	3.10	3.60
F	5.5	4.1	3.2	-	3.05
G	6.2	3.9	3.2	-	3.0

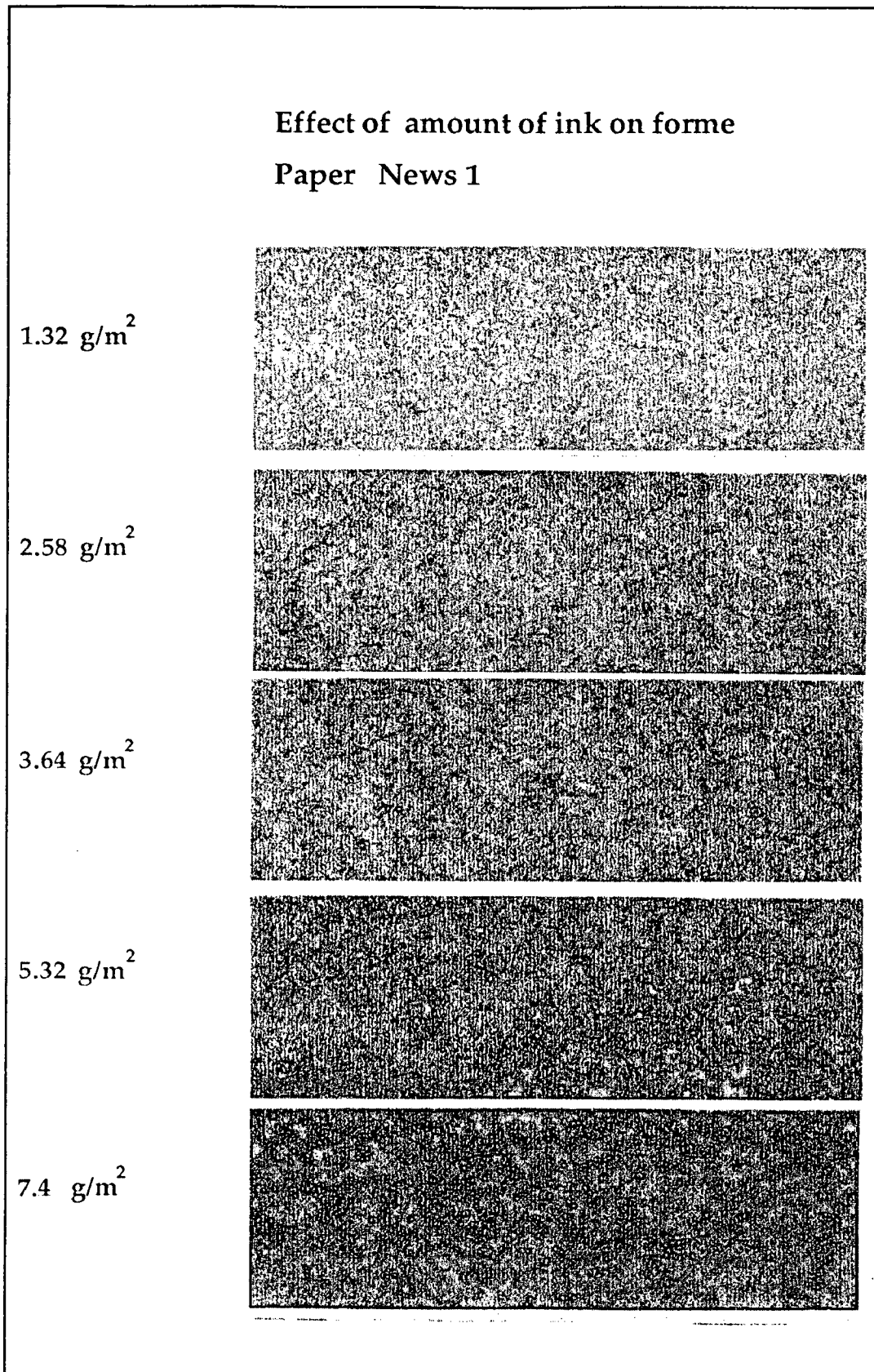


Figure 2.1 Examples of partial coverage prints showing the effect of increasing amount of ink on the forme

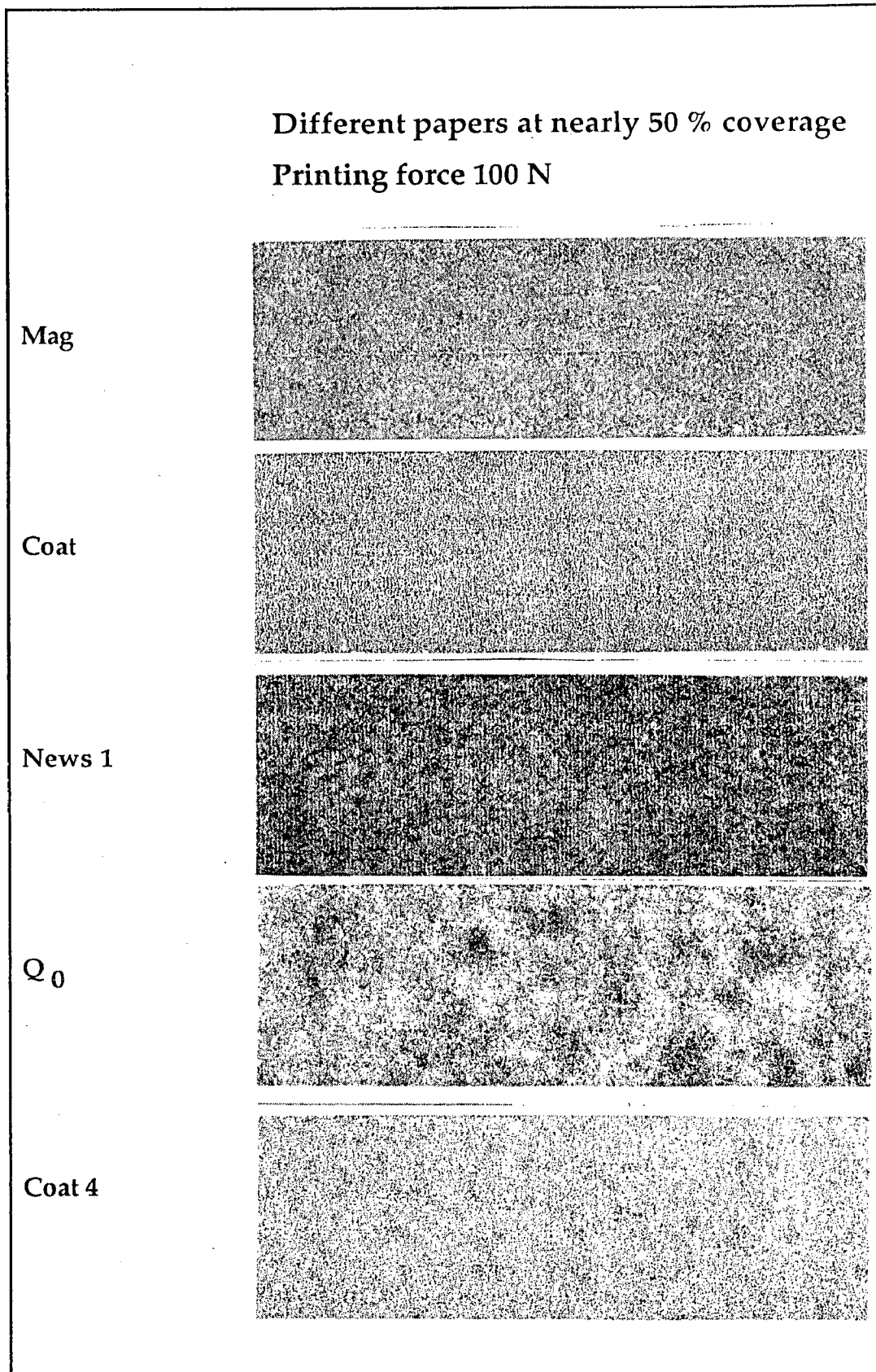


Figure 2.2 *Partial coverage printing of different papers with the same printing force and to the same degree of coverage reveals textural differences in different papers*

This is slightly shorter than the circumference of the standard disc because a special disc was used having a special wedge which was replaced with a clean wedge after the inking procedure. The disc was weighed without the wedge. Examples of the prints obtained are shown in Figure 2.1.

Figure 2.1 shows a series in which the amount of ink on the forme has been progressively increased.

Figure 2.2 shows prints for five different papers printed under the same printing force and to about the same degree of coverage. Here the potential of the method to reveal the texture in different surfaces is demonstrated.

The prints were evaluated by two different methods, using (a) the Elrepho reflectometer and (b) a Kontron IBAS image analyser.

2.3 Elrepho Reflectometer Measurements

The reflectance factor of the prints was determined using an Elrepho reflectometer with a FMY/C filter, each print being placed over a pad of the unprinted paper. Average values were obtained for three independent measurements on circular fields with a diameter of 30 mm. The area of the printed region was then determined by assuming that the reflectance factor was the mean value of the reflectance factors of the full-tone print and of the unprinted paper weighted in proportion to the areas of the printed and unprinted regions, according to the expression:

$$R = A R_p + (1-A)R_\infty$$

$$\text{i.e. } A = (R_\infty - R) / (R_\infty - R_p) \quad [2.4]$$

where

- R = reflectance of the printed strip
- R_∞ = intrinsic reflectance of the paper
- R_p = reflectance of a thick layer of ink, and
- A = fraction of the paper surface covered by the ink.

The value of R_p has been assumed to be equal to 2 % for all the papers. Strictly speaking this value is paper-dependent and should be measured experimentally for each paper but the differences are small and under conditions of partial coverage the error caused in

the calculation of area of coverage is of the order of 2-3 %. The difference is much less than the internal variations in the prints.

2.4 IBAS Image Analysis

The prints were viewed in a TV camera under uniform illumination and the image was converted to a 512 x 512 pixel matrix recording 256 grey levels in a Kontron IBAS image analyser. The image analyser was used to analyse the prints in three ways:

- a) assessment of the fractional area of the surface covered by the inked regions. The test area was 10.4 x 10.4 mm and the values recorded are the means of three independent measurements.

The primary scan showed that the print consisted essentially of printed and non-printed areas as shown in Figure 2.3. For the purpose of these measurements, the image was normalized, sharpened and converted to a pure binary image by discriminating at the middle grey tone level.

- b) assessment of the number and mean length of chords of inked regions along parallel lines on the prints
- c) determination of spatial distribution of variance of grey levels of the inked regions, and assessment of the typical wavelength discernible if the print was scanned with band-pass windows of different sizes. In this analysis, the image is not treated as a binary image. Instead the variance is determined and then sub-divided into regions of different wavelength

Details of the image analyser routines are given in Appendix A.

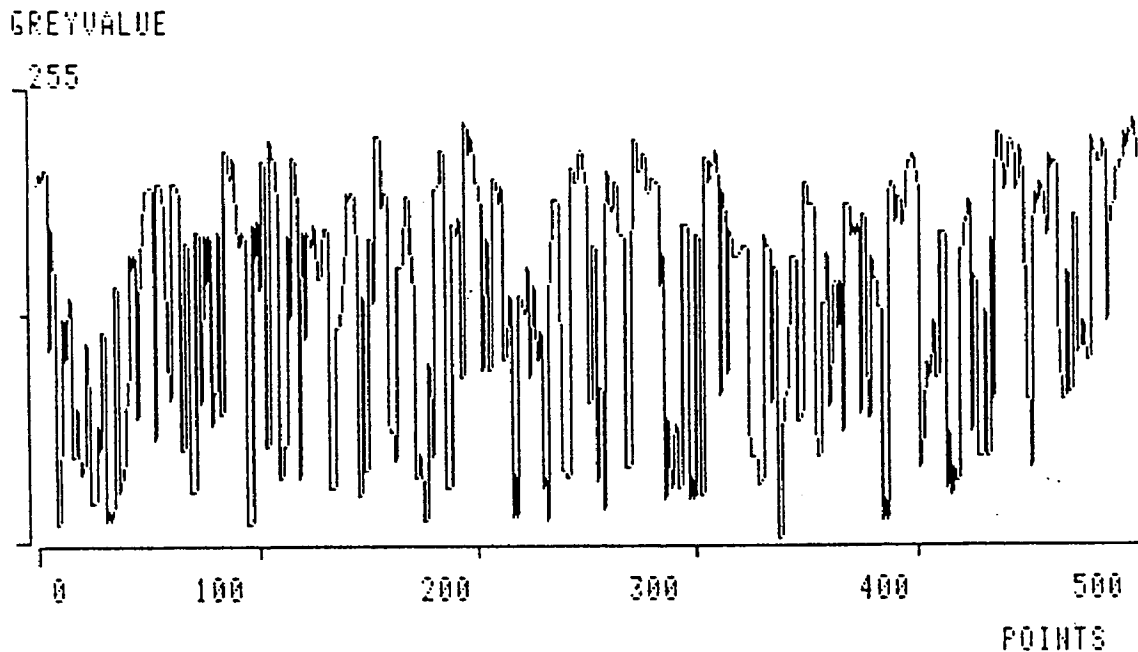


Figure 2.3 A typical greytone level scan obtained by the image analyser (IBAS)

3. VISUAL OBSERVATIONS ON THE PRINTS

The paper strips printed by this method present the surface structure in a manner suitable for visual examination. The prints obtained are similar to photomicrographs taken under grazing illumination, but these prints present the picture of the surface as it meets the inked printing forme in a dynamic printing nip and are free from the complications of optical effects, exposure times, developing conditions etc. At the same time, the area examined is much larger than that which is measured by most of the smoothness measuring heads. The method provides two-dimensional details. Since the printing experiments are carried out with varying amounts of ink on the printing disc, strips of different papers with almost the same area of the surface covered can be chosen for the purpose of close comparisons. The variation in the

amount of ink on the paper or in the area covered by the ink may provide a third dimension to the viewer if sufficient experience and skill is gathered in interpreting these prints. The following information is readily available from an observation of these prints. An experienced observer should be able to judge whether the features observed are likely to be detrimental to print quality in the intended printing process, and also what the likely causes are.

1. The contrast between adjacent areas. A low contrast signifies smoother surfaces.
2. Wiremarks, calender or coater streaks or any other type of marks are clearly visible.
3. The degree to which uneven features are oriented in the surface. A pronounced orientation may indicate a poor printing surface.
4. Fineness or coarseness of structure.

Information of this nature may be more important than the derivation of a numerical value which represents only some average value, and which may quite often be a measure of surface structure which is quite different from that which is essential for the performance of the paper in the printing press.

4. MEASUREMENT OF AREA OF COVERAGE

4.1 Comparison between Elrepho and IBAS Measurements

Figure 2.4 shows a number of typical curves in which the fractional area covered as determined using the Elrepho reflectometer is plotted against the ink quantity on the disc. It should be noticed that the independent variable is here the ink quantity on the printing forme. The coverage in relation to the ink quantity on the paper involves properties such as paper absorptivity and may be interesting in other contexts. It is the coverage in relation to the ink quantity on the forme which is a measure of the roughness.

Figure 2.5 shows a similar plot where the area of coverage has been measured by the IBAS image analyser. The general behaviour is the same as that observed in the Elrepho instrument, but the scatter in these data is slightly greater than that in Figure 2.4, perhaps because the test area is smaller.

Coverage Area (ELREPHO)

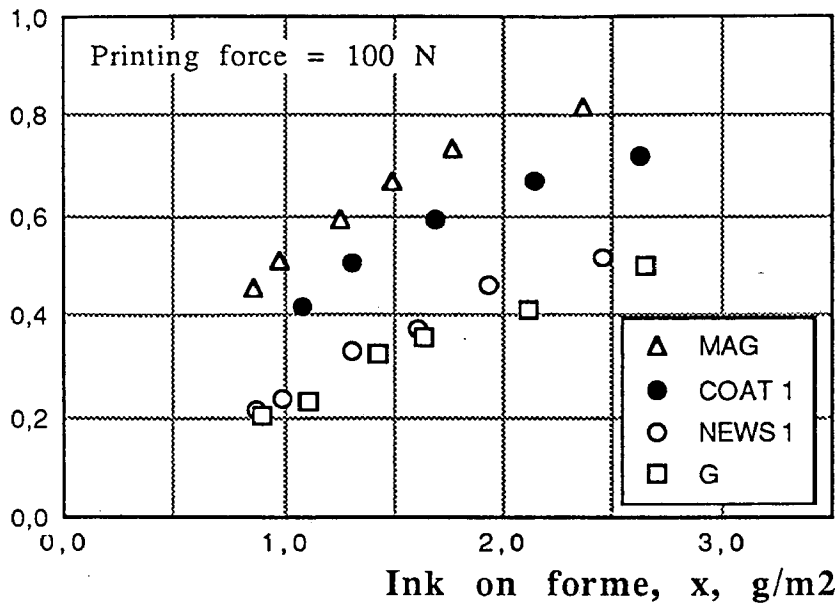


Figure 2.4 Plot of coverage area determined using the Elrepho reflectometer against the amount of ink on the printing disc for different grades of paper

Coverage Area (IBAS)

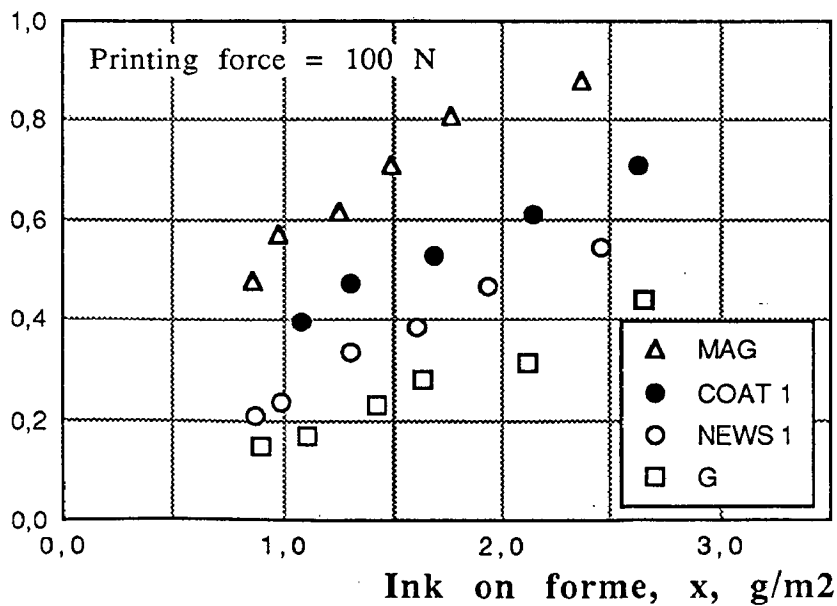


Figure 2.5 Plot of coverage area determined using the image analyser (IBAS) against the amount of ink on the printing disc for different grades of paper

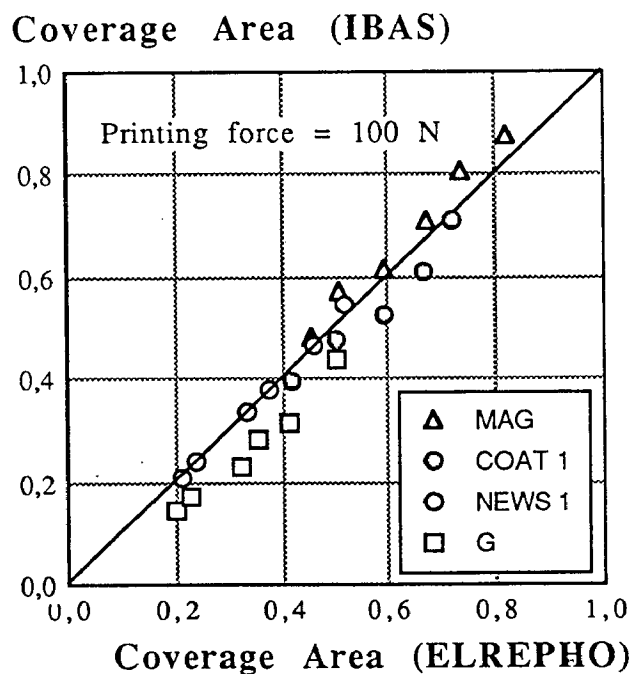


Figure 2.6 Relationship between coverage area (IBAS) and coverage area (Elrepho) for different papers

Figure 2.6 shows a plot of the area measured on the image analyser versus the area measured on the Elrepho. It is clear that, although the agreement between the two methods is basically very good, the two methods do not give exactly the same results.

Among the possible reasons for the deviation are (a) the assumption that the prints are truly binary may not be correct, (b) the blackness of the print depends upon the amount of ink actually transferred to the paper for a given coverage and hence R_p is not a constant, and (c) the linearity of the Elrepho instrument may be poorer than that of IBAS.

Further, the opacity of the paper influences the result. If the paper is translucent, light can enter the paper and be scattered beneath the inked regions so that the reflectance factor of the uninked regions is less than R_∞ , the so-called Yule-Nielsen effect (Ruckdeschel and Hauser, 1978). To some extent, this phenomenon may also affect the IBAS determination of area.

It is evident that the Elrepho indicates more area coverage than the IBAS for a relatively rough paper, G, while the Elrepho area is less than the IBAS area for a smooth paper, Mag. This is apparently due to the fact that a rough surface receives more ink per unit area than a smooth surface for a given fractional area

coverage. For rough papers the printed portions reflect an amount of light equal to the reflectance of a thick ink layer on paper and the unprinted portions reflect less light than R_{∞} due to the Yule Nielsen effect, which gives an impression of a larger coverage. On the other hand, for smoother papers, the thin ink film on the printed regions reflect more light than the thick ink film on rougher papers and gives an impression of less coverage.

The Elrepho area is also affected by the Y-value of the papers. For any given value of x , Elrepho areas for papers News1 and G are nearly equal whereas News1 is judged smoother by IBAS. The large difference in intrinsic reflectance between News1 and G tends to neutralize the effect of smoothness differences in the Elrepho measurement.

Although the IBAS measurement also lacks accuracy when the area covered is very small ($A = 0$) or very large ($A = 1$) due to difficulty in discriminating between printed and non-printed portions, the IBAS measurements are fairly accurate between $A = 0.1$ and $A = 0.9$.

Figure 2.7 shows the area covered as a function of the amount of ink on the printing disc at different printing pressures, and Figures 2.8 and 2.9 show prints of these effects at 50 % and 70 % coverage respectively. Under a higher printing force, a given coverage area is achieved with less ink and there is less contrast in the print. Figure 2.7 shows the relationship between the area of coverage measured by IBAS and that measured by the Elrepho for these two papers at the different printing pressures. The deviation between the IBAS and the Elrepho measurements increases as the printing pressure is increased. This is apparently due to the fact that the amount of ink required for a given coverage decreases with increasing pressure so that the reflectance R_p of the printed regions of the paper increases and a lower value of coverage area is thus obtained from the Elrepho reflectance measurement.

4.2 Relationship between Coverage Area and Ink on Forme

It is evident that for a given amount of ink on the disc a greater degree of surface coverage is achieved on a smoother paper than on a rougher paper, and also that the coverage can be increased by increasing the pressure in the printing nip. To compare different

Coverage Area (IBAS)

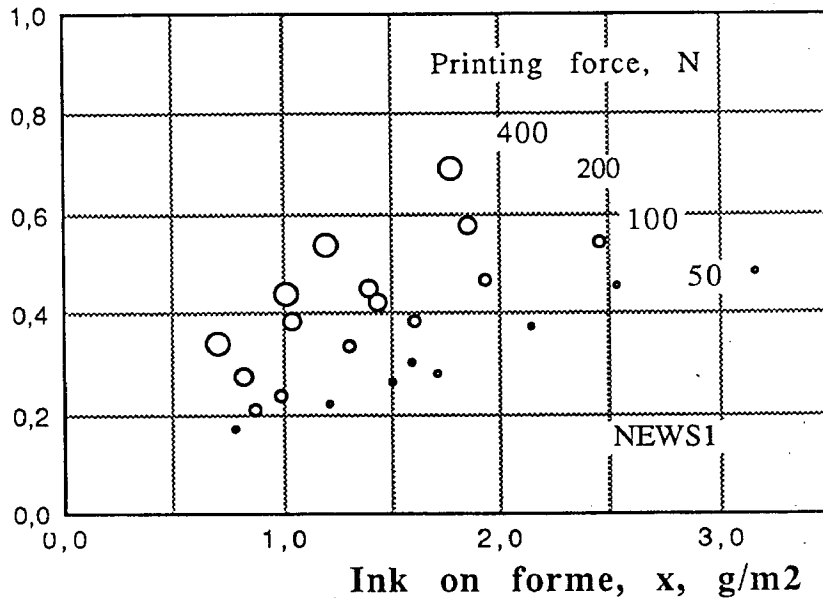


Figure 2.7(a) Plot of coverage area (IBAS) against the amount of ink on the printing disc for the newsprint, News1, at different printing pressures

Coverage Area (IBAS)

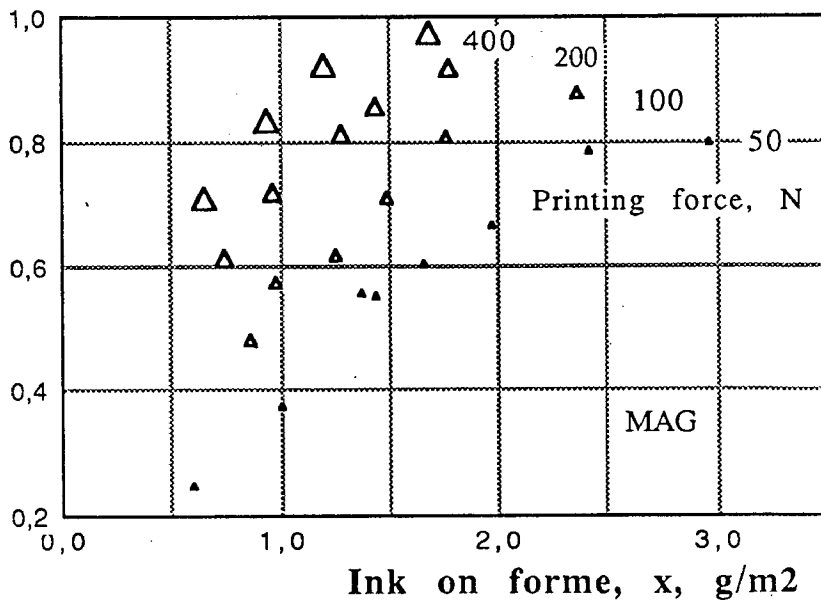


Figure 2.7(b) Plot of coverage area (IBAS) against the amount of ink on the printing disc for the magazine paper, MAG, at different printing pressures

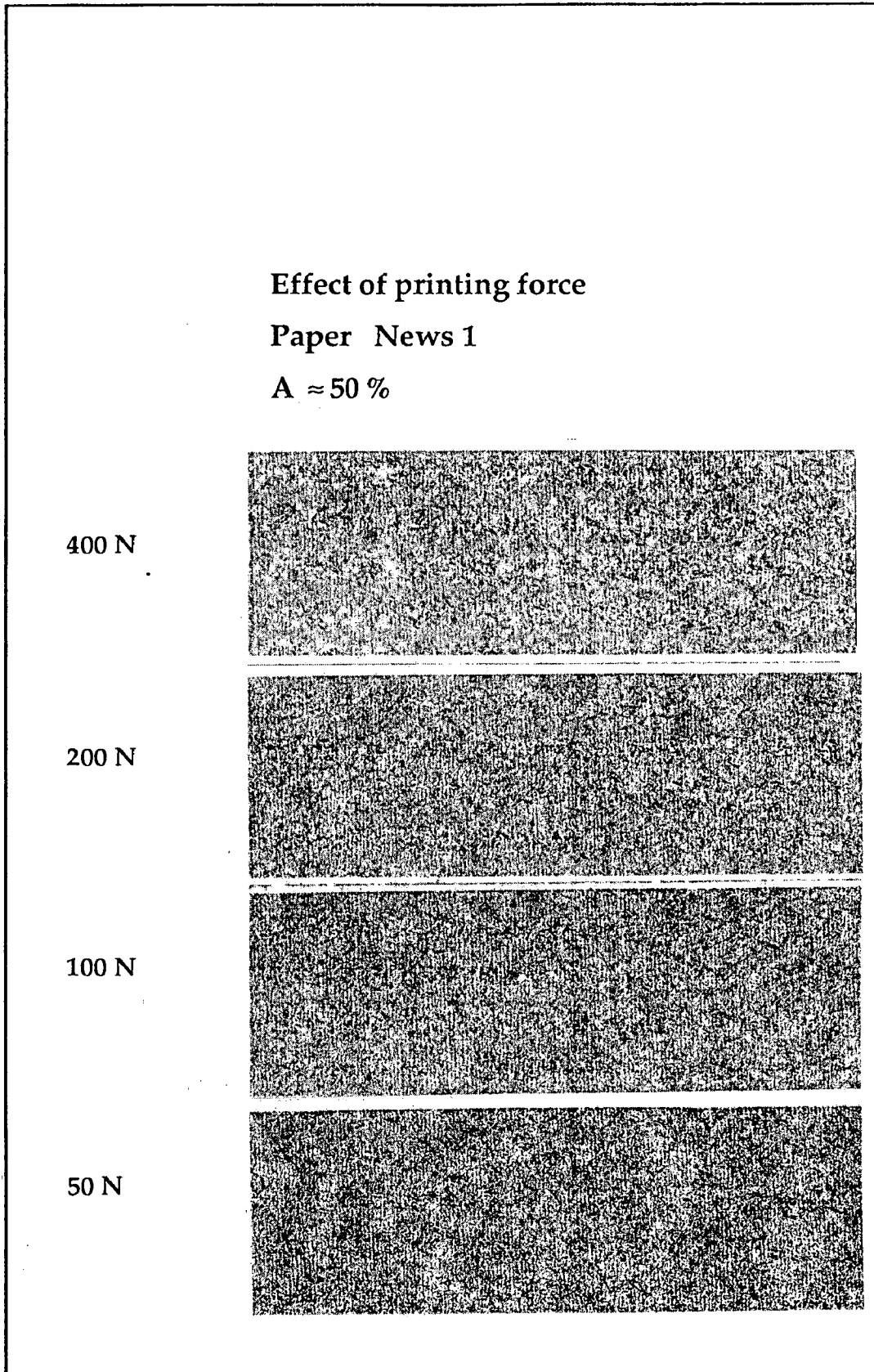


Figure 2.8 The effect of printing force on the appearance of prints on newsprint at 50 % coverage

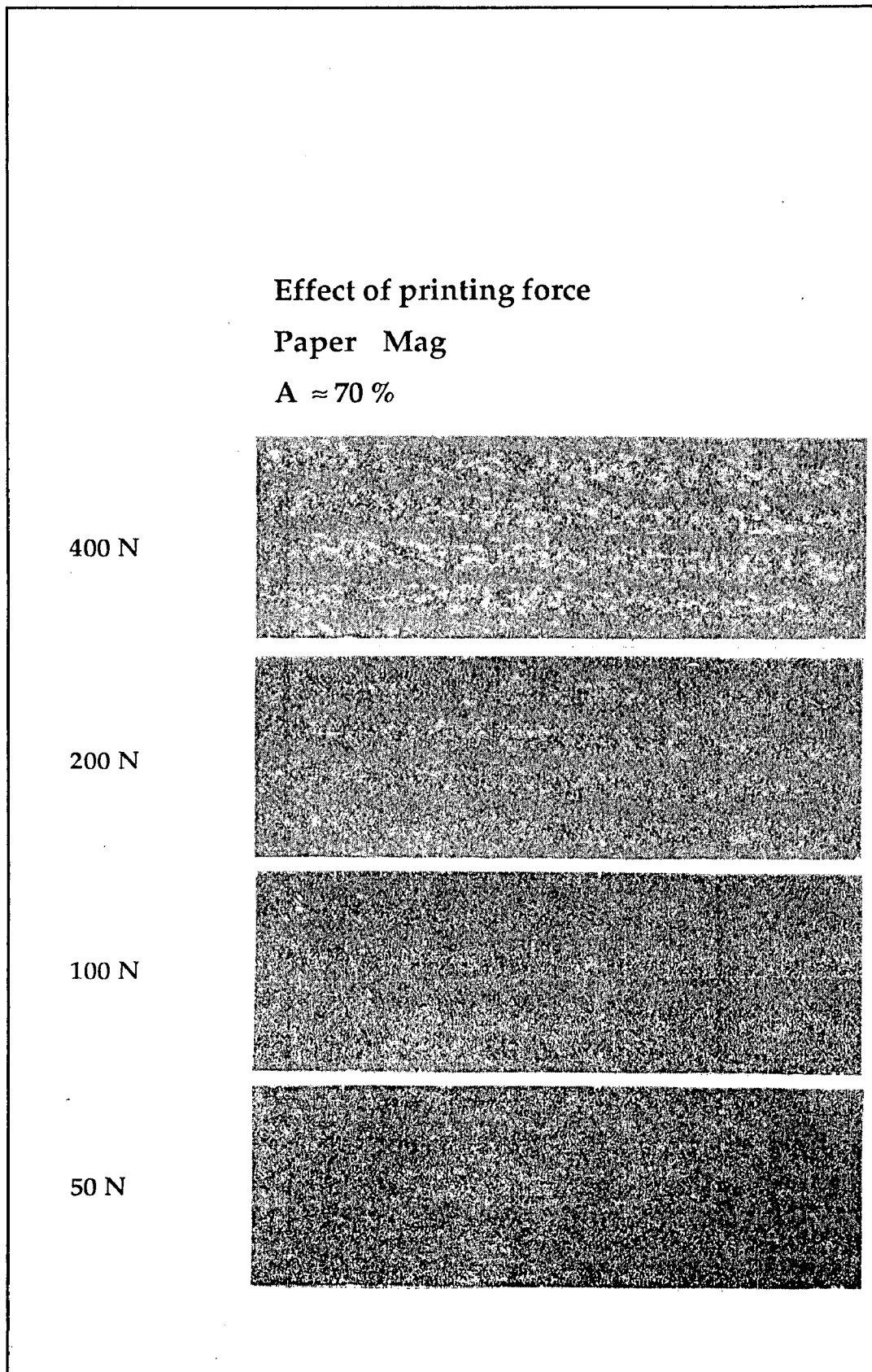


Figure 2.9 *The effect of printing force on the appearance of prints on a magazine paper at 70 % coverage*

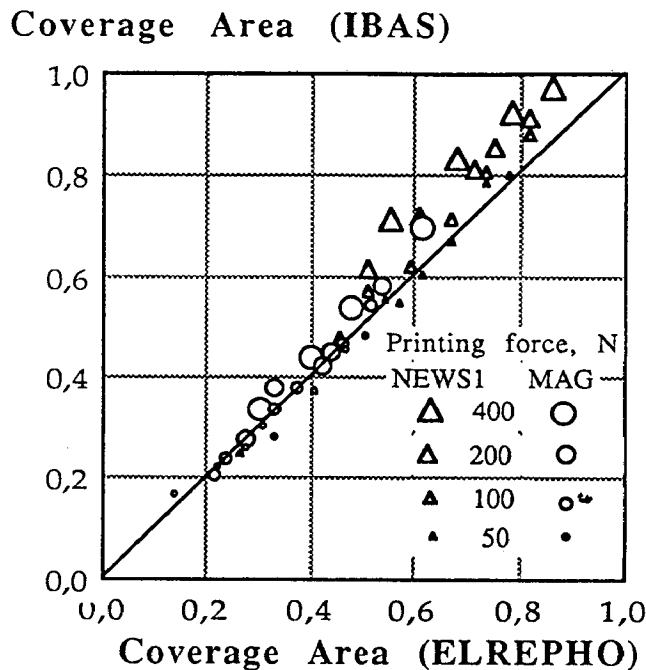


Figure 2.10 Effect of printing force on the relationship between the coverage area (IBAS) and the coverage area (Elrepho)

papers, standard conditions were adopted in which the speed was 1 m/s and the printing force was 100 N on a 31.5 mm wide strip. The low value of printing force was selected to keep the printed surface only partially covered and allow the largest possible range of ink quantities on the disc so that the ink transfer data could be determined accurately. The amount of ink required for 50 % coverage of the surface at a given printing pressure is a good printing smoothness index. The choice of 50 % coverage has the advantage that the area measurement techniques are most accurate in this range.

Hsu has observed that the distribution of depressions in the paper surface is a Gaussian function of $\log x$ with the mean at x when $A = 0.5$. The gradient $(dA/dx)_{0.5}$ may also have different values for different papers although the ink requirement for 50 % coverage may be the same. This gradient is a measure of the shallowness of the cavities. The shallower the cavities in the

surface, the more rapidly will they be filled when the ink thickness on the disc is increased and the greater will the gradient $(dA/dx)_{0.5}$ be.

4.3 Mathematical Relationship between A and x

Attempts were made to fit the experimental data relating A and x to a suitable mathematical expression. The equation of Fetsko and Walker, $A = 1 - e^{-kx}$, gave a poor correlation particularly for the small values of x. When the expression $A = 1 - (1 - A_0)e^{-kx}$ was used, after inserting the term A_0 , to account for the contact between the printing forme and the paper surface at $x = 0$ due to the printing pressure as suggested by Karttunen (1970), the relationship was still found to be unsatisfactory. The values of A_0 obtained were unrealistic (sometimes negative) and in any case the assumption that A_0 is a constant does not conform to the theory behind the introduction of this term.

Hsu observed that the area of coverage A could be related to the ink on the forme x by the equation [2.3] viz:

$$A/(1-A) = k x^n \quad [2.5]$$

and this equation has been found to give a good fit to the present data as indicated in Figure 2.11 which shows a plot of $\ln(A/(1-A))$ versus $\ln x$ for one sample of uncoated paper. (The coefficient of determination, r^2 , has been found to be greater than 0.97 in most cases.)

To characterize the papers tested, the values of k and n were therefore determined for different papers and the values of $x_{0.5}$ and $(dA/dx)_{0.5}$ at 50 % coverage were determined using equation [2.2]. The values are given in Tables 2.3 and 2.4.

The two constants k and n are not correlated. The constant k is basically a smoothness parameter, since k is equal to $A/(1-A)$ when x is equal to one and a higher value of k is therefore associated with a higher degree of coverage. There is a correlation between PPS and k, as shown in Figure 2.12 but no correlation between PPS and n, as is evident in Figure 2.13. It is difficult to assign any structural significance to the constant n, but it is noteworthy that it is not greatly changed by calendering, which may indicate that it is related to structural features which are not directly associated with the roughness.

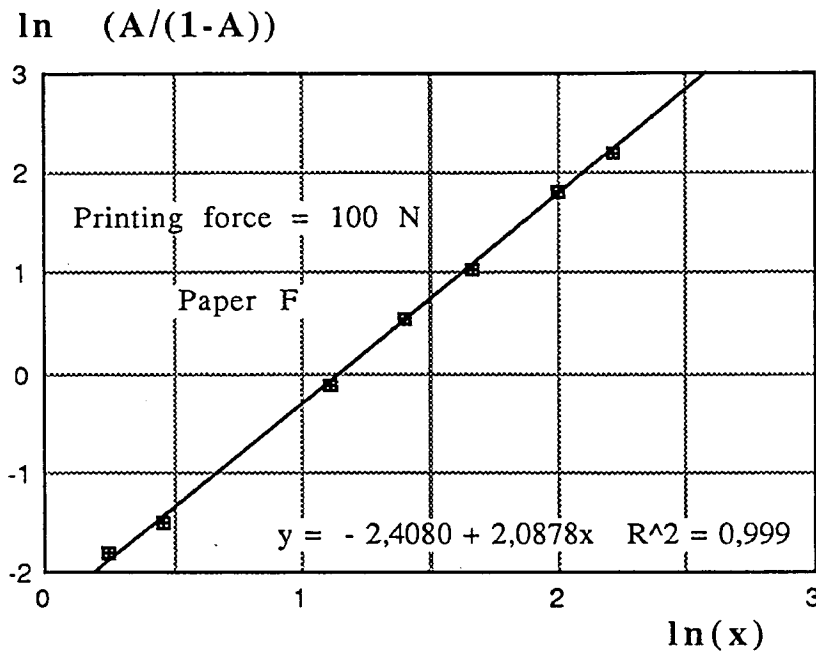


Figure 2.11 A plot showing the goodness of fit of the experiment data to the equation $(A/(1-A) = k x^n)$

Since the values of $x_{0.5}$ and $(dA/dx)_{0.5}$ are only functions of k and n , they do not in principle provide any additional information, but they do provide information which is more closely related to the physical notion of roughness and the distribution of roughness. A high value of $x_{0.5}$ indicates high roughness of the surface whereas a high value of $(dA/dx)_{0.5}$ says that the surface voids are shallow and further coverage would be easy to achieve either by increasing the ink quantity on the printing forme or by increasing the printing pressure.

The effect of a laboratory calendering is illustrated on two sets of prints on two different papers in Figures 2.14 and 2.15. Here it is seen that structural characteristics of the paper become more evident as the calendering is increased but that supercalendering gives a surface with a different printing texture.

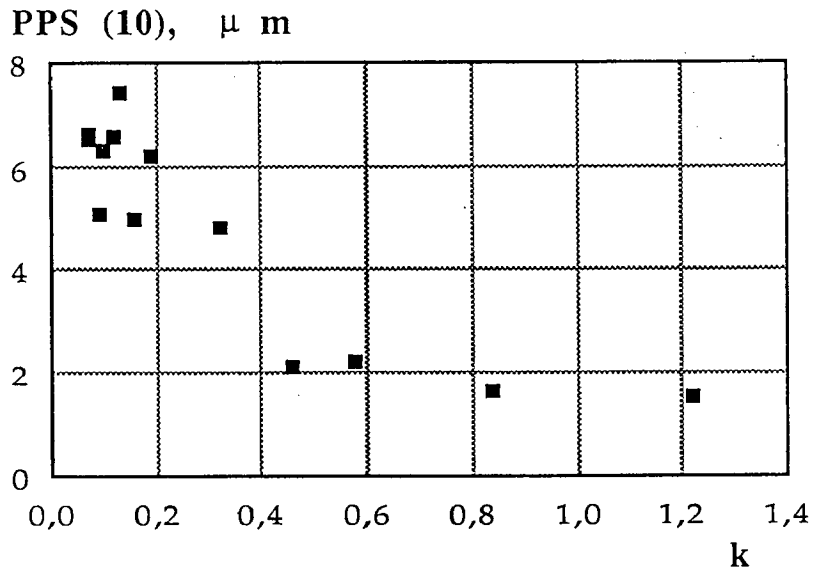


Figure 2.12 Relationship between PPS values and k

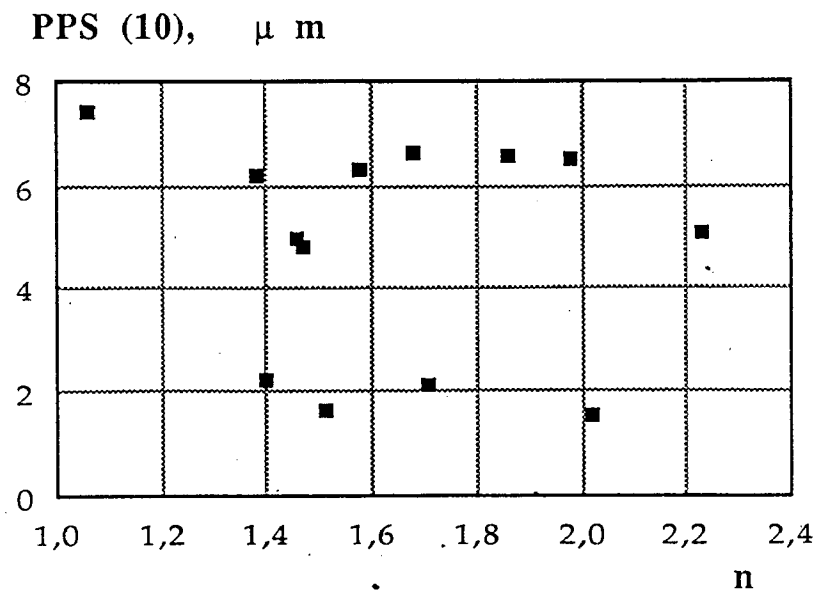


Figure 2.13 Relationship between PPS values and n

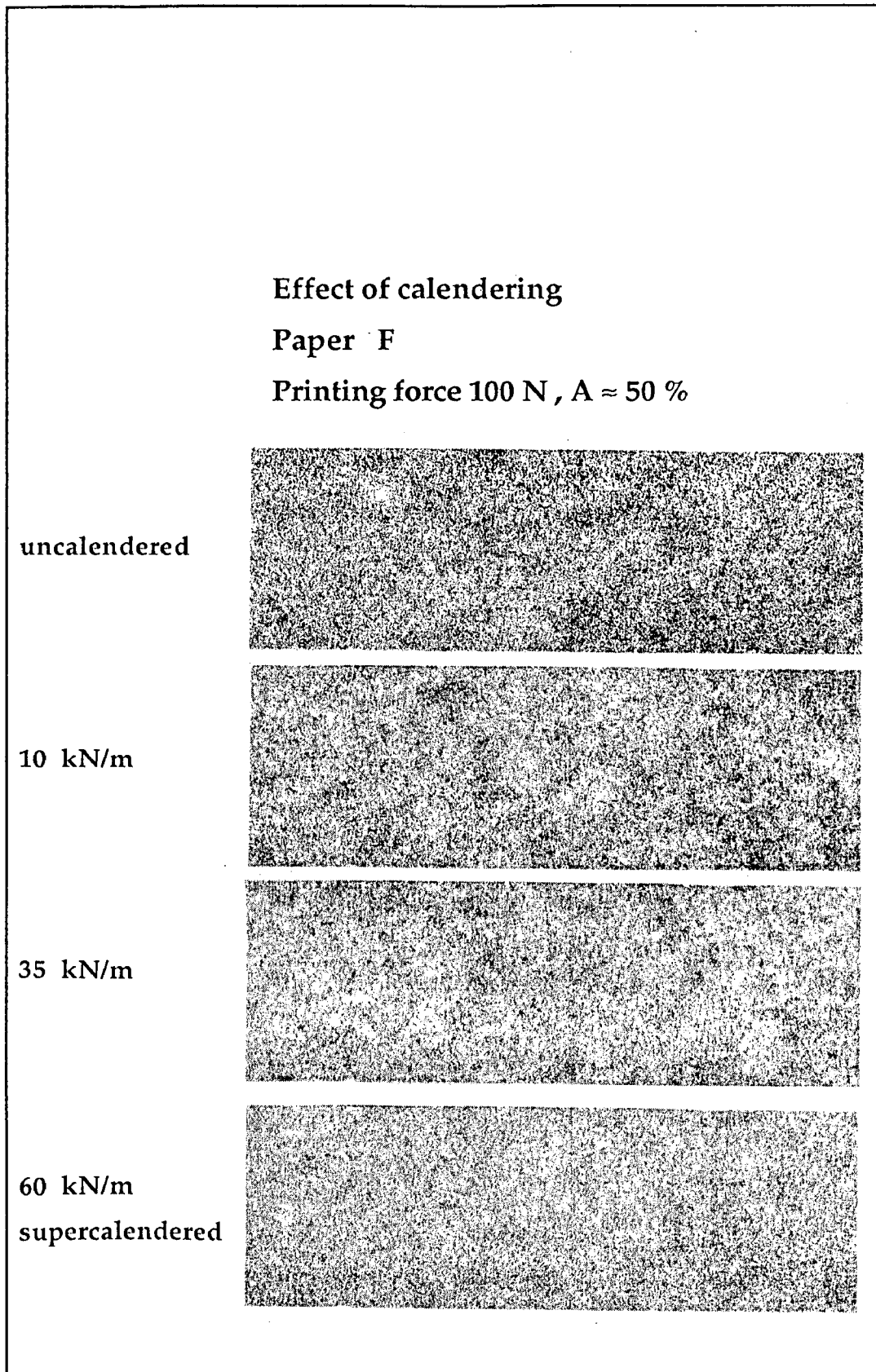


Figure 2.14 The effect of calendering on the texture of the print under a printing force of 100 N at a coverage area of 50 %

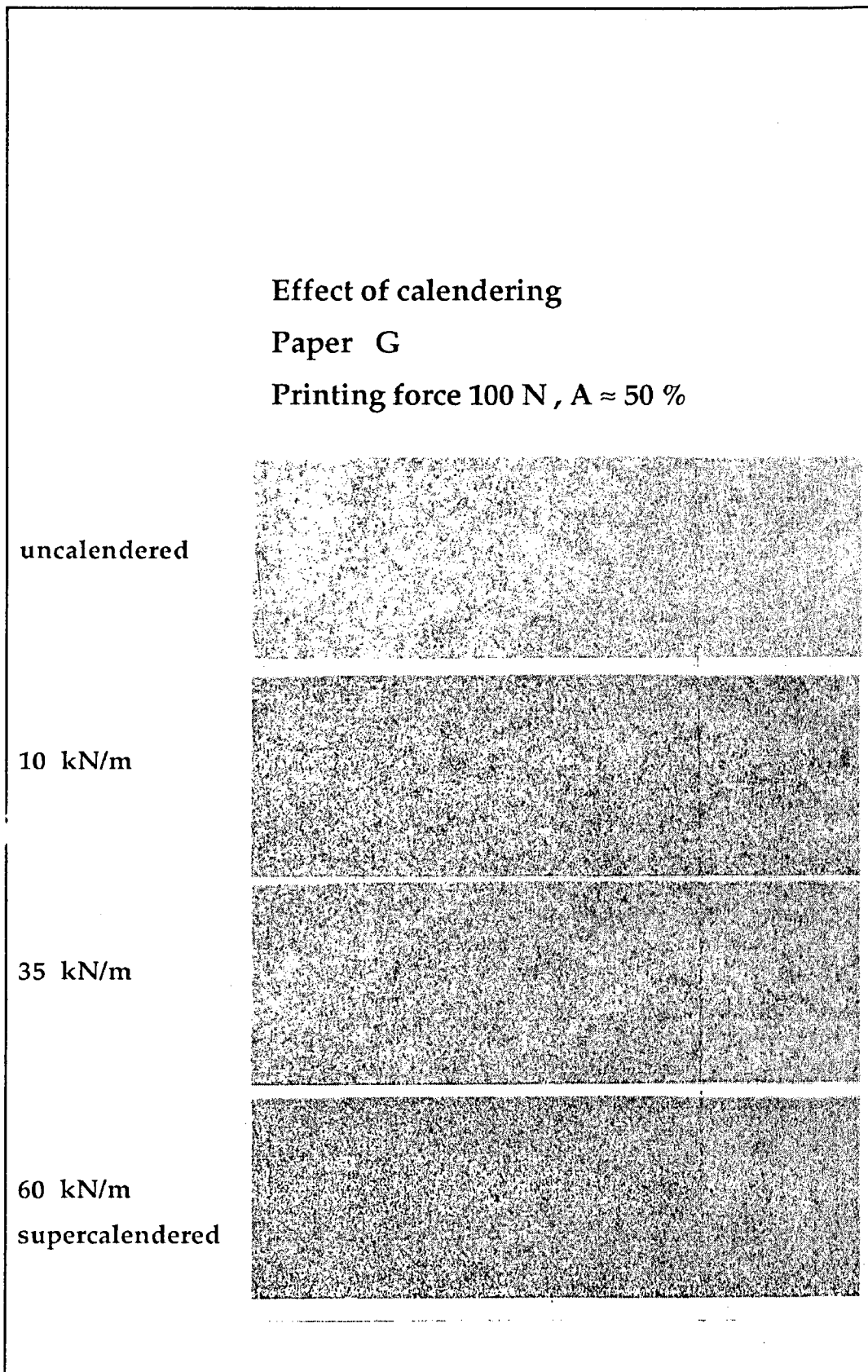


Figure 2.15 The effect of calendering on the texture of the print under a printing force of 100 N at a coverage area of 50 %

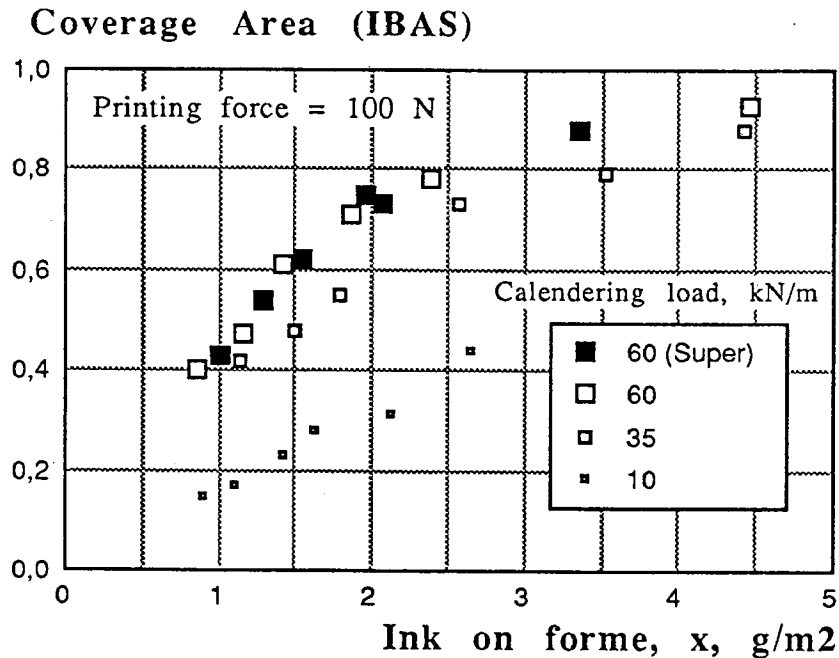


Figure 2.16 Plot of coverage area (IBAS) against the amount of ink on the printing disc for paper G, calendered at different nip loads

Figure 2.16 shows the effect of calendering on the ink coverage for an uncoated paper. As the degree of calendering is increased, the ink requirement to achieve 50 % coverage, $x_{0.5}$, decreases, and at the same time, the gradient $(dA/dx)_{0.5}$ increases. Supercalendering tends, however, to lead to a relationship which departs somewhat from the general pattern. In comparison with the machine calendered paper having the same ink requirement, $x_{0.5}$, experiments have indicated that the supercalendered paper tends to have a lower gradient $(dA/dx)_{0.5}$.

For a smooth surface able to achieve complete contact with a thin ink layer, the value of $x_{0.5}$ should be small and the value of $(dA/dx)_{0.5}$ should be large. The product of $x_{0.5}$ and $1/(dA/dx)_{0.5}$ gives a combined measure of these two effects, and it has been found empirically that the square root of this product, Z , i.e.

$$Z = [x_{0.5}/(dA/dx)_{0.5}]^{1/2} \quad [2.6]$$

is very close to the PPS-value as shown in Table 2.3. A plot of PPS values against Z is shown in Figure 2.17. One interpretation of this is that by calculating both $x_{0.5}$ and $(dA/dx)_{0.5}$ the information provided by the PPS-measurement is broken down into two complementary components representing different features of the paper structure.

Figure 2.18 shows the relationship between $x_{0.5}$ and $(dA/dx)_{0.5}$. Although there is a general hyperbolic relationship between these two parameters, there are significant differences for different papers. Theoretically, the product of these two variables is equal to $n/4$, so that deviation from a simple hyperbola merely reflects differences between or changes in values of n . Figure 2.19 shows the relationship between PPS and $(x)_{0.5}$.

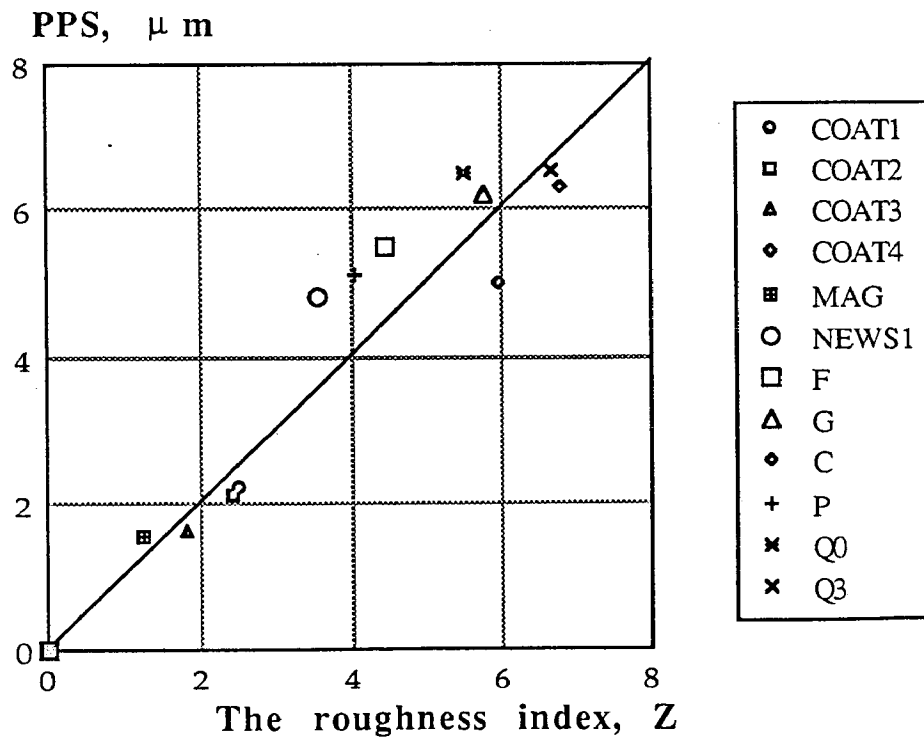


Figure 2.17 Plot of PPS against the roughness parameter Z showing some agreement between these two measures of roughness

Ink on forme, x , at $A = 0.5$, g/m²

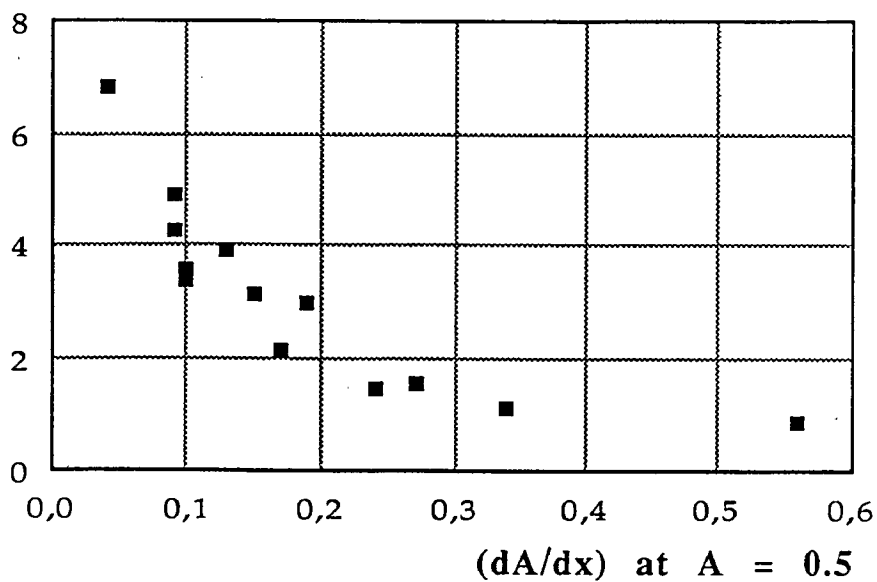


Figure 2.18 Relationship between $x_{0.5}$ and $(dA/dx)_{0.5}$ for different grades of paper

PPS (10), μ m

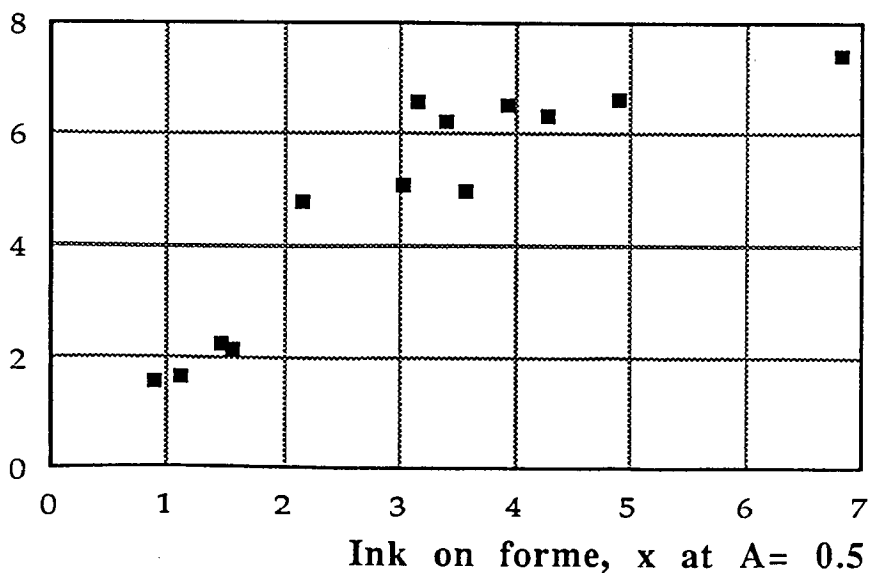


Figure 2.19 Relationship between PPS(10) and $x_{0.5}$ for different grades of paper

Table 2.3 Values of surface characteristics for different papers

Sample code	k (g/m ²) ⁻ⁿ	n	$x_{0.5}$ g/m ²	$(dA/dx)_{0.5}$ m ² /g	Z g/m ²
Coat 1	0.58	1.40	1.47	0.24	2.48
Coat 2	0.46	1.71	1.57	0.27	2.40
Coat 3	0.84	1.51	1.12	0.34	1.82
Coat 4	0.16	1.46	5.57	0.10	5.98
Mag	1.22	2.02	0.90	0.56	1.26
News1	0.32	1.47	2.15	0.17	3.55
News2	0.13	1.06	6.82	0.04	13.04
G	0.19	1.38	3.38	0.10	5.76
F	0.09	2.09	3.17	0.16	4.45
S	0.07	1.68	4.89	0.09	7.37
SD1	0.04	2.13	4.52	0.12	6.14
SD2	0.09	1.71	4.20	0.10	6.48
Q0	0.07	1.98	3.94	0.13	5.50
Q3	0.12	1.86	3.14	0.15	6.68
C	0.10	1.58	4.27	0.09	6.81
P	0.09	2.23	3.01	0.19	4.05

4.4 Spatial distribution of covered regions

An essential feature of the partial coverage technique is that it presents a two-dimensional representation of the surface structure. It has therefore been important to use the potential of the image analyser to derive not only a single measure of roughness using the ink requirement for an area of coverage of 50 %, but also additional parameters describing the spatial distribution of these covered regions corresponding to the information derived from a visual survey of the print.

Table 2.4 Values of surface characteristics calculated at different calendering loads

Sample code	Calendering load kN/m	k (g/m ²) ⁻ⁿ	n	x _{0.5} g/m ²	(dA/dx) _{0.5} m ² /g	Z g/m ²
F	0	0.09	2.09	3.17	0.16	4.45
	10	0.39	1.79	1.69	0.27	2.50
	35	0.61	1.89	1.29	0.37	1.07
	60 (Super)	0.72	1.87	1.19	0.39	1.75
G	0	0.19	1.38	3.38	0.10	5.81
	10	0.51	1.70	1.49	0.29	2.27
	35	0.78	1.85	1.14	0.40	1.69
	60 (Super)	0.74	1.90	1.17	0.41	1.69
S	0	0.07	1.68	4.89	0.09	7.37
	10	0.14	1.88	2.88	0.16	3.77
	35	0.23	1.96	2.14	0.23	3.05
	60	0.33	1.86	1.82	0.26	2.65
	60 (Super)	0.32	1.63	2.00	0.20	3.16
SD2	0	0.09	1.71	4.20	0.10	6.48
	10	0.30	1.60	2.12	0.19	3.34
	35	0.47	1.47	1.67	0.22	2.76
	60	0.70	1.42	1.28	0.28	2.14
	60 (Super)	0.34	1.71	1.87	0.23	2.85

Two approaches have been used. Firstly, the distribution of chord lengths has been studied and secondly an attempt has been made to define the spatial distribution in terms of a characteristic dominant wavelength and the coefficient of variation of grey tone level.

4.4.1 Chord length analysis

This analysis has been based on the binary representation of the print and provides a measure of the size distribution of the covered regions.

The chords created by the intersections of a scanning line with the inked regions are counted and measured. The print has been scanned at 10 pixel intervals (= 0.2 mm) along parallel scans giving a total scanning length of 520 mm.

Figure 2.20 shows a plot of the mean chord length for a number of papers as a function of coverage area A . In general, the mean chord length is very low up to about $A = 50\%$ but then increases rapidly. The reason for this is evident in Figure 2.20b which shows that during the initial stages, the increase in coverage area is associated with an increase in the number of covered spots, whereas in the later stages the number of spots decreases as the printed regions merge together with increasing coverage.

The mean chord size for a given area of coverage varies slightly for different papers, and it is also evident that calendering leads to a shorter mean chord length and an increased number of counts for a given area of coverage. It is thus apparent that the mean chord length provides additional information concerning the nature of the surface.

4.4.2 Wavelength analysis

In this approach, the print has no longer been represented by a binary distribution. Instead, the spatial distribution of the variance in the grey-tone levels has been studied and the typical

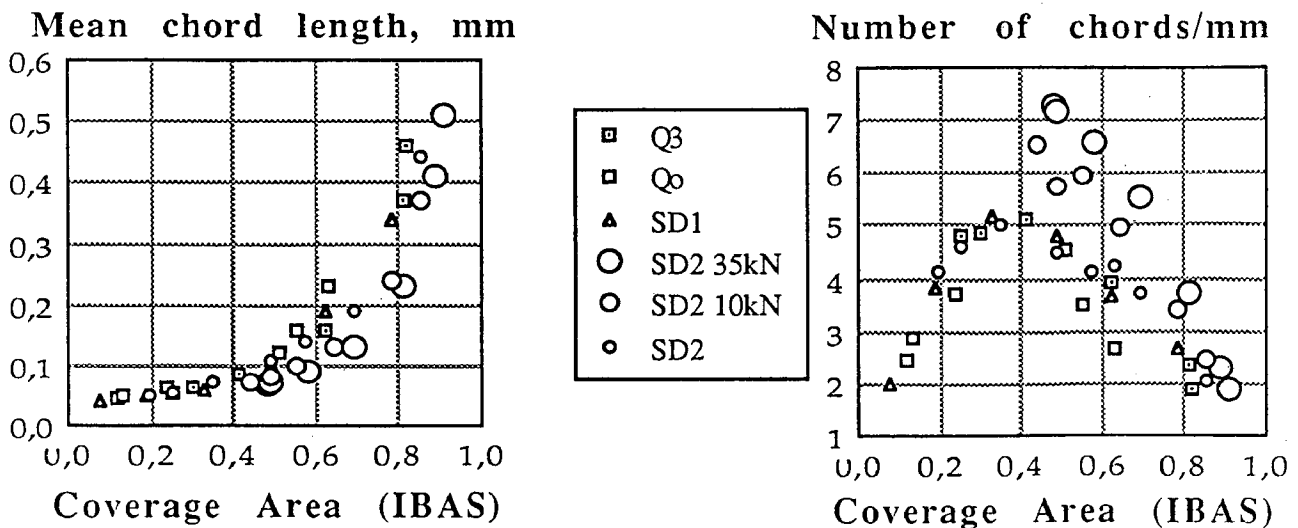


Figure 2.20 (a) Mean chord length and (b) Number of chords as functions of coverage area

spatial wavelength region with which the greatest variance is associated has been determined, (see Appendix A).

The coefficient of variance in grey-tone level increases with increasing area of coverage, but the coefficient of variation at $A = 0.5$ is a parameter characterizing the roughness and correlates reasonably with the PPS-value. The coefficient of variation decreased with increasing extent of calendering.

The typical wavelength is different for different papers and, for a given paper, it is almost independent of the degree of coverage and of calendering treatment, i.e. it is independent of roughness in the sense measured by air-leak and similar methods. This means that the typical wavelength may provide important additional information describing the pattern of structure and texture of the surface as it is influenced by other bulk properties of the paper, e.g. formation, rather than the surface roughness alone. Back et al. (1988) have reported that, even when the PPS-roughness of two sides of a paper are equalized by suitable calendering sequences, the speckle observed in a gravure print may be different on the two sides due to differences in surface structure which survive the calendering process and which are of a nature which is not detected by the PPS-instrument.

On the other hand, the coefficient of variation does measure roughness of the surface. Since the coefficient of variation depends on the coverage of surface by ink, samples of different roughness should therefore be compared at equal coverage. The 50 % coverage seems to be a good choice because of the greatest resolution in this range.

5. CONCLUSIONS

1. If a surface is printed under given conditions with a given quantity of ink, the degree of coverage of the surface will depend on the degree of contact between paper and printing forme. The degree of coverage is therefore a measure of the surface roughness.

It should be noted that this method compares the coverage with the ink quantity on the disc - not with the ink quantity on the paper. The coverage in relation to ink quantity on the paper is affected by the absorptivity; it is the coverage in relation to the ink quantity on the disc which is a measure of roughness.

2. The main feature of the present method is not, however, to determine the degree of coverage alone nor to determine the conditions required to give full coverage, but rather to seek to achieve partial coverage and then to use image analysis as a tool to characterize the nature of the surface patterns revealed by this type of printing.
3. It is readily apparent (Figure 2.2) that this type of printing reveals different characteristic patterns. Image analysis enables these patterns to be quantified.
4. At any specified set of printing conditions (speed, force, type of ink etc.) the fractional coverage of the paper surface depends on the amount of ink on the forme. The value of $x_{0.5}$ represents the depth and the value of $(dA/dx)_{0.5}$ represents the slope of the cavities in the paper surface. The value of the square root of the product of $x_{0.5}$ and $1/(dA/dx)_{0.5}$ has been found to be approximately equal to the Parker-Print-Surf value.
5. The analysis of chords provides information about the coarseness or fineness of the surface structure. The number of chords and the mean chord length at a given coverage area provide information about the surface texture.
6. The analysis of variance in the greytone values of the printing image yields a typical wavelength for the pattern which is a characteristic of the surface. The value of typical wavelength for a paper surface was found to be relatively insensitive to the calendering of paper suggesting that this is also related to the formation of the paper or to textural features of the surface which survive the calendering operation.
7. The advantage of the present method is that it characterizes the surface in terms of several parameters. These parameters are different measures of the surface features and describe the surface structure much more exhaustively than any of the methods which give only a single quantity for the total surface structure.

CHAPTER III

SURFACE EVALUATION BY ANALYSIS OF MICROCONTOUR INK STAINS

1. SCOPE

Ink stain tests have long been in use for the qualitative evaluation of absorptivity and surface roughness of coated papers and boards. The microcontour ink which is used for roughness assessments rather than for absorptivity evaluation contains a blue pigment suspended in a colourless oil. When this ink is spread over the surface of a paper the solid phase pigment is retained in the cavities of the surface while the colourless oil is absorbed in the paper. When the excess ink is wiped from the surface a mottled blue stain is left. The ink is especially suited for accentuating the surface irregularities of paper. The evaluation of these stains has traditionally been only visual, an intense coloration indicating a high roughness. Bristow and Bergenblad (1982) have reported that a reflectance photometer can be used to quantitatively measure the amount of coloration on these stains. A microcontour value similar to the K&N value has been reported as a measure of roughness.

In the present study, the microcontour ink stains for a variety of both coated and uncoated papers have been analysed by an image analyser as well as by the Elrepho reflectometer. Several types of image analysis are presented.

2. EXPERIMENTAL

1. Microcontour ink supplied by Lorilleux was used to study a number of paper samples with wide differences in surface characteristics.
2. Stains were prepared according to the recommended standard procedure given in TAPPI RC-19 K&N through the following stages.

- a - An excess of ink was applied to a 50 mm x 50 mm surface of the paper.
 - b - The ink was allowed to remain on the paper for 2 minutes.
 - c - The excess of the ink was wiped from the surface by hand using cleaning tissue.
3. The reflectance factor (R) of these stains was measured using the Elrepho instrument with a FMY/C filter and with an opaque pad of the paper as backing. The microcontour value was determined by the following equation

$$Q = \frac{100(R_{\infty} - R)}{R_{\infty}} \quad [3.1]$$

where Q = microcontour value for a paper
 R = reflectance factor of the stain
 R_{∞} = intrinsic reflectance factor of the paper

4. The stains were studied on an IBAS image analyser. The mean and the variance of the greytone values of these stains were determined. The spatial distribution of variance in greytone values was determined and a typical wavelength was calculated. The fraction of the paper surface covered and the classification of chord lengths of inked portions on the surface were also determined. The IBAS routines used are the same as those used for the evaluation of partial coverage prints and are explained in Appendix A.

3. RESULTS AND DISCUSSION

The various quantities determined for different papers are presented in Table 3.1.

Table 3.1 Results from Analysis of Microcontour ink stains

Paper	PPS(10)	Q Elrepho	A % IBAS	Mean Chord length	Count of chords	Typical wavelength λ_T , mm	Grey- tone CV
Coat 1	2.20	51	32.6	.094	1725	0.62	0.45
Coat 3	1.62	17.4	2.4	.050	200	0.80	0.50
Coat 2	2.12	35	7.4	.056	670	0.63	0.85
Coat 4	5.0	46	16	.075	1060	0.60	1.67
Mag	1.45	47	19.0	.085	1140	0.70	0.74
News1	4.8	77	81	0.415	1060	0.68	2.99
F	5.5	83	92	0.73	675	0.65	1.56
G	6.2	80	90	0.60	820	0.58	2.3
Qo	6.7	82	88	0.52	920	0.68	1.67
S	6.8	62	58	0.20	1550	0.62	2.76

3.1 Microcontour values (Elrepho)

A visual examination of these stains indicates that the intensity depends not only on the surface roughness but also on the absorptivity of the paper, since the intensity of stain on uncoated papers was higher than that on coated papers.

The microcontour ink stains present the surface in an inverted form of the patterns produced by low pressure printing. In the case of printing, the hills of the surface receive ink while the valleys remained unprinted, but in microcontour stains the pigment is retained in the valleys. There is however an important difference. Printing merely indicates the positions of the hills and not

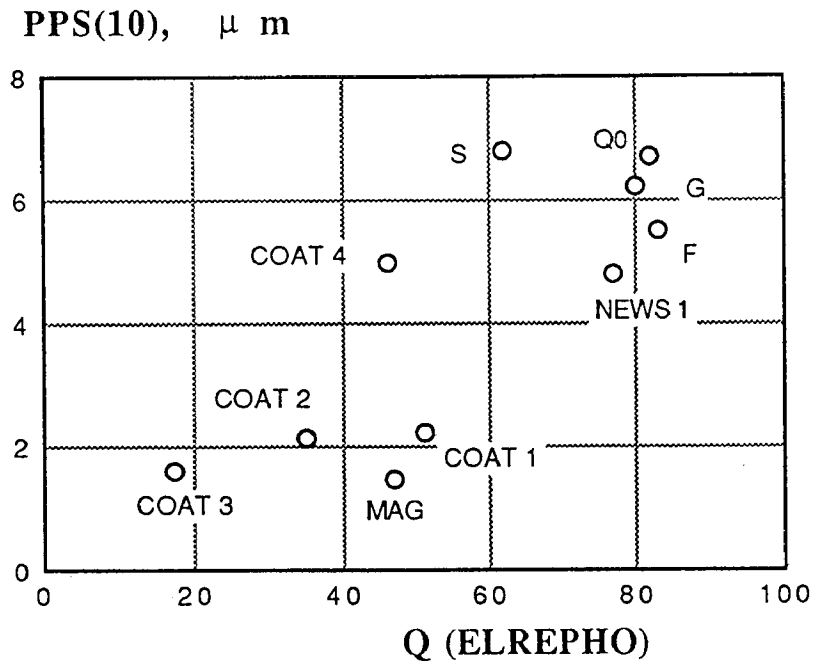


Figure 3.1 PPS value versus microcontour ink stain value for a number of different papers

their heights, whereas in the microcontour test the quantity of pigment retained is proportional to and provides information about the depth of the valleys.

Figure 3.1 shows a plot of Parker Print-Surf roughness at a clamping pressure of 1 MPa, PPS(10), against the microcontour value of the stain determined from the Elrepho reflectance values. There appears to be a general agreement between the two quantities but there are nevertheless significant deviations, indicating that the two methods complement each other in their characterization of the surface. Samples Mag, Coat 1 and Coat 4 have almost the same microcontour value, but the Coat 4 has a much higher PPS(10) value than the other two. On the other hand, sample Coat 4 and News1 have almost the same PPS(10) value, but sample News1 has a very high microcontour value indicating its intense colouration. Apparently the uncoated papers have high absorptivity and the pigment also moves into the paper structure along with the oil, whereas the coated surface holds the pigment on the surface most of which is removed during wiping. For very smooth papers, however, the microcontour value seems to show a greater resolution than the PPS- value.

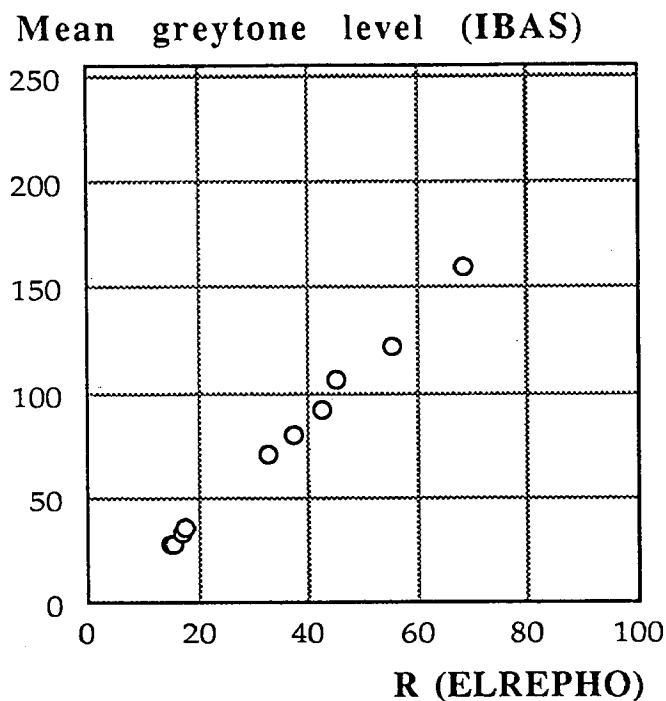


Figure 3.2 Mean greytone level recorded in IBAS versus the Elrepho reflectance value for a number of different papers

Figure 3.2 shows a plot of mean greytone of the stains measured by IBAS against the reflectance values measured by the Elrepho. The values correlate fairly well with each other indicating a linear response of the IBAS. Since the IBAS was not calibrated against any standard value it is not possible to determine a quantity similar to the microcontour value, Q , determined from Elrepho reflectance measurements.

3.2 IBAS Image Analysis

The fraction of the total area covered by the pigmented regions was determined by IBAS using the same technique as that discussed in Chapter 2 (cf. Appendix A). The reliability of the area determination is, however, poor in this case. Since the routine for area determination assumes that the image being analysed is binary, it discriminates stained and unstained portions by the middle greytone value. Actually, on these stains there are no significant unstained portions. All the cavities retain pigment; it is only the quantity that differs from cavity to cavity. The fractional coverage area determined by IBAS is in fact well corre-

lated with the microcontour value, Q , as is evident in Figure 3.3. The discrepancy is probably mainly due to the fact that the Elrepho determination is more sensitive to variations in the maximum intensity R_p of the stain. Actually Q is a special case of the coverage area, as defined in equation [2.4]. Q is the area covered if the value of R_p is zero. For a non-zero value of R_p

$$A = (1/100) \cdot Q R_\infty / (R_\infty - R_p) \quad [3.2]$$

In the case of smooth papers, the intensity of the stain is low, which yields a higher value of R_p and thus a value of Q greater than A . For rough papers the value Q approaches the value of A more closely. The Parker-Print-Surf roughness correlates with coverage area (Figure 3.4), no better than with Q .

The analysis of chords was also performed on these stains and the mean chord length and count of chords were determined (cf. Appendix A). Figures 3.5 - 3.7 show that for the samples here studied, the area of coverage, mean chord length and counts of chords are closely related quantities and that the chord analysis essentially yields no further information.

The analysis of variance of grey level values on these stains yielded two parameters, namely the coefficient of variation of the grey level of the stain and a typical wavelength of the variation pattern. The coefficient of variation is a measure of roughness. Figures 3.8 - 3.10 show plots of coefficient of variation against PPS, IBAS area and the Q -value. In all cases, there is a similar degree of correlation. Figure 3.11 shows a plot of the typical wavelength against the PPS-value and indicates that this type of wavelength analysis has a potential for identifying characteristics of the surface structure to which the PPS method is insensitive.

4. CONCLUSIONS

1. Microcontour ink stains provide an assessment of surface roughness, which may be different from other roughness measuring methods, for example PPS.

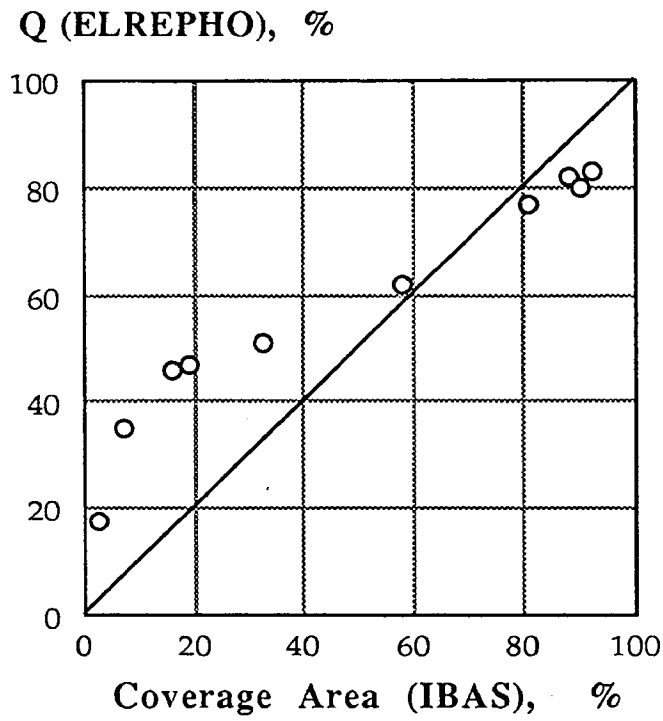


Figure 3.3 Fractional coverage area (IBAS) versus the microcontour value, Q, for different papers

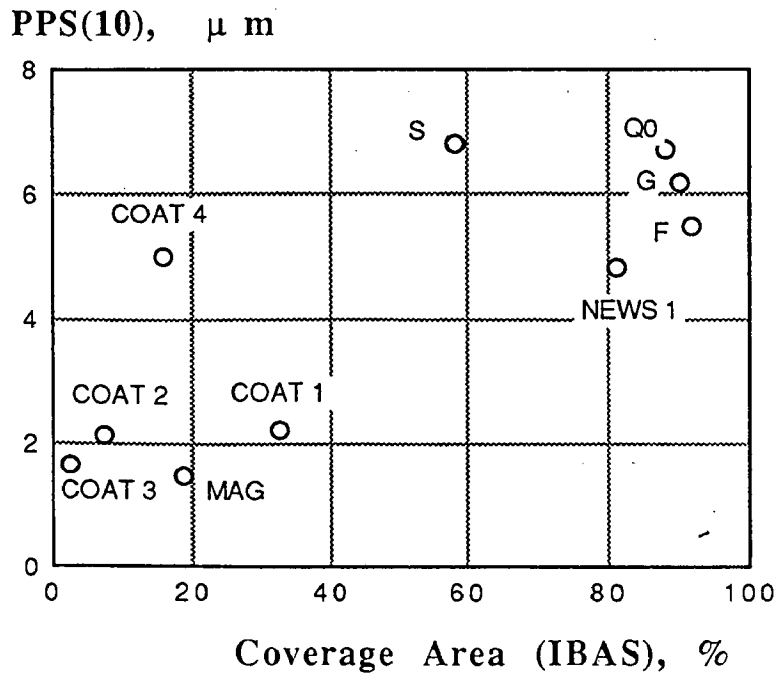


Figure 3.4 PPS value versus the fractional coverage area (IBAS)

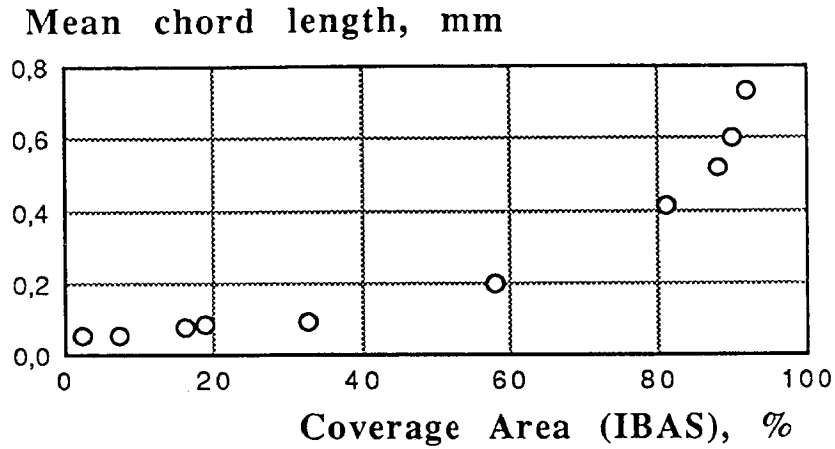


Figure 3.5 Mean chord length versus coverage area

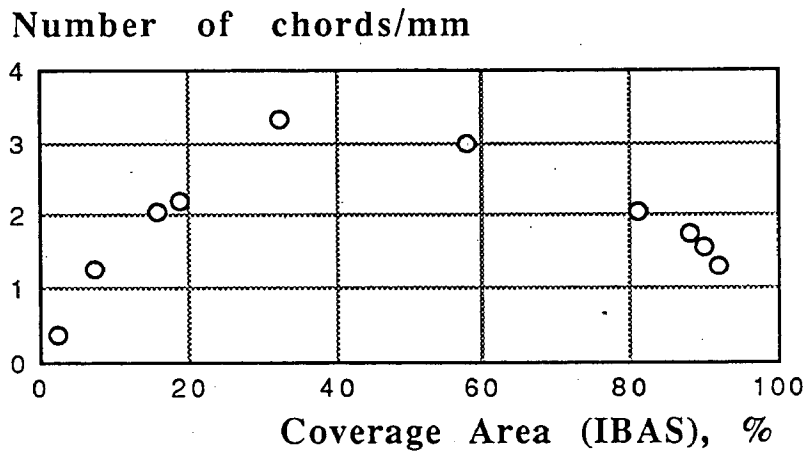


Figure 3.6 Number of counts versus coverage area

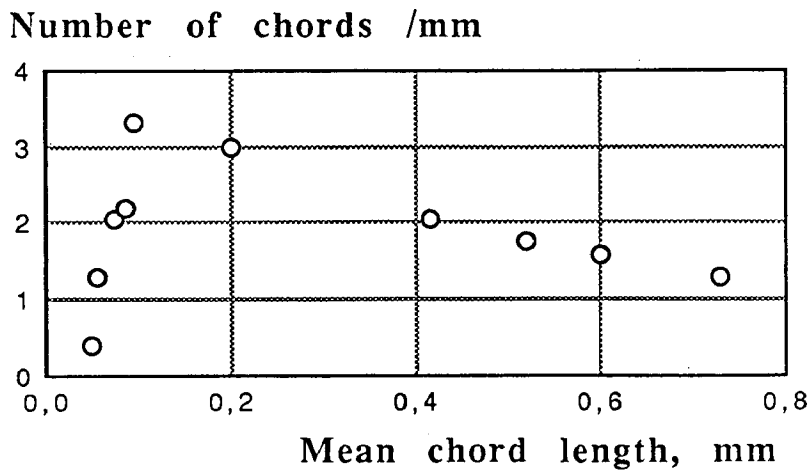


Figure 3.7 Number of counts versus mean chord length

Coeff. of variation

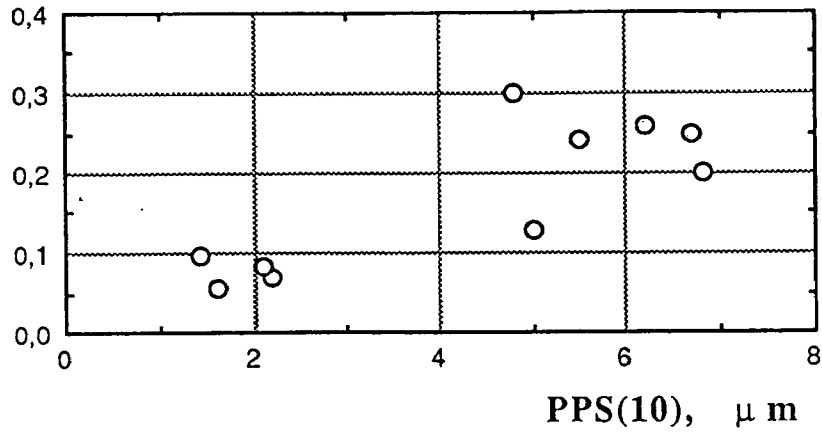


Figure 3.8 Coefficient of variation in greytone levels versus PPS value

Coeff. of variation

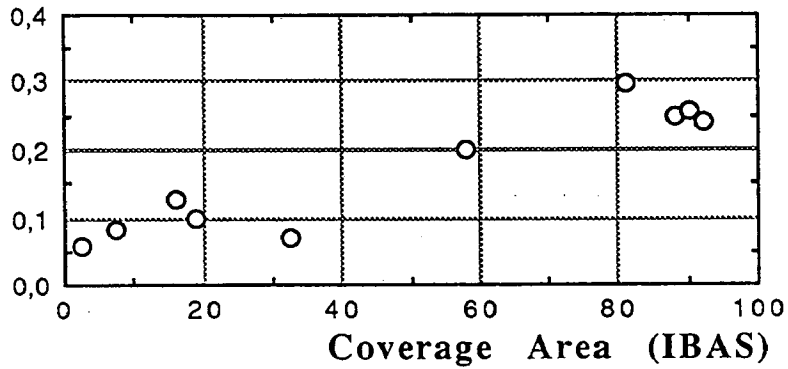


Figure 3.9 Coefficient of variation in greytone level versus coverage area

Coeff. of variation

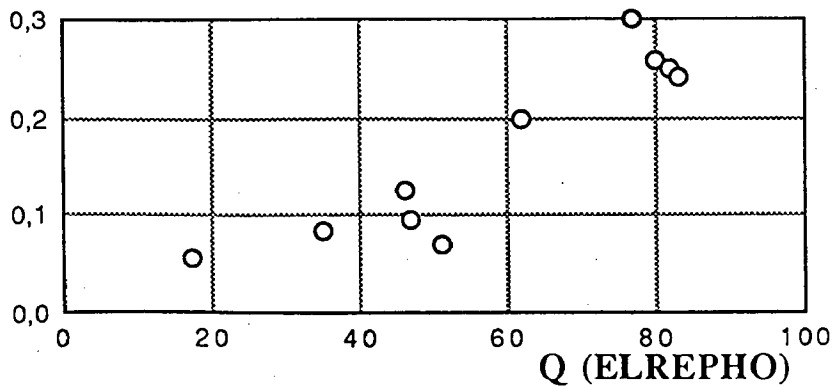


Figure 3.10 Coefficient of variation in greytone level versus microcontour value

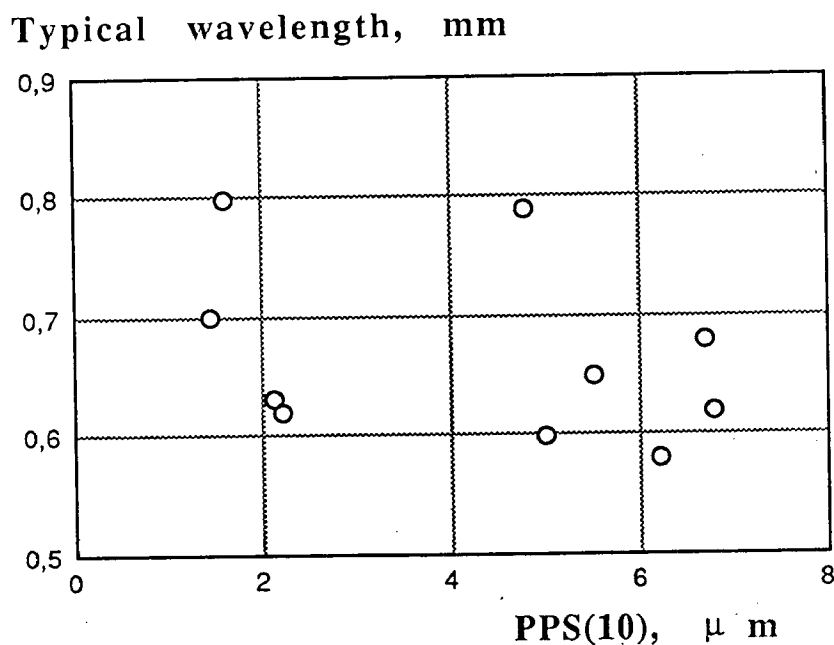


Figure 3.11 The typical wavelength as a function of PPS value

2. The coated and uncoated paper show marked difference in the intensity of colouration even though they have the same PPS roughness. Presumably the absorptivity of paper significantly affects the results and some pigment also penetrates into the pores of paper along with the oil.
3. The test is good only for the visual comparison of papers which have nearly the same absorptivity and optical properties. The microcontour value determined by the Elrepho may sometimes be misleading.
4. The IBAS analysis gives nearly the same information as that obtained by the Elrepho. The coefficient of variation of the intensity of stains is also a good measure of the roughness.
5. The determination by image analysis of a typical wavelength for the stain pattern has a potential to provide further information concerning the nature of the surface.

CHAPTER IV**ANALYSIS OF PROFILES****1. INTRODUCTION**

Surface profiling instruments, which have been in use for nearly 40 years to evaluate paper surface structure, provide the most exhaustive description of the surface characteristics. Most other methods of evaluating paper surface roughness produce only an average value describing the whole surface but, when considering paper as a substrate for printing, these average values have been found to be insufficient to predict the performance of the paper.

The profiles present a magnified visual picture of the topography of the surface. The major task is to extract quantitative data able to tell how the paper is going to behave in a given printing process. A number of studies are reported in the literature, and several printability indices have been determined from the surface profile records. These indices have been shown to correlate with the printability of paper but the available literature lacks a unified approach to the treatment of the recorded profiles.

In the present work, attempts have been made to establish methods of filtering out irrelevant information from the profile and calculating statistical properties from the relevant components only, in this case those components of the profile which are important to printability. Two methods of spatial analysis are presented. A band pass filtration technique based on moving averages can decompose a profile into its components of different wavelengths. An autospectrum of the profile on the other hand gives the distribution of the profile variance as a function of the wavelength. A detailed study has been made to establish the potentials and limitations of these methods of analysing the profiles.

1.1 General Characteristics of Profiling Techniques

The profiling technique was first developed for the study of surface finish of smooth metal surfaces, and this technique, more or less unchanged, has been adopted to characterize paper surfaces. Significant differences, however, exist between a metal surface

and a paper surface, particularly when the desire is to see the surface from the printability viewpoint, viz.:

1. Paper is a deformable viscoelastic material. Its surface smoothens out due to the application of pressure in the printing nip.
2. During the printing process, the paper has to pass through a narrow printing nip which may not be sensitive to the long-wave variation in the paper.
3. Paper is brought into contact with a fluid ink film which can easily bridge very fine cavities in the surface.
4. Paper is a porous material. It absorbs ink which continues to move in the bulk of the paper even after the paper has passed through the nip.

Surface cavities of all widths and depths are important in the case of rigid metallic surfaces whereas the profile recorded on a free paper surface contains extra irrelevant information which should be removed before the properties of these profiles are analysed.

Another important question is whether the irregularities in the paper surface are completely random or whether there are some periodic variations, for example wiremarks, or other predominant size scale variations arising out of certain features of the furnish or of the papermaking process. Can the intensity and the size of these components be determined from this analysis? To answer these questions a comparative study has been made between real paper surface profiles and profiles synthesized from various random and deterministic series. An approach to the interpretation of the autospectra of paper surface profiles based on these comparisons is presented.

There is a tendency to assume that the surface profile levels are normally distributed about the mean, but it was noticed that most of the paper surface profiles studied were skewed in their distribution. The probability distribution function of these profiles may therefore provide valuable information in addition to that given by other characteristic quantities.

Some examples showing the application of the techniques here developed for the characterization of paper and board surfaces are presented. Effects on surface structure of paper or board of some

of the surface smoothing operations such as coating, calendering and brushing are illustrated.

2. EXPERIMENTAL

A schematic diagram of the profiling equipment used in the present study is shown in Figure 4.1. The basic instrument was a Perthometer surface profiler consisting of a diamond stylus with a spherical tip of $3\ \mu\text{m}$ radius. The stylus is fitted in a small pick-up such that it can move freely in the vertical direction, and the vertical position of the stylus is measured with a positional transducer which generates a voltage proportional to the displacement of the stylus. The total range of the stylus is $250\ \mu\text{m}$. Any smaller measuring range can be chosen by altering the sensitivity of the amplifier. The output voltage was digitized by an 8-bit analog-digital converter (ADC) giving values between 0 and 255. These values were converted to actual distance by calibrating the sensitivity of the amplifier against a standard which consisted of a metal plate engraved with a groove $9.3\ \mu\text{m}$ in depth.

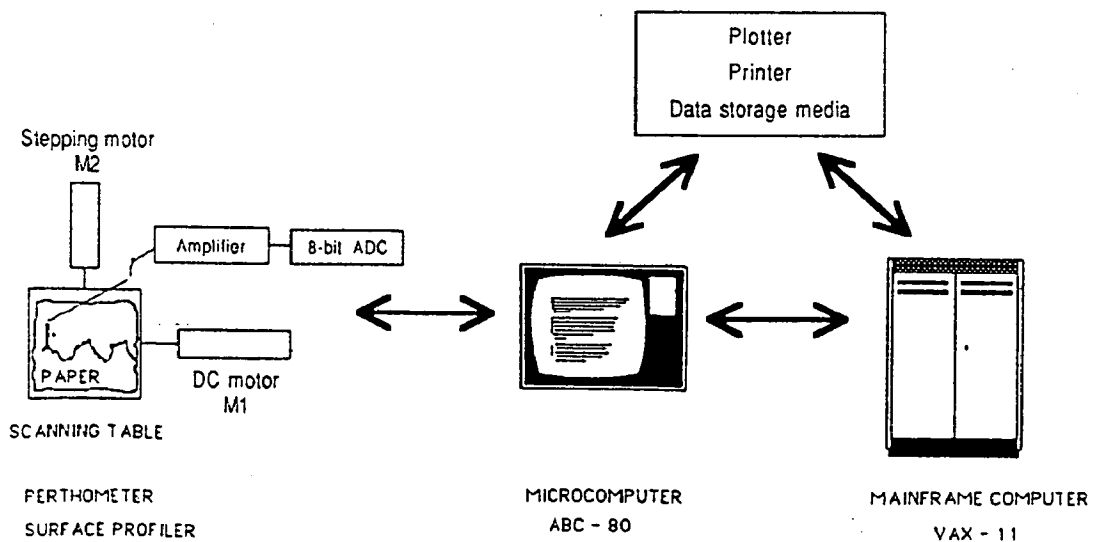


Figure 4.1 Schematic diagram of the surface profiling system

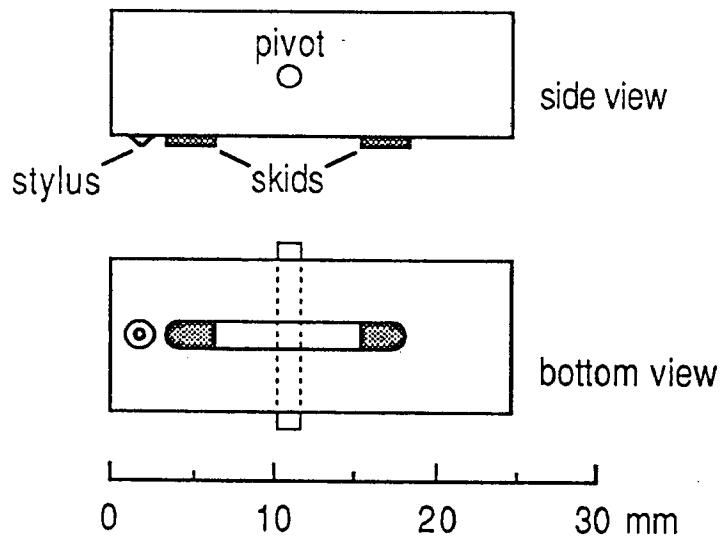


Figure 4.2 The stylus and the pick-up design

Figure 4.2 shows the shape of the pick-up in which the stylus is housed. During measurement, the pick-up slides on the paper surface on two shoes A and B, and the vertical position of the stylus tip is thus measured with reference to the line joining the shoes A and B. The effect of such a reference is to eliminate variations in the profile at wavelengths greater than the distance AB which is about 12 mm. The stylus point has an offset of 1 mm from the reference shoe A. Such an offset can result in a slight distortion of the true surface profile especially at wavelengths longer than 1 mm. Since no pick-up design is free from errors in profiling a surface and since variations with wavelengths longer than 1 mm were found to be not very important in characterizing paper surfaces, this instrument was considered to be satisfactory in the present work.

While being scanned, the paper specimen was mounted on a smooth flat metallic table 100 mm x 100 mm in area. The stylus with its pick-up was moved over the paper surface with the help of a

constant-speed motor M_1 . The direction of motion was such that the shoes passed over the surface before it was sensed by the stylus. The mass of the stylus acting on the paper was 80 mg. Repeated scanning of the same paper profile indicated that the paper surface itself was not changed by the action of either the shoes or the stylus. The table on which the paper sample was mounted could also be moved by another stepping motor M_2 in a direction perpendicular to the scanning direction to allow the surface to be scanned along close parallel lines. The profiling unit was connected to a microcomputer, ABC-80, to control the movements of motors M_1 and M_2 , and to record the profiles.

During the scanning of a profile, the stylus readings were recorded by the computer at fixed intervals of time, the speed of movement of the stylus and the recording times being adjusted so that the time intervals corresponded to distance intervals of 4.5 μm . After the complete profile was recorded, the data were used to plot the profile and to calculate statistical quantities.

In the beginning of this study an approach similar to that used by Kent (1984) and Climpson (1984) was adopted. The surface of the paper was scanned along parallel lines separated by 25 μm , and the data from these profile records were used to draw contour maps of the surface. The total variation in heights of the surface was divided into four levels and the regions of the surface lying within these levels were plotted in four different colours. The intention of such an approach was to use an image analyser to determine the distribution of portions of the paper surface at different levels, but the approach was later abandoned because it was exceedingly slow and allowed examination of only a very small area (5 mm x 5 mm) of the surface.

The techniques adopted in the present work to analyse profile data are similar to those used in time series analysis. A single 20.25 mm long profile (4500 points at intervals of 4.5 μm) was recorded for this analysis. Later it was found that sampling of the surface as close as 4.5 μm was not necessary and it was decided to read the profile at intervals of 4.5 μm but to record means of 3 consecutive points. Thus only 1500 points were recorded at intervals of 13.5 μm . This averaging at 3 points also helps avoid problems in the estimation of power spectra which are discussed in more detail together with the results. To enhance the computational speed and capabilities, the data were transferred from the microcomputer ABC-80 to a mainframe computer, VAX-11/780, for further analysis.

3. ANALYSIS

3.1 Basic Definitions and Notations

Figure 4.3 shows a typical surface profile recorded in the present study. Since the recorded profile is a sequential output from the Perthometer it can be regarded as a time series. In a deterministic function, for example a sine wave, the complete behaviour of the output signal is known by determining only a few parameters and it is possible to predict all future values exactly. The surface profile record, on the other hand, is non-deterministic and its future values cannot be accurately predicted. Such stochastic signals can only be described by statistical laws and only mean values of signal properties can be predicted. Methods of statistical analysis of such fluctuating or random signals were first practically applied in communication engineering. Subsequently these methods have been found to be powerful tools of analysis in many areas where stochastic processes are encountered. The technique is generally referred to as time series analysis, (Jenkins and Watts, 1968; Bendat and Piersol, 1958).

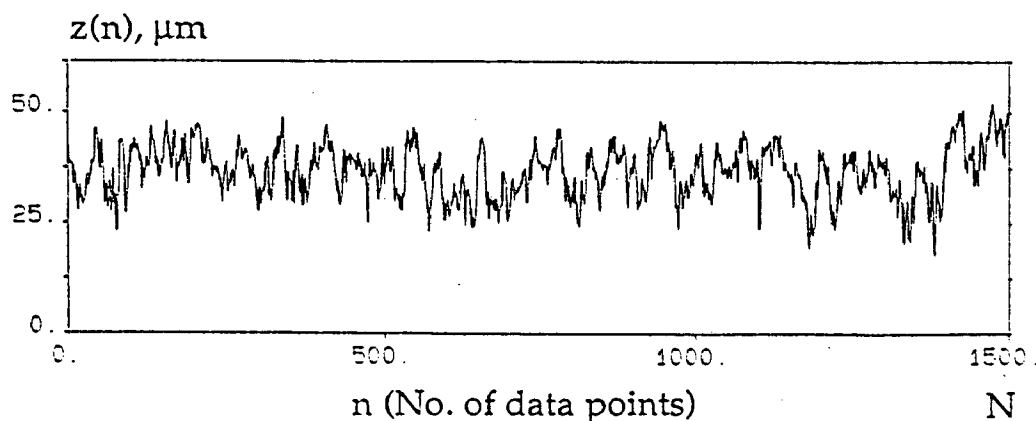


Figure 4.3 A typical surface profile

The output signal from the Perthometer may be expressed as $z(t)$, where $z(t)$ is the vertical position of the stylus at time t . The profile in terms of the space coordinate can then be expressed as $z(x)$ where $x = t \cdot v$, v being the speed of the stylus and x its displacement along the surface at time t . For computational ease, the surface profile is recorded as a discrete series. The transducer output is recorded at fixed intervals of time. This series may be expressed as $z(n)$ for $n = 1, 2, \dots, N$, where N is the total number of data points recorded. If Δt is the time interval between two consecutive records then the distance between adjacent points or the sampling interval will be $h = \Delta t \cdot v$. Subsequent expressions can be simplified if v is assumed to be equal to unity. The choice of sampling interval depends on the smallest size of the details of the surface structure which it is desired to study and the speed with which the profiles can be recorded and mathematically analysed.

The mean, \bar{z} , and the standard deviation, σ_z , of the profile are then defined as

$$\bar{z} = \frac{1}{N} \sum_{1}^N z(n) \quad [4.1]$$

and

$$\sigma_z = \left[\frac{1}{N-1} \sum_{1}^N (z(n) - \bar{z})^2 \right]^{\frac{1}{2}} \quad [4.2]$$

An important concept in time series analysis is the concept of stationarity. Although the properties of a stochastic process are time dependent, a simplifying assumption often made is that the series is in some form of steady state or equilibrium in the sense that the statistical properties of the series remain unchanged if the series is lengthened. A simple test for stationarity is that the mean and standard deviation of the series are independent of time, i.e. that \bar{z} and σ_z do not vary when the value of N is further increased. The analysis used in the present work is applicable only to stationary time series. It has therefore been essential to ensure that the profile records fulfil the condition of stationarity, otherwise the estimated parameters may contain large errors. The profiles recorded in the present study were 20.25 mm long. Due care was taken to place the paper sample flat on the scanning table and no disturbing trends were visible in the profile records. The mean and standard deviation of half of the length of the profile, i.e. 10 mm, were nearly the same as those

of the total profile length. The profiles were therefore considered to be stationary and it was not necessary to attempt to remove trends from the profile data.

3.2 Analysis of Variance

The simplest and the most commonly used statistical property of a series is the mean of the data, but in the case of profile data the mean does not relate to any physical property of the surface since it is the deviation from the mean which is of interest. Subsequent formulae and calculations may be greatly simplified by transforming the data to a zero mean, the new profile record being expressed by $y(n)$ such that

$$y(n) = z(n) - \bar{z} \quad [4.3]$$

with mean $\bar{y} = 0$.

The other most commonly determined statistical property of a series is the variance of the data about their mean, which is equal to the mean square value when the mean is zero and N is large, defined as

$$\sigma_y^2 = \frac{1}{N-1} \sum_1^N y(n)^2 \quad [4.4]$$

The variance of the profile data gives some measure of the roughness of the surface. Profiles of smooth surfaces will have less variance than those of rough surfaces.

If the profile curve in Figure 4.3 crosses the mean line frequently this indicates the presence of narrow irregularities or a profile variation of a small wavelength. If, on the other hand, the curve crosses the mean less often, this indicates the presence of wider cavities or variations of longer wavelength. A glance at a paper profile reveals that a paper surface contains variations of no definite amplitude or wavelength. It can be regarded as consisting of a large number of waves of varying wavelengths and amplitudes. It is possible to decompose a profile into its components. Two methods are presented here.

3.2.1 Band pass filtration by moving averages

In Figure 4.4a, the profile heights have been plotted with reference to the common mean of the profile. If, instead of being considered as a whole, the profile is viewed through a narrow window which is moved from one end of the profile to the other, the effect is to suppress wavelengths longer than the width of the window while shorter wavelength variations can still be seen.

As the window traverses the profile, each point is replaced with a value which is equal to the deviation of that point from the mean value of the profile viewed through the window when the point concerned is in the middle of the window. Mathematically the height of the n th point with a window having a width of $2W + 1$ data points is recorded as

$$y_W(n) = y(n) - \left(\frac{1}{2W}\right) \sum_{n-W}^{n+W} y(i) \quad [4.5]$$

$$n = (W+1), (W+2), \dots, (N-W)$$

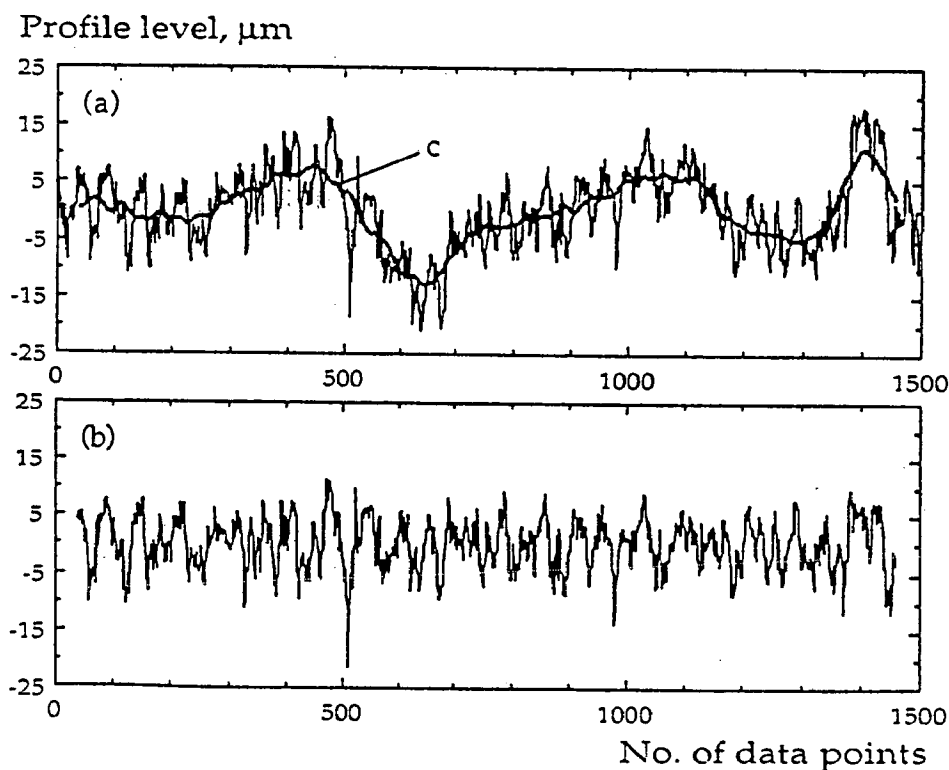


Figure 4.4 Total surface profile and the profile with reference to a moving average

Thus the profile is recorded with respect to a moving average. The resulting profile in Figure 4.4b contains no longwave components. All deviations having wavelengths shorter than the width of the window are absent from profile c, which contains the longwave component and is also the moving average of profile a. The technique of deriving profile b from profile a is called high-pass filtration because the low frequency (long wavelength) variations have been removed and the high frequency variations have passed the filter. It should be noted here that filtration also means that the length of the resulting profile is shorter due to a loss equivalent to half the width of the window at each end.

This filtration procedure can be repeated. A profile from which variations of wavelength longer than $2W_1$ and shorter than W_2 have been removed is called a bandpass filtered signal, and can be represented as:

$$y_{2W_1-2W_2}^{(n)} = (1/2W_1) \sum_{n-W_1}^{n+W_1} y(i) - (1/2W_2) \sum_{n-W_2}^{n+W_2} y(i) \quad [4.6]$$

$$n = (W_2+1), (W_2+2), \dots, (N-W_2)$$

The bandpass filtration technique can be applied to decompose a profile into many components although a simple averaging window is not a perfect filter. Figure 4.5 shows the decomposition of a deterministic signal which was generated by adding three sine waves of different wavelengths. Although the separation is very good, it can be seen that the components of the signal obtained by the bandpass filtration contain variations with wavelengths outside their band widths, which means that the technique cannot be meaningfully used for high resolution with very narrow bands. Johansson (1983) has shown that the technique is very useful for the study of stochastic signals.

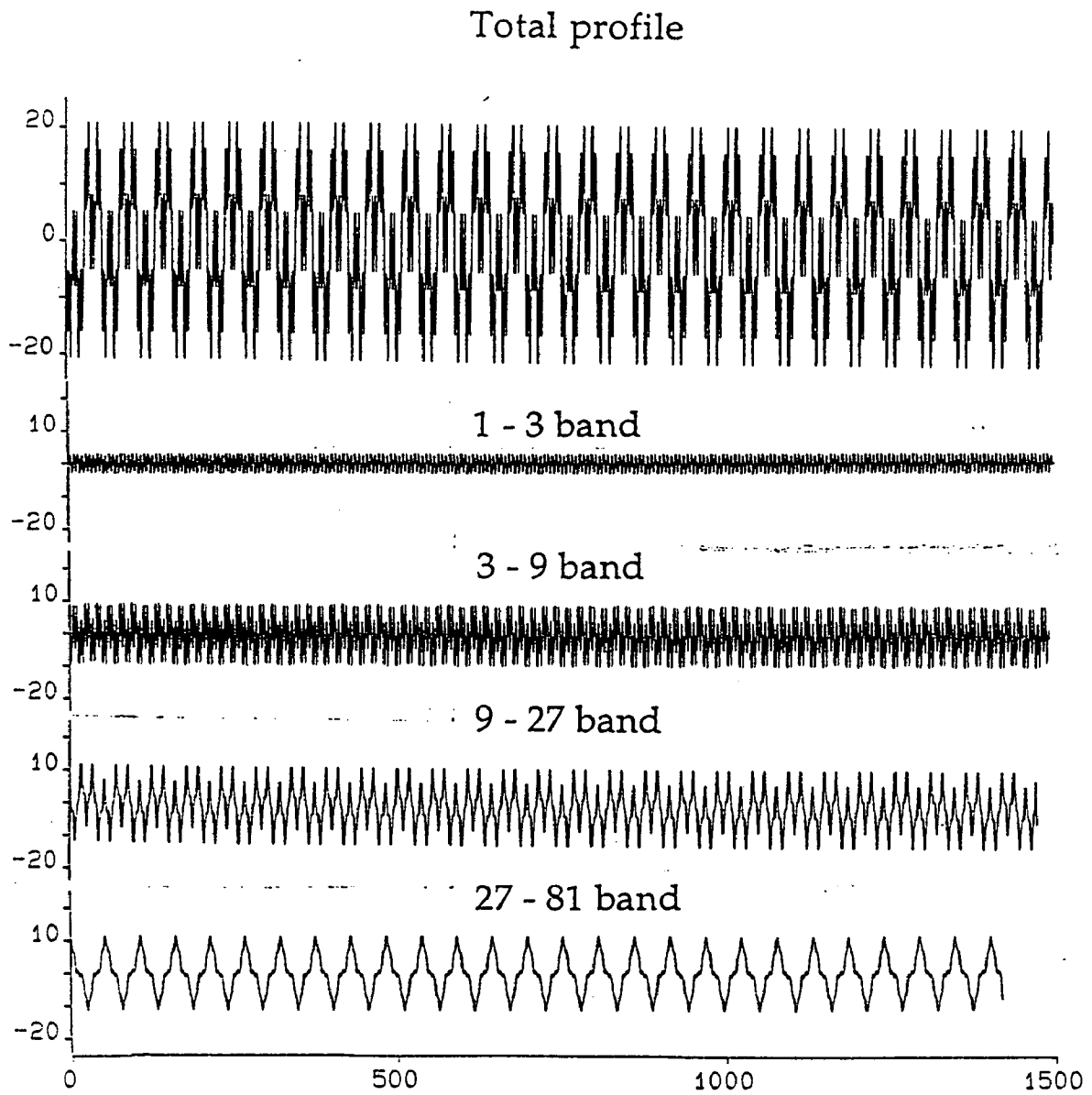


Figure 4.5 Decomposition of a deterministic signal consisting of three sine waves:

$$Z(n) = 40 \sin \left(\frac{2\pi n}{6} \right) + 40 \sin \left(\frac{2\pi n}{18} \right) + 40 \sin \left(\frac{2\pi n}{54} \right)$$

Table 4.1 lists the wavelength bands chosen for the characterization of paper surfaces.

Table 4.1 Wavelength bands for surface characterization

Band No	Window width No of data points	Window width μm
1	1 - 3	13.5 - 40.5
2	3 - 9	40.5 - 121.5
3	9 - 27	121.5 - 364.5
4	27 - 81	364.5 - 1093.5

These nominal bandwidths correspond to a simple model of the behaviour of the windows. Other limits can be assigned if consideration is given to their unsharp cut-off characteristics.

Figure 4.6 shows how an original profile decomposes into these bands. The residue after this separation contains wavelength components longer than 81 data points. When all these components are summed, they give a signal equal to the original profile.

Figure 4.7 shows for three profiles from the same grade of paper (a) the variance in these four wavelength bands, (b) the variance in a single band derived with a window having 81 data points, and (c) the total variance. It is evident that the total variance of a profile has a poor reproducibility, but that when the variance data are compared after decomposing the profile into its components most of the irreproducibility lies in the residual longwave component and that the variance in the bands up to a wavelength of 81 data points (≈ 1 mm) is fairly reproducible. The variations attributed to a wavelength greater than 1 mm have presumably come from distortions due to the effect of the design of the pick-up of the profiler or from some waviness of the sample which is not characteristic of the surface.

The variance in the 1-81 window width band is not quite equal to the sum of the variances in the four component bands, indicating some degree of correlation between profile components or to limitations in the filtering technique with regard to the boundaries between bands.

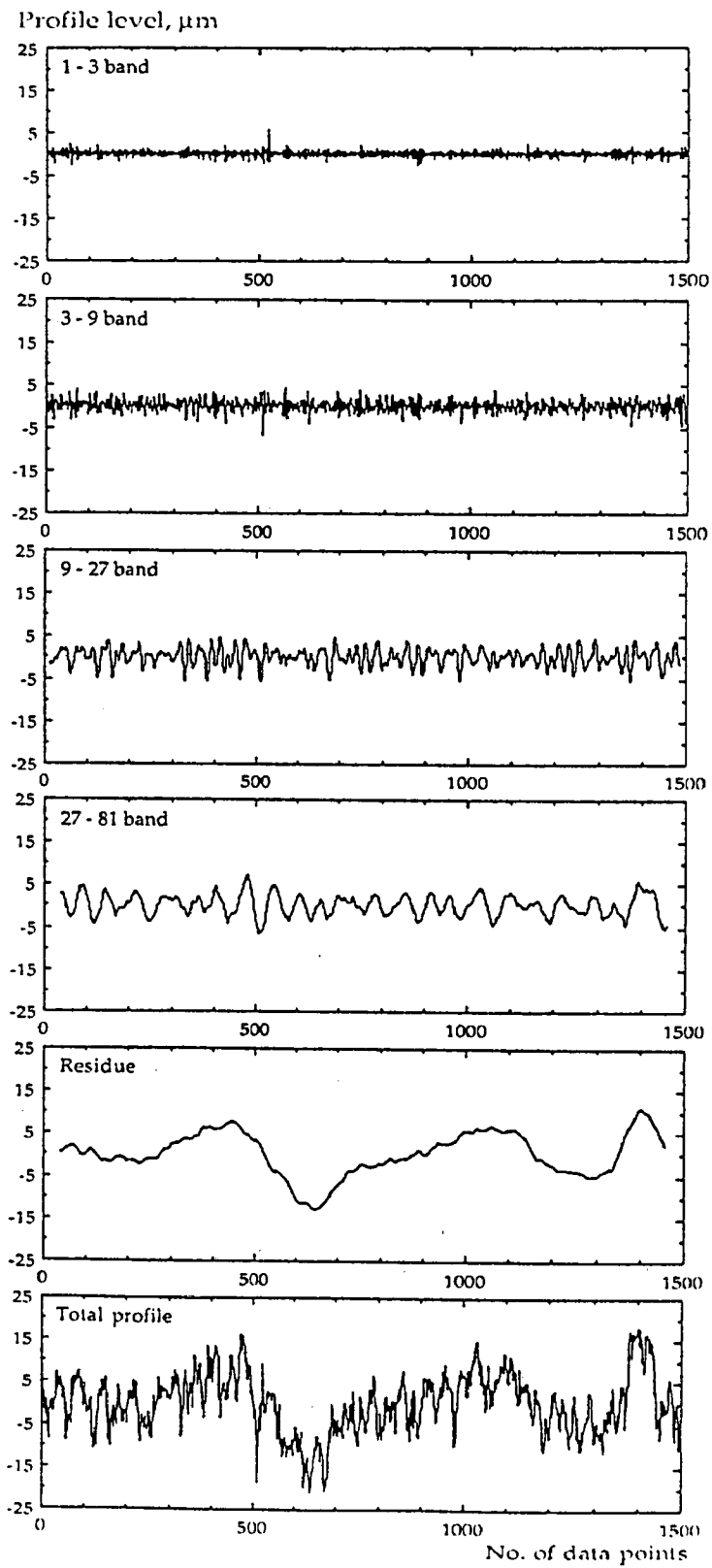


Figure 4.6 Components of a paper profile decomposed by moving average bandpass filtration

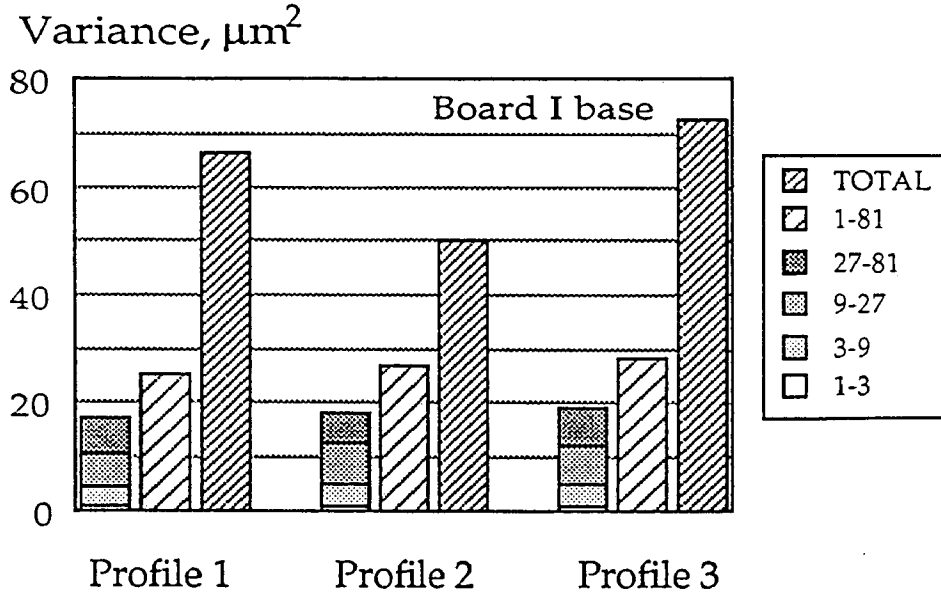


Figure 4.7 Distribution of variance in four wavelength bands - shown for three profiles of the same paper sample

In Figure 4.8 the variance in four bands has been plotted for an uncalendered paper and for the same paper calendered at two different pressures. The figure shows that the variance decreases in all these bands as a result of the smoothing effect of calendering, but it is interesting to note that the greatest reduction is in bands 3 and 4 and that there is little reduction in the first two bands. Information of this type is potentially valuable in the study of the printability of paper.

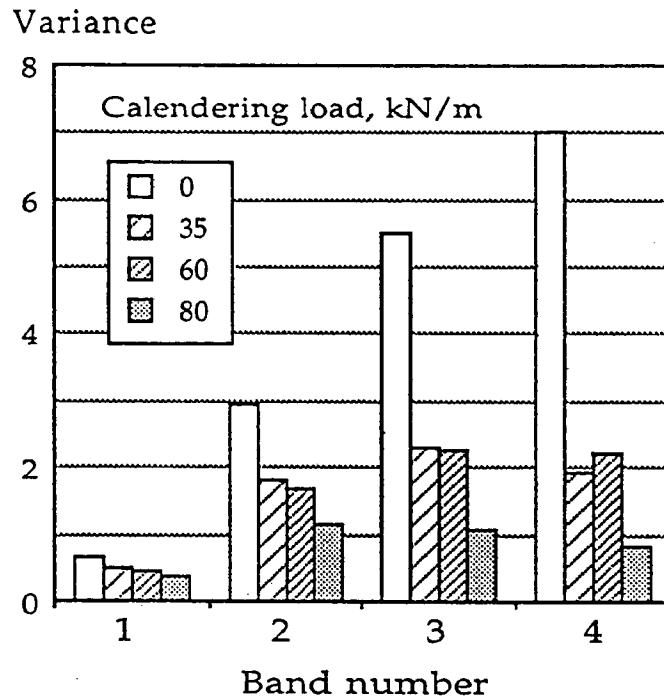


Figure 4.8 Effect of calendering on the variance of the profile in the four wavelength bands

In fact, there is a fairly good correlation between the variance in each of these bands and the PPS-value as shown in Figure 4.9, which combines data for a series of coated, calendered and brushed boards. It is necessary, as indicated above (Figure 4.7), to eliminate the long wavelength variance, but separation of the remaining variance into these sub-groups does not provide information which correlates either more or less with the PPS-value than the total variance in the single 0-1 mm band.

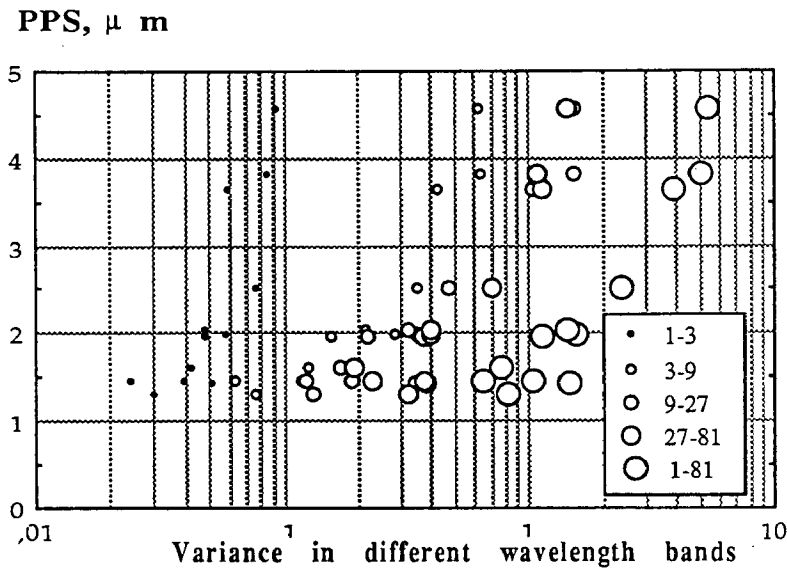


Figure 4.9 The variance in different wavelength bands as a function of the PPS-value for a number of different paper samples

3.2.2 Autocorrelation function

A variance distribution obtained by the method of moving averages has only 4 or 5 bands with successively increasing bandwidths. The technique is quite simple and the results obtained are easy to interpret and quite useful for the characterization of paper surfaces. When an analysis of the wavelength components into narrower bands is required, the technique of determining the autocorrelation function and autospectrum has a greater efficiency. These latter techniques also provide means of determining the presence in the profile of any periodic components, their amplitudes and periods.

The variance of a series is obtained by averaging the squares of the distances of the data points from their mean over the entire profile length. The covariance is obtained when the products of corresponding data points in two series are averaged. Autocovariance is obtained by displacing a profile relative to itself by some fixed interval, multiplying the original profile by the displaced one over the overlapping lengths of the profiles, and averaging the product values. Repeated calculation of the autocovariance with different displacements yields the autoco-

variance function, $c_{yy}(u)$, defined for a profile $y(n)$ as

$$c_{yy}(u) = \frac{1}{(N-u)} \sum_{n=1}^{N-u} y(n) \cdot y(n+u) \quad [4.7]$$

for $u = 0, 1, 2, 3, \dots, U$

The displacement u is called the lag and U is the total number of lags for which the function is determined. The autocovariance at zero lag is equal to the variance of the signal.

It is sometimes convenient, particularly when comparing profiles with different total variances, to normalize the autocovariance function by dividing it by the variance of the profile. The new function is called the autocorrelation function, $\rho_{yy}(u)$, and is given by

$$\rho_{yy}(u) = \frac{c_{yy}(u)}{c_{yy}(0)} \quad [4.8]$$

$u = 0, 1, 2, \dots, U$

When the lag, u , is zero, the correlation coefficient is unity. As the lag increases, the correlation between the points decreases. If a periodicity is present in a profile, the autocorrelation coefficient rises as the lag approaches the periodicity length or an integral multiple thereof. The autocorrelation function plotted against lag may be regarded as a new profile derived from the original, which will generally contain less noise than the original and thus enhance the visual impression of any periodicity in the profile.

3.2.3 Autospectrum

The autospectrum, also known as the power spectrum, is an alternative method of expression of the spatial information. The autospectrum is the fourier transform of the autocovariance function of a series

$$P(f) = \int_{-\infty}^{\infty} c_{yy}(u) e^{-j2\pi fu} du \quad [4.9]$$

$$-\infty \leq f \leq \infty$$

where $j = \sqrt{-1}$. $P(f)df$ represents the variance of the series over the frequency range f to $f+df$. The area under the power spectrum curve is equal to the total variance of the series, i.e.

$$\sigma_y^2 = \int_{-\infty}^{\infty} P(f)df \quad [4.10]$$

Hence $P(f)$ shows how the variance of the profile $y(n)$ is distributed with respect to frequency. A normalized power spectrum obtained by dividing $P(f)$ by the variance is called the power spectral density function (PSD). This density function is the fourier transform of the autocorrelation function and the integrated value of PSD is unity. PSD is useful for comparing the nature of the distribution of variance of profiles with different total variances.

The power of a random series is uniformly distributed over the entire frequency range. A smooth series has most of its power at low frequency and a highly oscillating series has most of its power at high frequencies. If the series contains a periodic component, the power tends to concentrate at the frequency of that component and appears as a sharp peak in the autospectrum.

There are two commonly employed methods for computing power spectra: (1) the classical Blackman-Tukey method (cf. Jenkins and Watts, 1968) based on computing the autocovariance function for a suitable number of lags and then computing its fourier transform; (2) the direct fourier transform or Cooley-Tukey method (ibid) based on computing the power spectrum from a finite range fast fourier transform (FFT) of the original data. Although the direct fourier transform method has a higher computation efficiency, the earlier method was used in this study since it provided observation of autocovariance functions while computing the autospectra. The standard software packet IDPAC (Wieslander, 1980) was used on a VAX-11/780 main frame computer for these analyses.

The definition of power spectrum given in eq. [4.9] is for an infinitely long continuous time series. Since profiles of finite length were recorded, only an estimate of the true power spectrum can be determined from these data. The spectral estimates are given by

$$\bar{P}(f) = h \sum_{u=-(U-1)}^{(U-1)} c_{yy}(u) e^{-j2\pi fuh} \cdot W_{BH}(u) \quad [4.11]$$

$$-(1/2h) \leq f \leq (1/2h)$$

where $W_{BH}(u)$ is the Blackman-Harris lag window (Harris, 1978) used to smoothen the spectral estimates.

Since $\bar{P}(f)$ is an even function of frequency, it is only necessary to calculate it over the range $0 \leq f \leq 1/2h$. When only the real terms are used, the formula becomes

$$\bar{P}(f) = 2h [c_{yy}(0) + 2 \sum_{u=1}^{U-1} c_{yy}(u) \cos(2\pi fuh) \cdot W_{BH}(u)] \quad [4.12]$$

and the variance is given by

$$\sigma_y^2 = \int_0^{\infty} \bar{P}(f) df \quad [4.13]$$

The autocovariance function, c_{yy} is calculated for positive lags, ($u \geq 0$) only. Usually the values of $\bar{P}(f)$ are determined for

$$f = \frac{i}{U} \frac{1}{2h}$$

$$i = 0, 1, 2, \dots, U$$

The maximum frequency ($1/2h$) is also called the Nyquist frequency.

The width of the Blackman-Harris smoothing window is equal to $1/Uh$ and two frequency components f_1 and f_2 can be resolved in the spectrum only when the width of the window is smaller than $f_2 - f_1$ i.e.

$$\frac{1}{Uh} \leq f_2 - f_1 \quad [4.14]$$

Hence to increase the resolution in the spectrum, the number of lags must be increased. On the other hand, each lag increase leads to a reduction in the effective profile length and hence to a reduction in the accuracy of the estimates. A normalized standard error in the estimate of spectral density is given by

$$\epsilon = (U/N)^{1/2} \quad [4.15]$$

The choice of number of lags for which the autocovariance function is calculated is a compromise between the accuracy of the estimated spectral density and the resolution in the frequency. In the present case, a maximum lag of about 10 % of the record length was a good choice in the analysis.

Another factor which affects the accuracy of the spectral estimates is called aliasing which is dependent on the sampling interval. Theoretically the maximum possible frequency of the signal is $1/2h$ and any frequency above this should not contribute any power to the spectrum, but frequencies higher than $1/2h$ do contribute some power in the spectral density estimates. This leakage of power from higher frequencies is called aliasing. To avoid aliasing a sampling interval should be chosen which is about one half of the sampling interval corresponding to the desired maximum frequency, then the data should be low-pass filtered so that the information for frequencies above $1/2h$ is no longer contained in the filtered data. In the present case, the problem of aliasing was avoided by taking readings at $4.5 \mu\text{m}$ and averaging these in groups of three to yield data points at $13.5 \mu\text{m}$ intervals.

3.2.4 Wavelength spectrum

Conventionally the power spectrum is calculated as a function of frequency, but in the case of a paper surface, the wavelength of the profile corresponds directly to the width of the surface cavities and is better related to the physical nature of the surface. Moreover the concept of wavelength is compatible with the method of bandpass filtration using moving averages. The frequency spectrum was transformed into a wavelength spectrum using the method suggested by Norman and Wahren (1972).

The wavelength and the frequency are related as

$$f = \frac{1}{\lambda} \quad [4.16]$$

$$\text{i.e. } df = -\frac{1}{\lambda^2} d\lambda \quad [4.17]$$

Substituting df in equation (4.13) yields

$$\sigma_y^2 = \int_0^{\infty} \frac{1}{\lambda^2} \bar{P}(f) d\lambda \quad [4.18]$$

or

$$\begin{aligned}\bar{P}(\lambda) &= \frac{1}{\lambda^2} \bar{P}(f) \\ &= f^2 \bar{P}(f)\end{aligned}\quad [4.19]$$

$\bar{P}(\lambda)$ gives spectral estimates as a function of wavelength.

The estimation of the autospectrum depends greatly on the number of lags (U) used for the computation of the autocovariance function. A greater value of U will allow a better resolution in the estimates of $\bar{P}(f)$ between two frequencies. On the other hand, as the number of lags is increased the overlapping length of the profile over which the autocovariance is determined is reduced and the accuracy of the estimate of $\bar{P}(f)$ decreases. A compromise is made between the resolution among frequencies and the accuracy of the spectrum while choosing the number of lags. This limitation leads to a distortion when a power spectrum is transformed from a frequency scale to a wavelength scale using the technique of equation [4.19].

3.3 Probability Density Function

The autocorrelation function and the autospectrum of a series provide no information about the nature of the distribution of data about their mean. There is a tendency to assume that the profile data are normally (Gaussian) distributed, although the present work indicates that this is often not true. If the distribution is non-Gaussian, the probability density function of the data must be determined in order to characterize the profile completely.

The probability density function describes the probability that the data will assume a value within some defined range. The probability that $y(n)$ assumes a value between y_1 and y_2 may be obtained by taking the ratio of the number of data points falling inside the range to the total number of data points. If the total range in which the profile data may lie is divided into K classes, then

$$p(i) = \frac{N_i}{N} \frac{K}{\beta - \alpha} \quad [4.20]$$

$$i = 1, 2, \dots, K$$

and

$$y(i) = \alpha - (i - \frac{1}{2})(\beta - \alpha)/K \quad [4.21]$$

where

$p(i)$ = probability that a data will lie within class i

$y(i)$ = middle value of class i

α = the minimum value of $y(n)$

β = the maximum value of $y(n)$

N_i = number of data points lying in class i

N = total number of data points

4. ANALYSIS OF SURFACE PROFILES USING AUTOSPECTRA

The basis of the determination of autospectra is the assumption that any series of data can be divided into a number of periodic functions (e.g. sine functions) with different amplitudes, frequencies and phases. The various components can be determined exactly for a deterministic series, but for a stochastic series such as a paper surface profile the number of these components is infinitely large and only average values of their amplitudes can be determined. The autospectrum shows the estimated contribution to the total variance of the series of the components of different frequencies; a peak in the autospectrum signifies a high variance at the corresponding frequency and the presence of a periodic component.

Traditionally the autospectrum is calculated as a function of frequency and plotted on a log-log scale, but the transformation of the autospectrum to a wavelength scale has been found to be more consistent with the terms used to describe paper surface such as width of cavities, waviness of the surface etc. Such a transformation results, however, in the distortion of some information about the surface.

To provide background data with which to assess the significance of fractions in autospectra of paper surfaces, a pseudo-random data series has here been analysed. The whole analysis was

done on a VAX-11/780 computer using the IDPAC (Wieslander, 1980) software for time-series analysis. The actual commands used are given in Appendix B.

4.1 Comparison of a paper surface profile with a random profile

A pseudorandom signal having a normal distribution with 3000 data points with a mean of 127 and a standard deviation of 20 units was generated. These values were adopted to achieve compatibility with the Perthometer surface profile recording system.

Figure 4.10 shows a plot of a paper surface profile and of the random signal generated on the computer.

The profile data in (a) appear to show the presence of long-wave periodic components superimposed upon stochastic variations. At least one long-wave periodic component having a wavelength of about 3 mm is clearly visible. The shorter wave components show a skewed distribution about the local mean, the depths of valleys in the surface appearing to be greater than the heights of the hills.

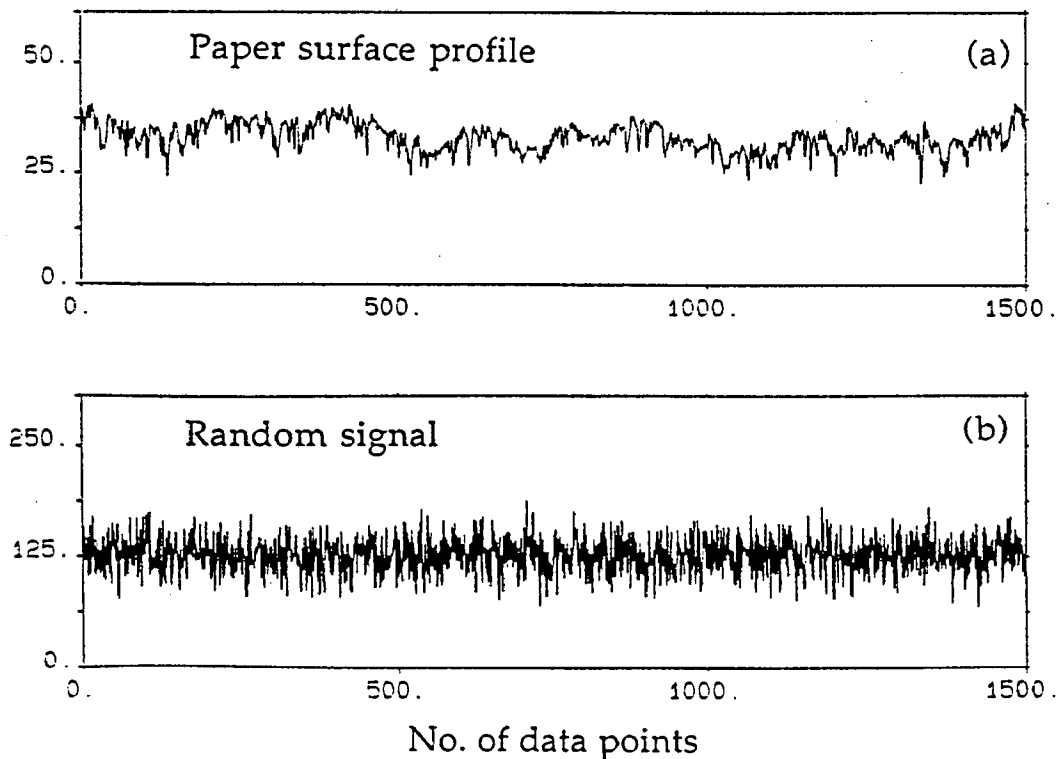


Figure 4.10 Plots of a paper surface profile and the pseudorandom signal

Figure 4.11 shows the autocorrelation functions of the paper surface profile and of the random signal. The function *a* provides some confirmation of the visual observation that there is a long-wave component in the profile with $\lambda = 3$ mm.

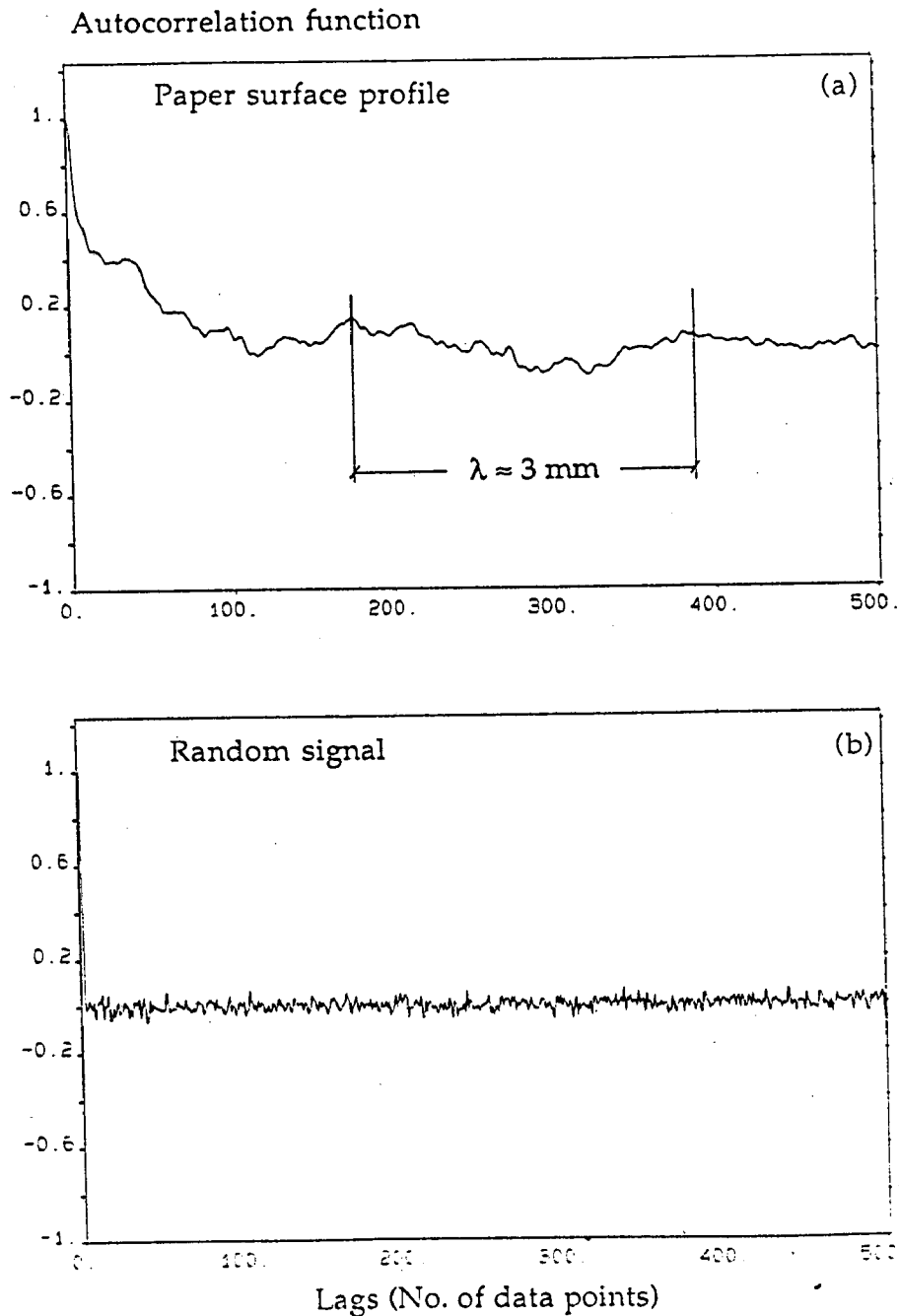


Figure 4.11 Autocorrelation function of the paper surface profile and that of the random signal

The correlation coefficients for the random signal quickly fall to zero for all lags greater than 0. A comparison of the autocorrelation functions a and b reveals that there is a greater correlation between the adjacent undulations in the paper profile than there is in a random series.

Figure 4.12 shows the autospectra of the paper surface profile and that of the random signal.

The autospectrum was determined from the autocorrelation function determined over 150 lags for profiles consisting of 1500 data points. At short wavelengths, the autospectra of both the random signal and the paper profile have a sawtooth-like shape indicating the presence of many low-power peaks in this region. The theoretically calculated autospectrum of a completely random signal should be a straight line with a slope of -2 on a log-log plot. When the procedure was repeated with different random data series generated with the same function, the details were different but the general pattern was found to be the same. It is thus apparent that it is difficult to judge whether any of the short-wave peaks is related to any characteristic of the paper surface.

The real profile shows much less spectral density at short wavelengths than a purely random signal, presumably due to the finite size of paper furnish components.

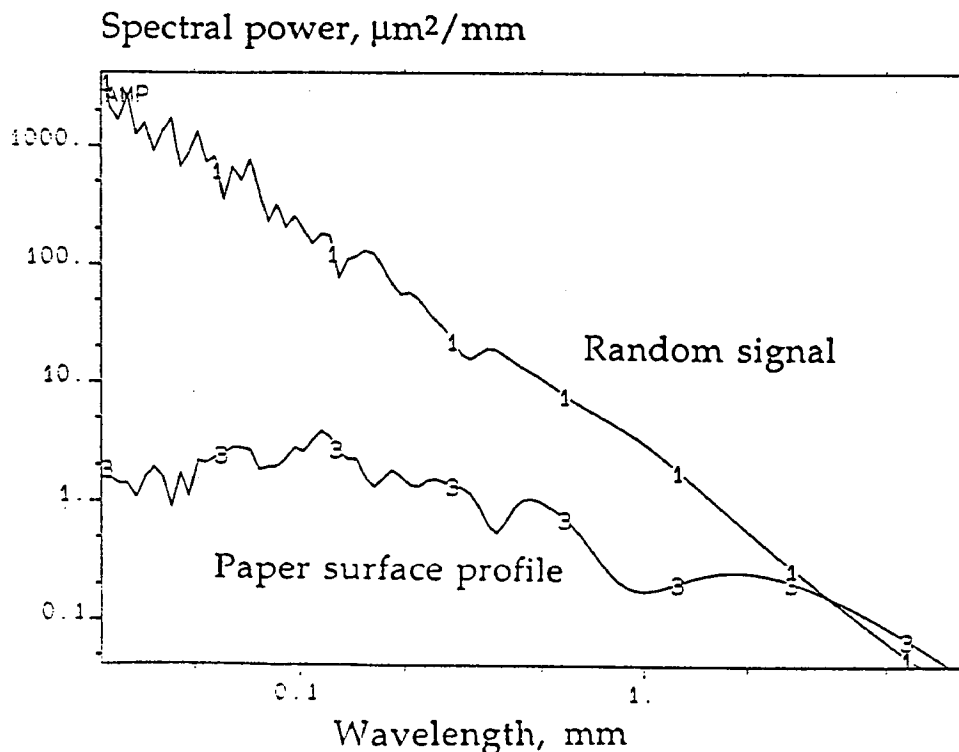


Figure 4.12 Autospectra of the paper surface profile and that of the random signal

4.2 Development of Synthetic Profiles

To acquire a better understanding of these autospectra, profiles were synthesized from various random and deterministic components.

A sine wave with a wavelength of 0.6 mm and an amplitude of 5 units was added to the previously generated random signal. The sum of the random signal and sine wave was then given a slightly skew distribution by cutting off the peaks of values greater than 150 units.

Since it was evident in Figure 4.12 that paper surfaces are free from very high frequency variations, the signal was passed through a low-pass digital filter to cut off frequencies equivalent to wavelengths shorter than 0.2 mm. To avoid errors in the profile data due to instability of the low-pass filter at the beginning of the profile, only the last 1500 points were selected for further investigations. Finally, a long wave sine function with a wave length of 4 mm and an amplitude of 10 units was superimposed to simulate the wavy part of the paper surface profile.

Figures 4.13 shows the generated signal at its various intermediate stages. The final synthesized profile looks quite similar to an actual paper surface profile.

Figure 4.14 shows the autocorrelation function of the synthesized profile. A high correlation coefficient at a displacement of 4 mm represents the long-wave sine component. The other sine wave component ($\lambda = 0.6$ mm) is not so clearly visible, although a component with a wavelength of 0.6 mm was included in the signal. Apparently a stronger long-wave component tends to hide the short-wave components.

Figure 4.15 shows the autospectra of the synthetic paper profile and of the random signal. The autospectrum of the synthetic profile is similar to the autospectrum of an actual paper surface, shown in Figure 4.12.

The two sine wave components added in the profile show up in the autospectrum as peaks at a and b. Peak a is situated at a wavelength of 0.6 mm whereas peak b appears at a wavelength of slightly less than 2 mm rather than at its exact value of 4 mm. This shift in the position of the peak is a drawback of the transformation from a frequency spectrum to the wavelength spectrum. The conversion is highly dependent on the number of lags selected in the calculation of the autospectrum.

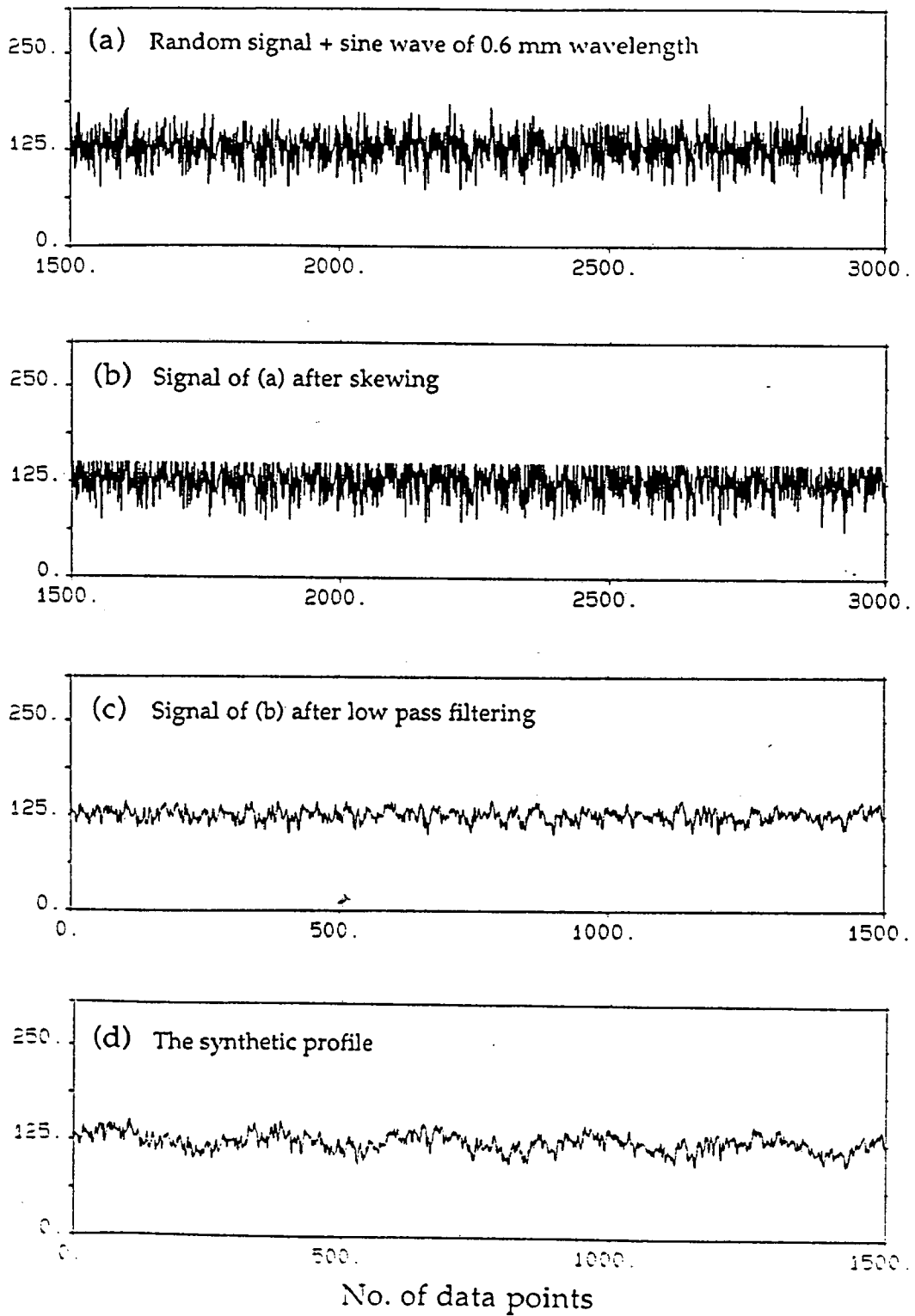


Figure 4.13 Development of the synthetic paper profile showing its intermediate stages

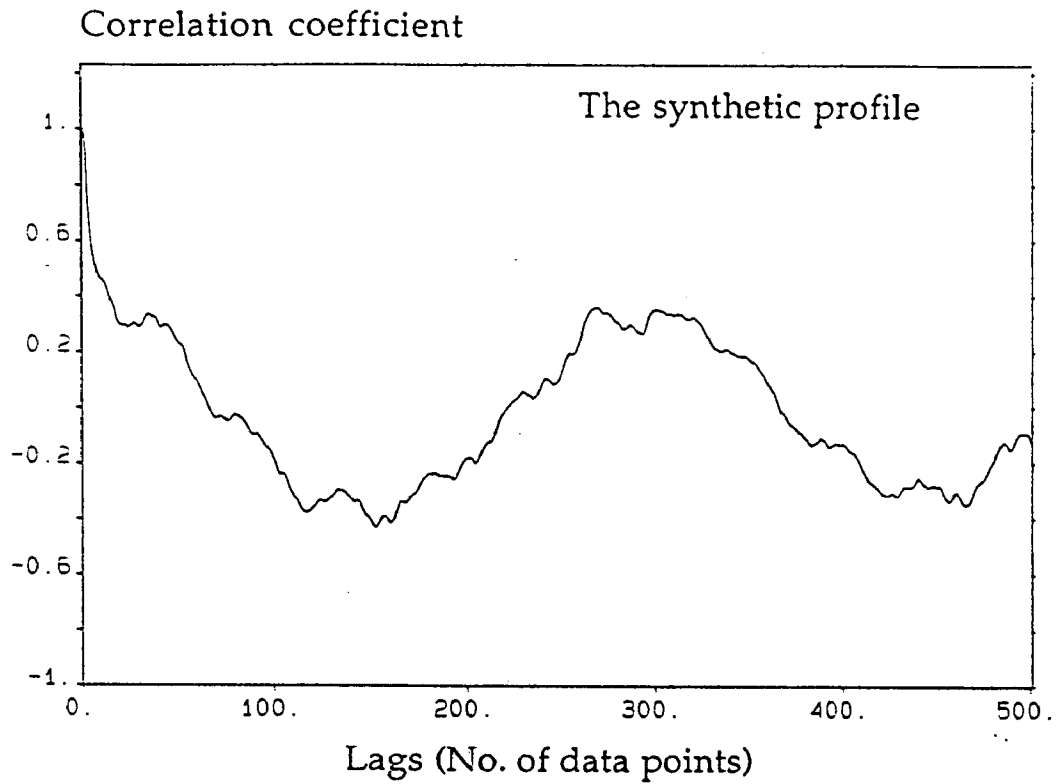


Figure 4.14 Autocorrelation function of the synthetic paper profile

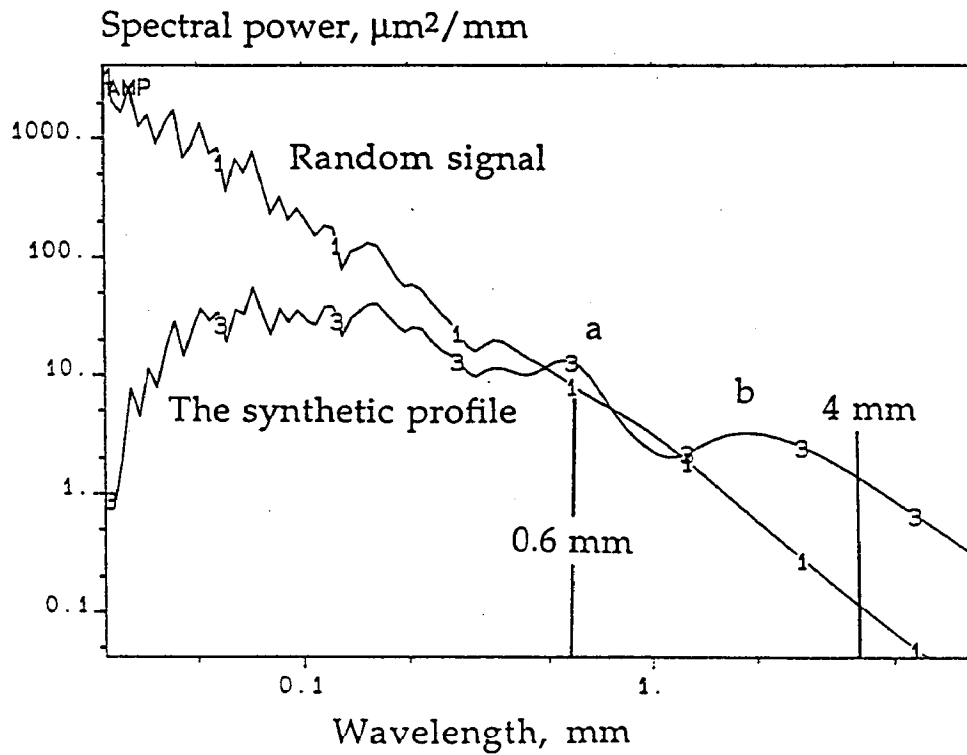


Figure 4.15 Autospectra of the synthetic paper profile and of the random signal

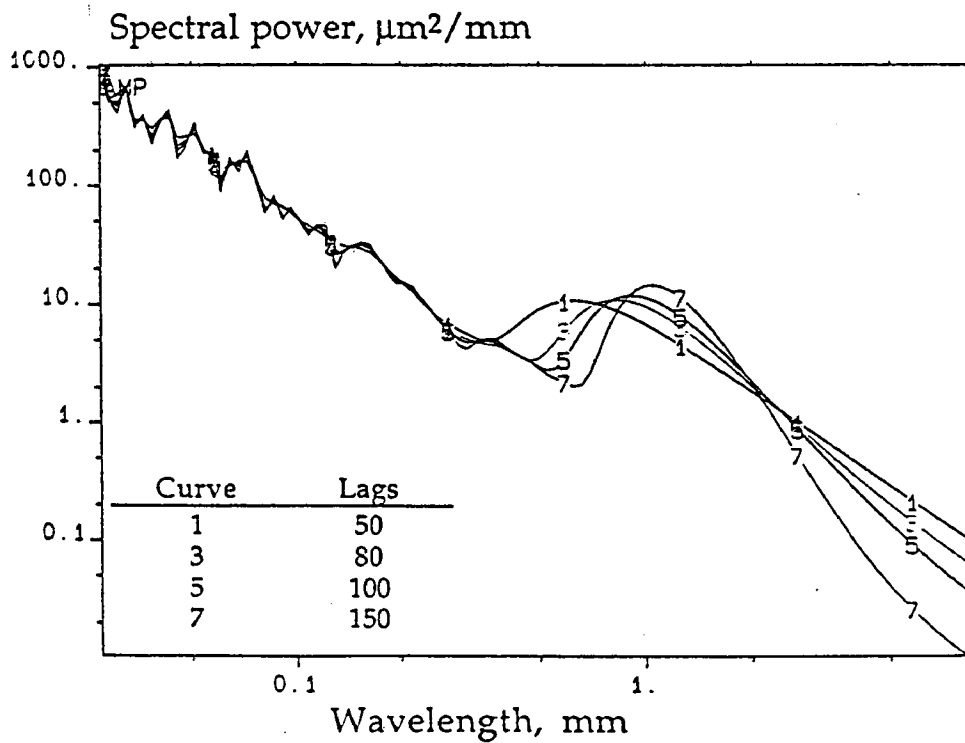
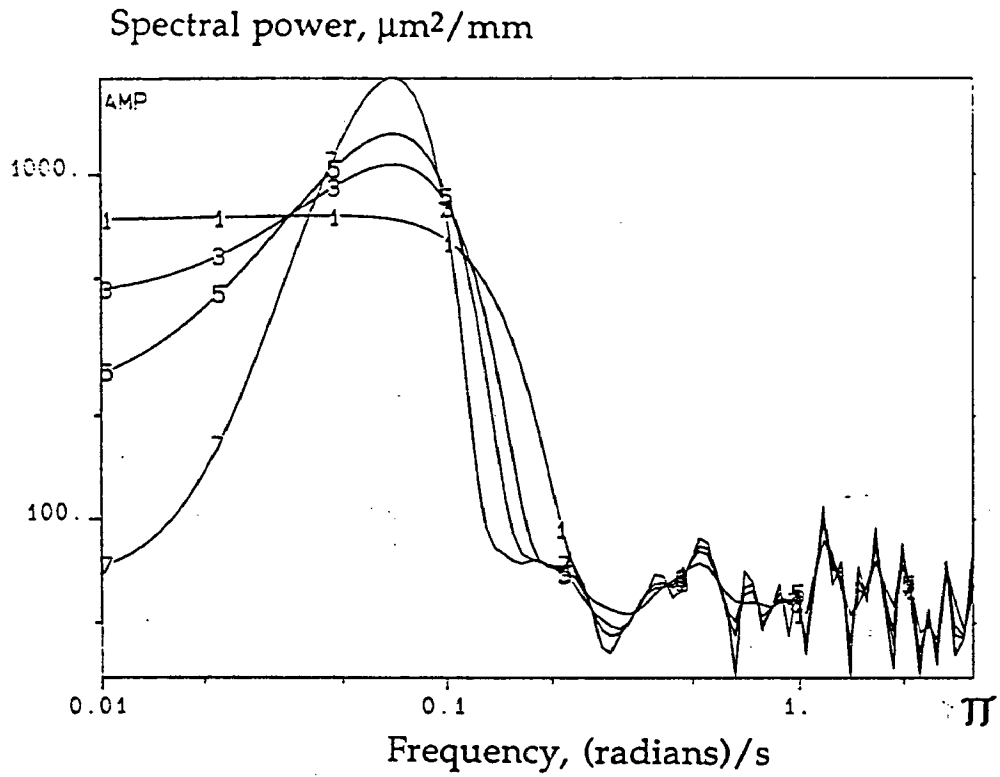


Figure 4.16 Effect of number of total lags on the location of a peak in the autospectra. The autospectra are plotted on (a) a frequency scale and (b) a wavelength scale.

The effect of number of lags on the location of the peak was separately studied for a sine wave of known wavelength. Figure 4.16 shows the autospectra of a signal generated by adding a random signal and a pure sine wave of 3 mm wavelength calculated using different values of the maximum lag from 150 points to 50 points. When plotted on a frequency scale, the autospectra for all values of lags show a peak at a frequency corresponding to a wavelength of 3 mm. On the other hand, transformation to a wavelength scale causes the peak of the sine wave to be highly displaced when the maximum number of lags was only 50. The location of the peak shifts towards its true value as the maximum number of lags increases, but increasing the lags too much also sharpens some of the insignificant peaks in the short wavelength range.

4.3 Decomposition of the Profile by Bandpass Filtration

Figure 4.17 shows the two components of the synthesized profile; one containing variations at wavelengths less than 1 mm and the other containing signal components at wavelengths greater than 1 mm. The decomposition was achieved using a moving average filtration technique.

Figure 4.18 shows the autocorrelation functions of the components shown in Figure 4.17. The two periodic components are very clearly visible from these figures at their correct wavelengths.

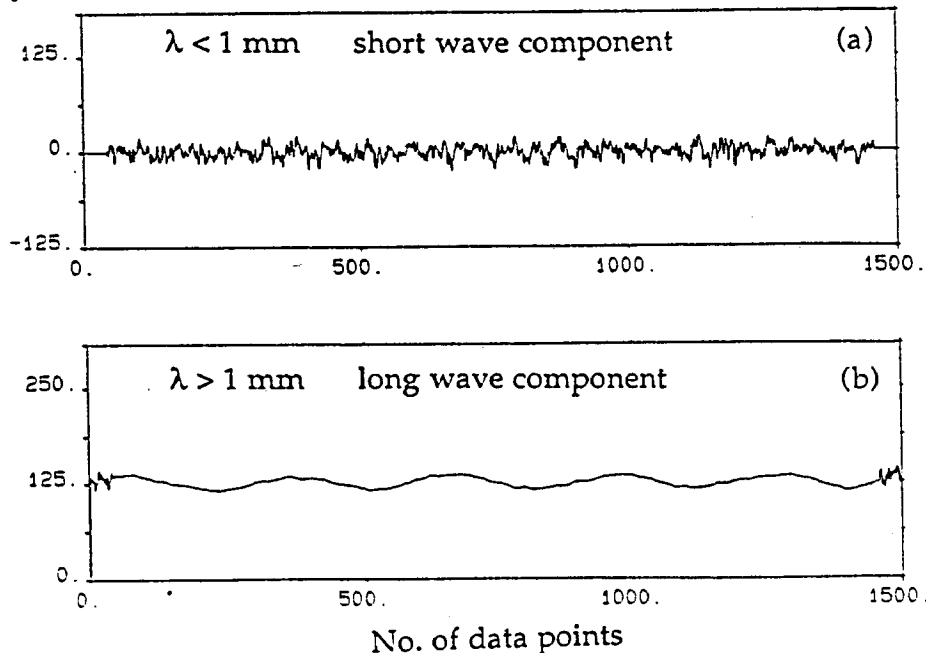


Figure 4.17 Decomposition of the synthetic profile using bandpass filtration

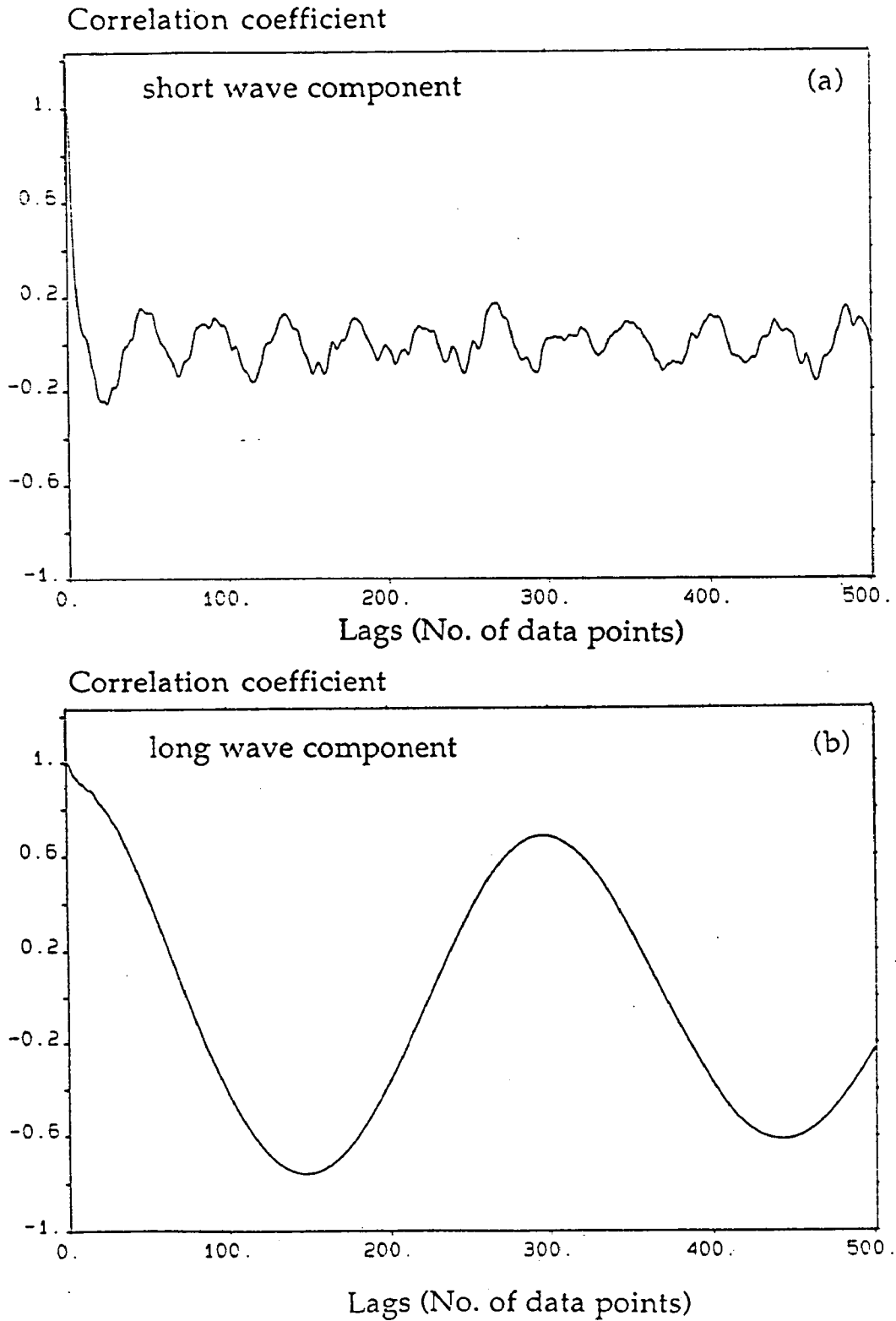


Figure 4.18 Autocorrelation functions of the longwave and the shortwave components of the synthetic profile

Figure 4.19 shows the autocorrelation function of the profile component before the addition of the longwave component (Figure 4.13c). The autocorrelation function of this signal is almost identical to the autocorrelation function obtained for the decomposed profile, which confirms that the moving average filtration method here used to decompose a profile into its components is accurate with regard to periodic components in the profile.

Figure 4.20 shows the components of a real paper profile; one shortwave component and one longwave component (> 1 mm). Figure 4.21 presents the autocorrelation function of the shortwave component, which shows that there is some periodicity in the profile at about 0.6 mm which can be considered as a characteristic wavelength for the surface of the paper analysed. The profile should be decomposed into further components if all the periodic components are to be determined.

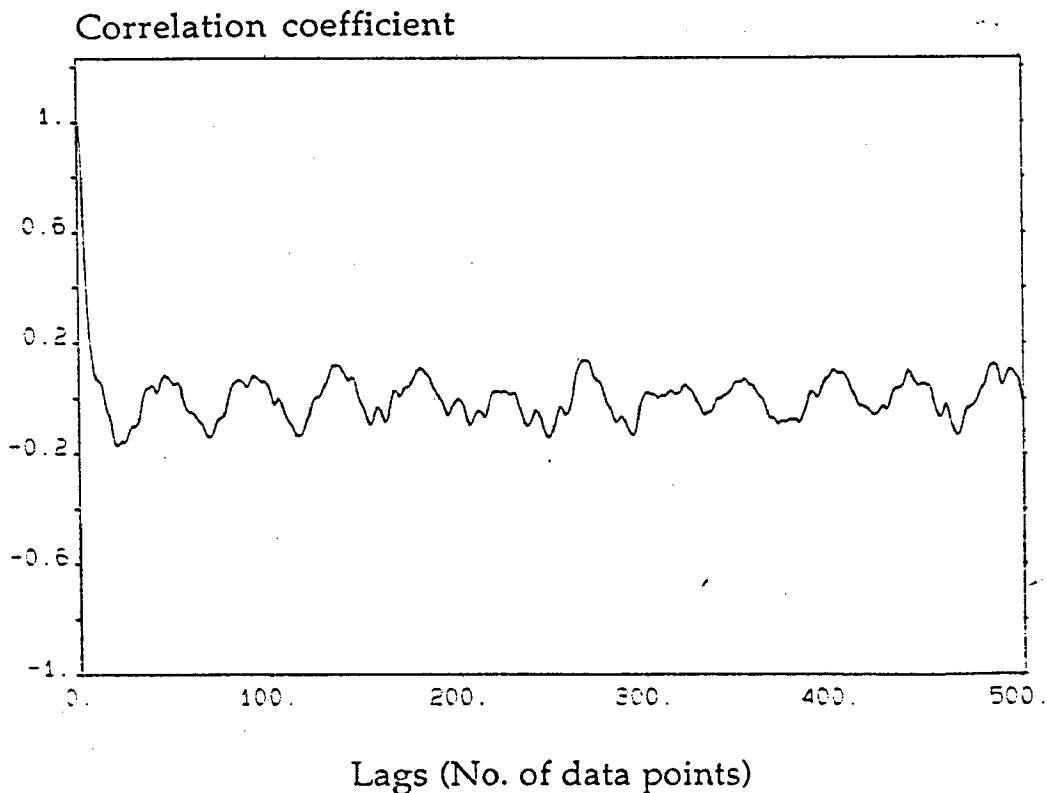


Figure 4.19 Autocorrelation function of the profile shown in Figure 4.13c

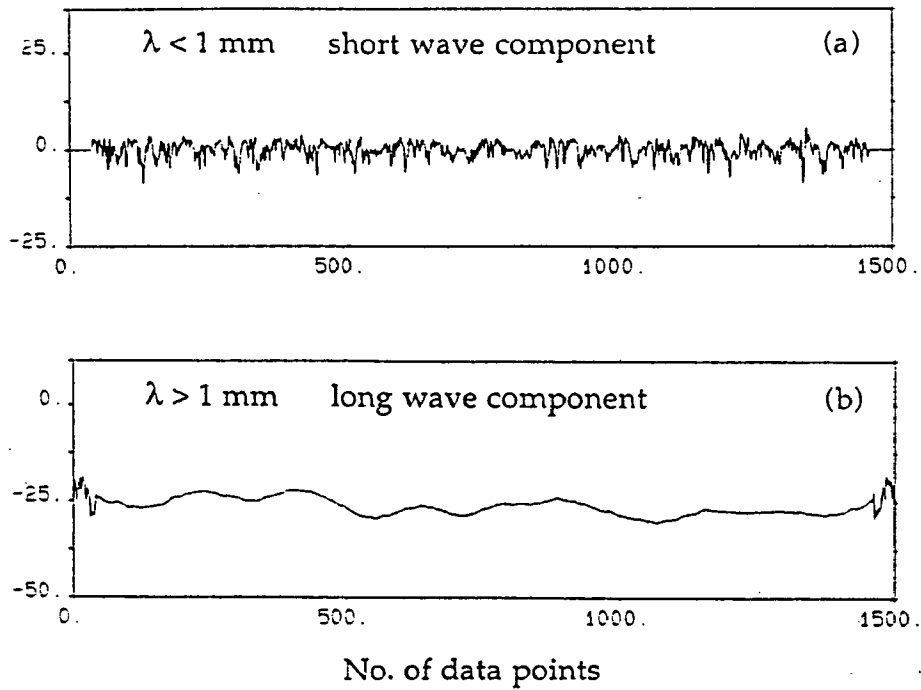


Figure 4.20 The shortwave and the longwave components of the real paper profile

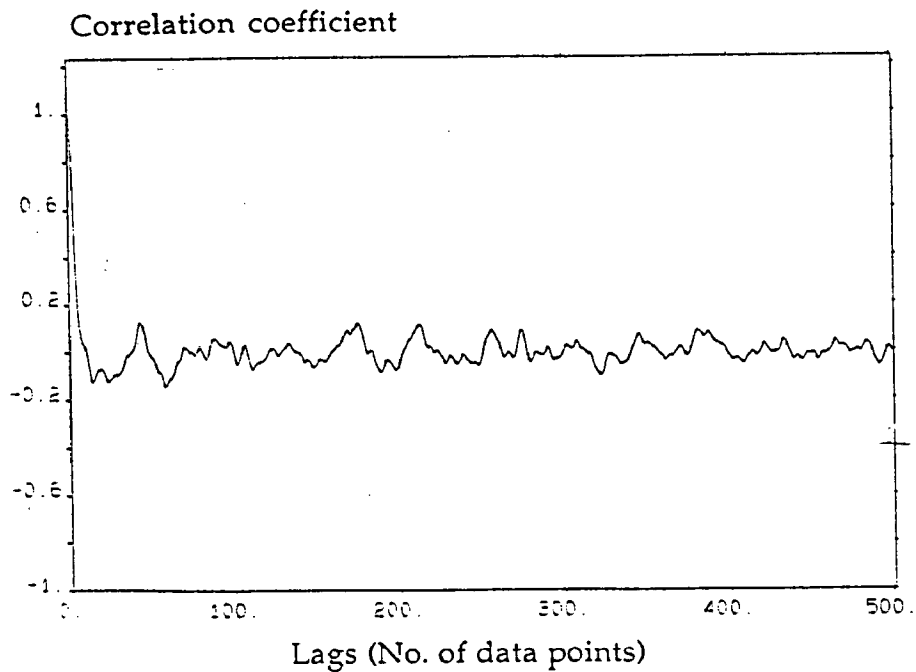


Figure 4.21 Autocorrelation function of the shortwave component of the real paper profile

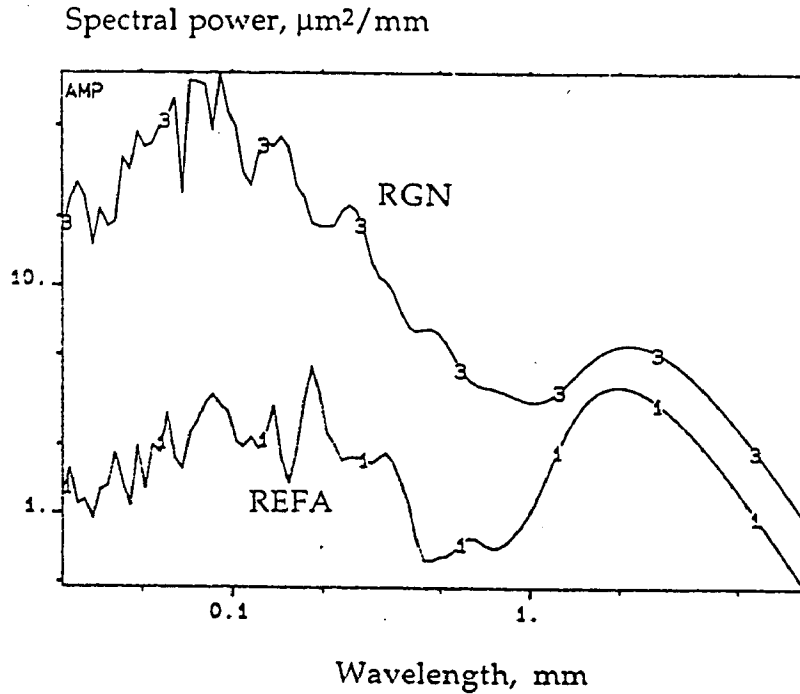


Figure 4.22 Comparison of autospectra of two paper profiles

4.4 Conclusions

1. Paper surface profiles contain random variations and often periodic variations superimposed thereon. Some of the predominant wavelengths in a surface profile must have arisen due to characteristic sizes of the furnish components or to features of specific process steps.
2. The contribution of short wavelength variations ($\lambda < 100 \mu\text{m}$) to the total variance in profiles is much less than that in a random profile, presumably because of the finite size of fiber and other furnish components.
3. The autospectrum function gives the distribution of the total variance of the profile data in its various wavelength bands. In general, smooth papers have less variance than rough papers in all the bands. (The paper REFA in Figure 4.22 was found to be smoother than the paper RGN when measured by Parker-Print-Surf roughness tester.)
4. A wavelength spectrum appears to be more informative than a frequency spectrum for the study of paper profiles because it gives a better feel of sizes of the irregularities. When a

frequency spectrum is transferred into a wavelength spectrum, however, the shape of the spectrum is distorted and the peaks of periodic components do not show up at their correct wavelengths. The distortion is dependent on the number of lags used in the calculation of the autospectrum. An increase in the number of lags brings the peaks towards their exact wavelengths but, at the same time, reduces the accuracy of the estimated power of the spectrum.

5. An autocorrelation function gives more accurate information than the wavelength spectrum about the frequency of a periodic component if its existence is very obvious.
6. A band pass filtration technique based on moving averages is fairly accurate in decomposing a profile into its components in different wavelength bands. The autocorrelation function of these components can be determined to check for periodicity in these components.

5. EFFECT OF COATING METHODS ON THE SURFACE STRUCTURE OF BOARDS

5.1 Scope

The techniques here described have been adopted to study the effect of coating methods on the surface structure of boards. Two types of boards, one MG duplex and the other MF homogeneous, were used for this study. The board samples were coated in a single stage by air-knife and blade coating methods and in two stages by combinations of air-knife and different blade-coating techniques. The coated samples were subsequently calendered and brushed.

Surface profiles were recorded to follow the development of the surface structure through these stages. The autospectra of the profiles were calculated to show the spatial distribution of the surface roughness after each stage, and the variance was also divided into its components in four bands by moving average filtration methods.

5.2 Experimental

The boards were coated in a pilot-coater in cooperation between STFI and KCL (Aschan et al, 1980). The MG duplex board was called "P" and the MF homogeneous board was called "I". Samples of these

boards were coated with clay to a coat weight of 20 g/m² by air-knife and bent-blade coating methods. Samples of board P were coated in two stages using bent-blade + air-knife, normal-blade + air-knife and normal-blade + bent-blade combinations, the coat weight applied at each stage being 10 g/m² so that the total was still 20 g/m². The type and concentration of the binder (17 parts/100 parts pigment) was mainly the same for all the coatings. The values of Parker-Print-Surf roughness at clamping pressure of 1 MPa, (PPS 10), and of 75° (Tappi) gloss for the samples studied are given in Table 4.2.

Surface profiles of these samples were recorded by the Perthometer profiler. Three profiles, each 20.25 mm long consisting of 1500 values at a displacement of 13.5 µm, were recorded on each sample. Mean values of autospectra determined for each profile are reported. Similarly, the bandpass filtration technique was used to determine the variance in four bands up to 1 mm wavelength for each profile and the mean of three values for each sample is reported.

Table 4.2 Parker-Print-Surf roughness and Tappi gloss value

Board	Type of coating	PPS(10)	75° Gloss
P	Base	3.35	14.5
MG	Air knife coated	2.50	24.7
Duplex	Air knife coated, calendered	2.03	37.9
	Air knife coated, calendered, brushed	1.98	45.8
	Bent blade coated	1.97	27.8
	Bent blade coated, calendered	1.62	41.7
	Bent blade coated, calendered, brushed	1.43	55.4
	Bent blade - Air knife coated	1.31	36.7
	Normal blade-Air knife coated	1.46	37.3
	Normal blade-Bent blade coated	1.46	31.5
	I	Base	5.82
MF	Bent blade coated	4.58	20.5
Homogeneous	Bent blade coated, calendered	3.82	22.0
	Bent blade coated, brushed	3.65	39.4

5.3 Results and Discussion

A plot of the profile recorded on the base board P is shown in Figure 4.23. The long-wave oscillation visible in the profile is probably due to flocs or thickness variations rather than to a roughness variation as such. Variations at shorter wavelengths up to about 1 mm are probably the type of roughness related to the surface of the board to which the printing forme or cylinder is sensitive and are responsible for the inability of the forme to achieve perfect contact with the paper. Variations with wavelengths longer than 1 mm were therefore removed by moving average filtration methods and the short-wave component is shown in profile b.

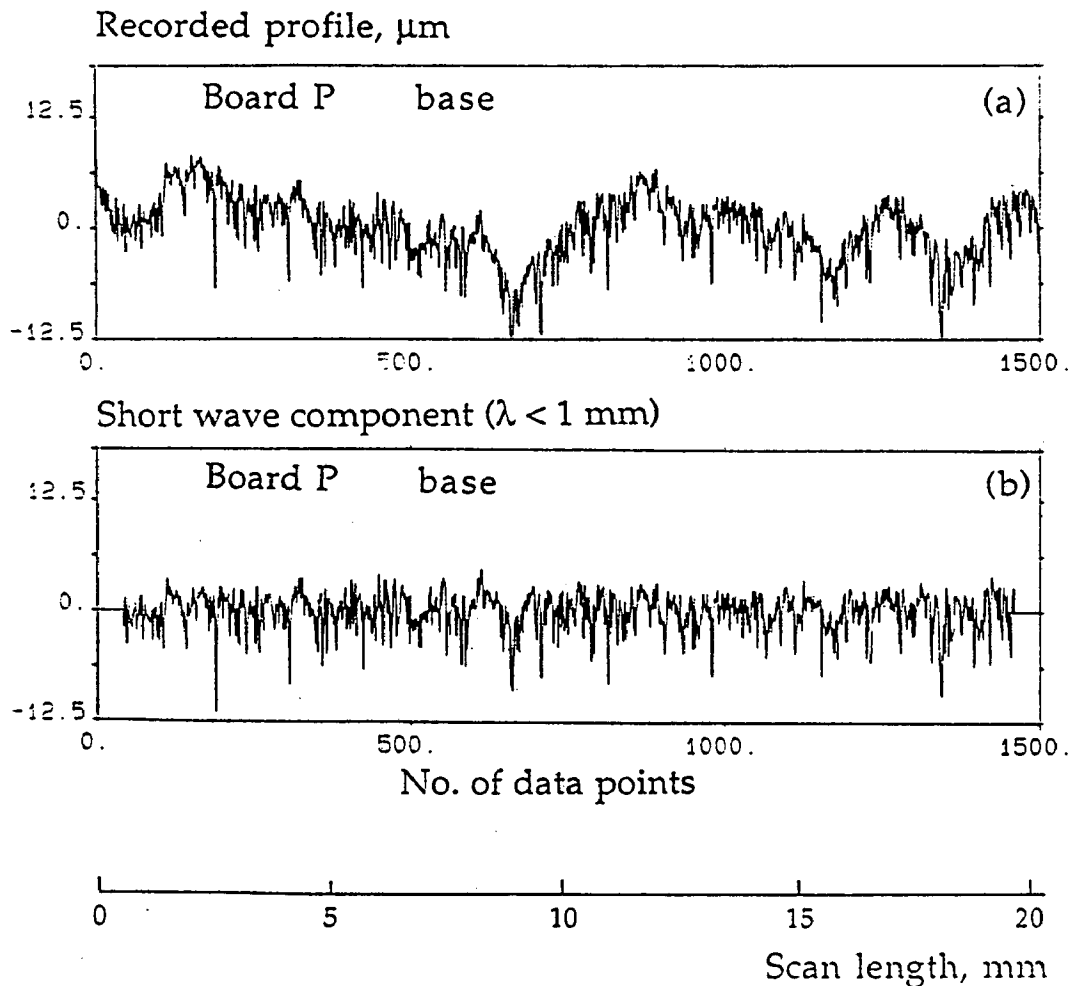


Figure 4.23 Plots of surface profile of board P (a) the total profile (b) the profile after filtering off the longwave components ($\lambda > 1 \text{ mm}$)

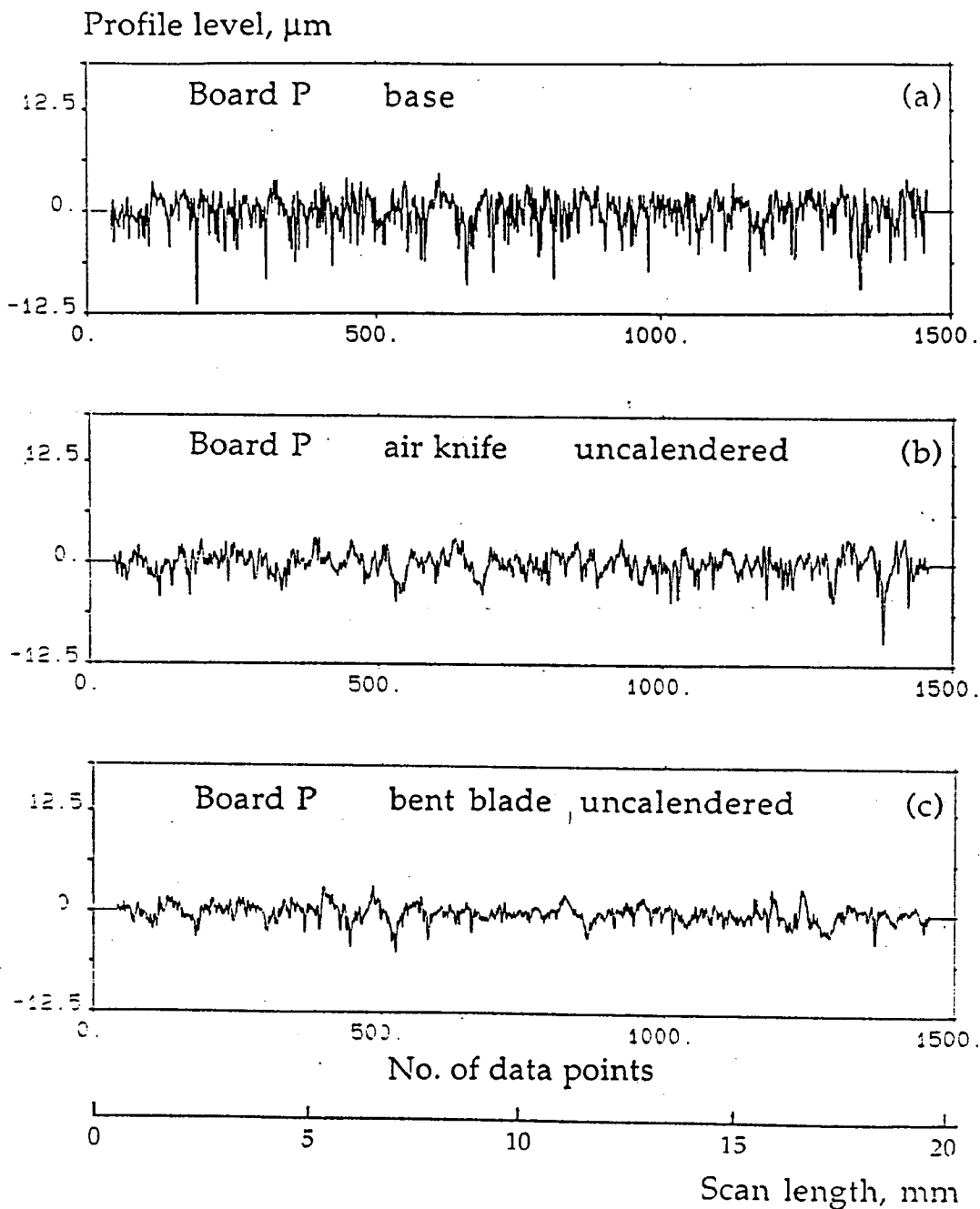


Figure 4.24 Surface profiles of air-knife coated and bent-blade coated board P

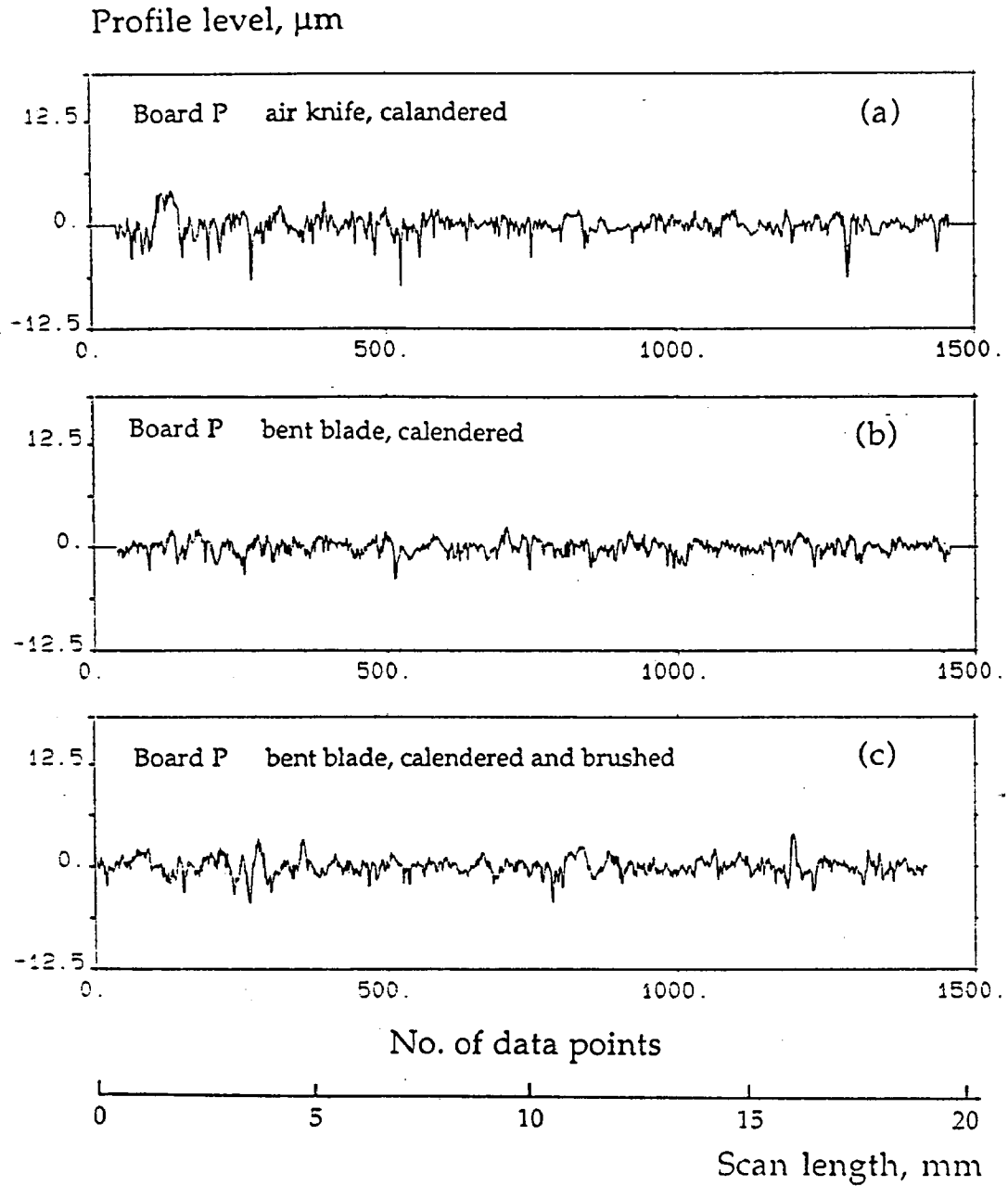


Figure 4.25 Effect of calendering on the surface profiles of air-knife coated and bent blade coated boards P

The effect of coating on the roughness component of the profile of board P is shown in Figure 4.24. Profile a shows the surface after air-knife coating and profile b that after bent-blade coating. It can be seen that the air-knife coater results in a reduction of variance of the profile, although the general profile of the surface remains similar to that of the base board. The bent-blade coater is able to fill up the narrow deep cavities better than the air-knife coater and produces a better smoothing effect.

Figure 4.25 shows the effect of calendering on the board coated by the air-knife and bent-blade processes. Calendering leads to a further reduction of the amplitude of the variations but it affects the peaks of the surface topography more than the cavities and leads to a skewed distribution of the surface. The profile for bent-blade coated board is less skewed because of the better filling of the cavities by the coating colour. Profile c shows the surface after brushing of the bent-blade coated and calendered board. The brushing does not seem to show any significant reduction in the amplitude variations.

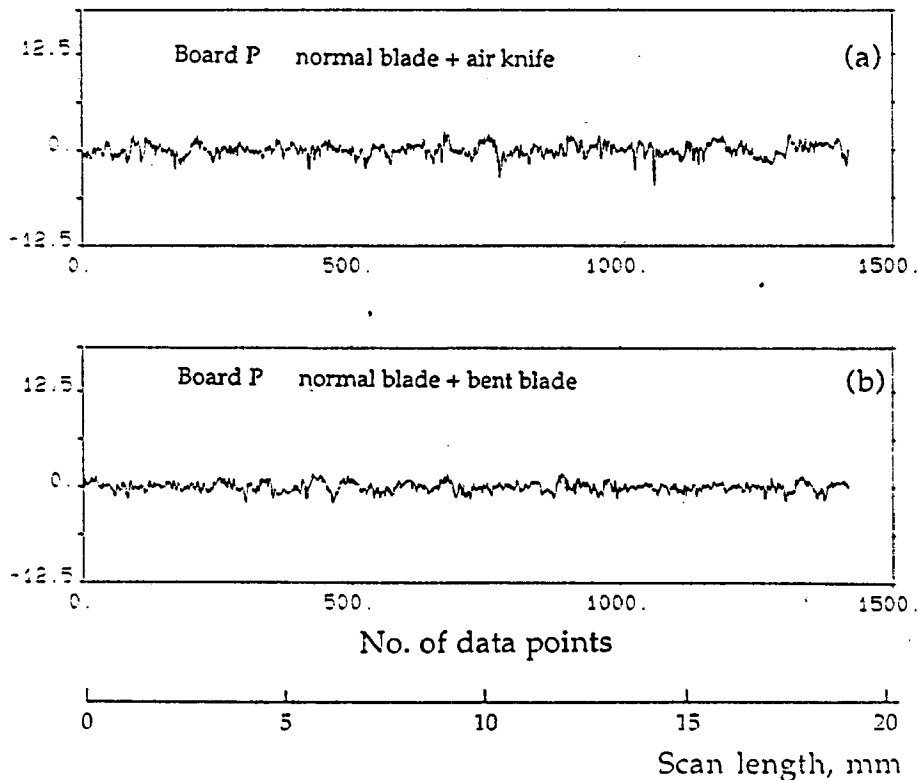


Figure 4.26 Surface profiles of board P after two-stage coating

The effect of two-stage coating is shown in Figure 4.26. Two-stage coating in general produces a smoother surface than a single-stage coating for the same coat weight. Bent-blade and air-knife appear to be the best combination since the bent blade fills the deep narrow cavities and the air knife levels up the surface, finally filling the wider valleys.

Figures 4.27 and 4.28 show how these effects appear in the autospectra. Autospectra of the base board, air-knife coated and bent-blade coated boards are plotted in Figure 4.27. The straight line marked 1 (which has a slope of -2) indicates an idealized random series. The power of the profiles decreases on coating in the region up to a wavelength of 1 mm. In the longer wavelength region the profiles of coated boards, curves 7 and 5, show more variation than that of the uncoated board, curve 3, confirming that these variations arise due to waviness of the surface rather than because of its roughness. The bent-blade coated surface shows less variation than the air-knife coated surface below a wavelength of 1 mm.

The autospectra in Figure 4.28 show the character of the base board and of the board after air-knife coating and then subsequent calendering and brushing. The effect of coating is greater than the effect of subsequent calendering. There is little difference between the spectra of the surface before and after brushing; very little reduction in the power is visible at the low wavelength end (near 0.05 mm).

Figure 4.29 shows the surface profiles of board I. Profile (a) is for the base board, profile (b) is for the bent-blade coated board and profile (c) is for the bent-blade coated and calendered surface. The base board I has a rougher surface than base board P, and even the most efficient bent-blade coating process could not level the surface as much as for the board P. This effect has been shown in terms of autospectra in Figure 4.30. Curves 3 and 7 show the base board and bent-blade coated surfaces of board I and curves 5 and 9 show the base board and bent-blade coated surfaces for board P. Bent-blade coating has a significant effect in the short wavelength region and this is probably responsible for the marked improvement in the gloss of the coated surfaces.

Figure 4.31 shows the autospectra of three board surfaces which had roughly the same Parker-Print-Surf roughness value at clamping pressure of 1 MPa.

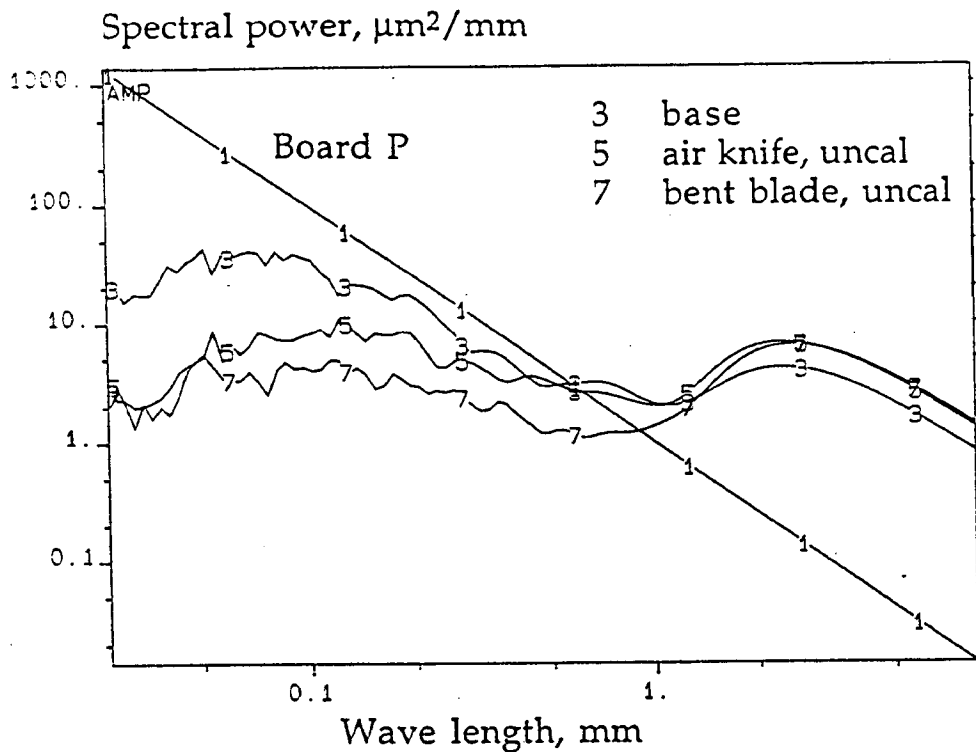


Figure 4.27 The autospectra of the base board, the air-knife coated and the bent-blade coated board P

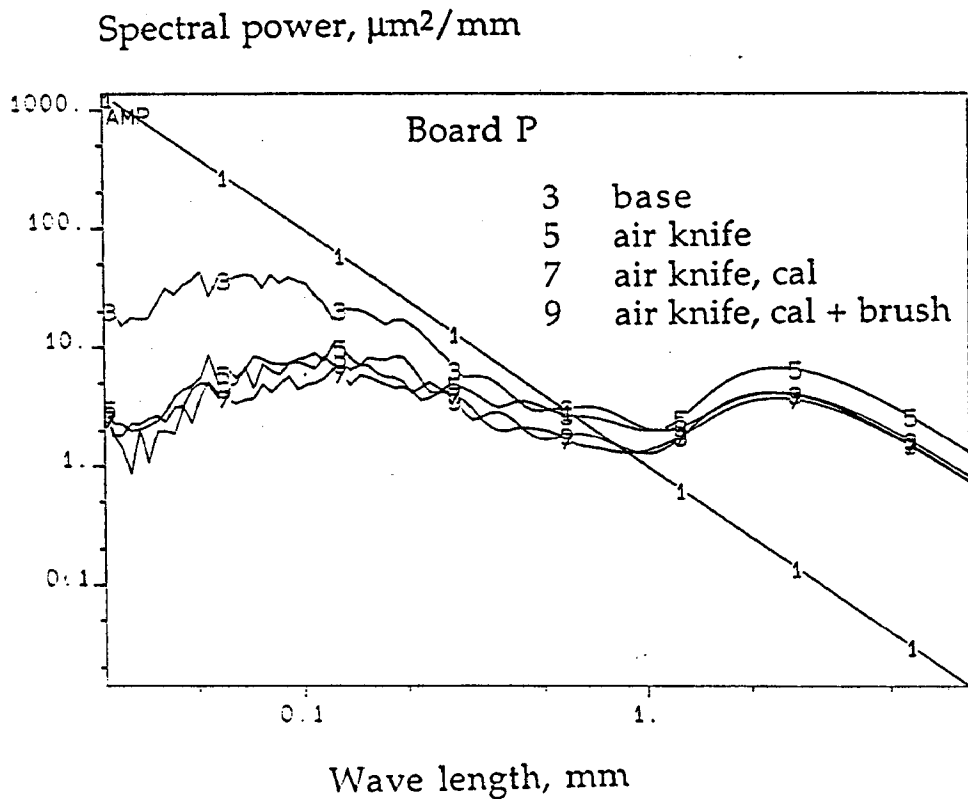


Figure 4.28 The autospectra showing the effect of air-knife coating and subsequent calendering and brushing on the surface profile of board P

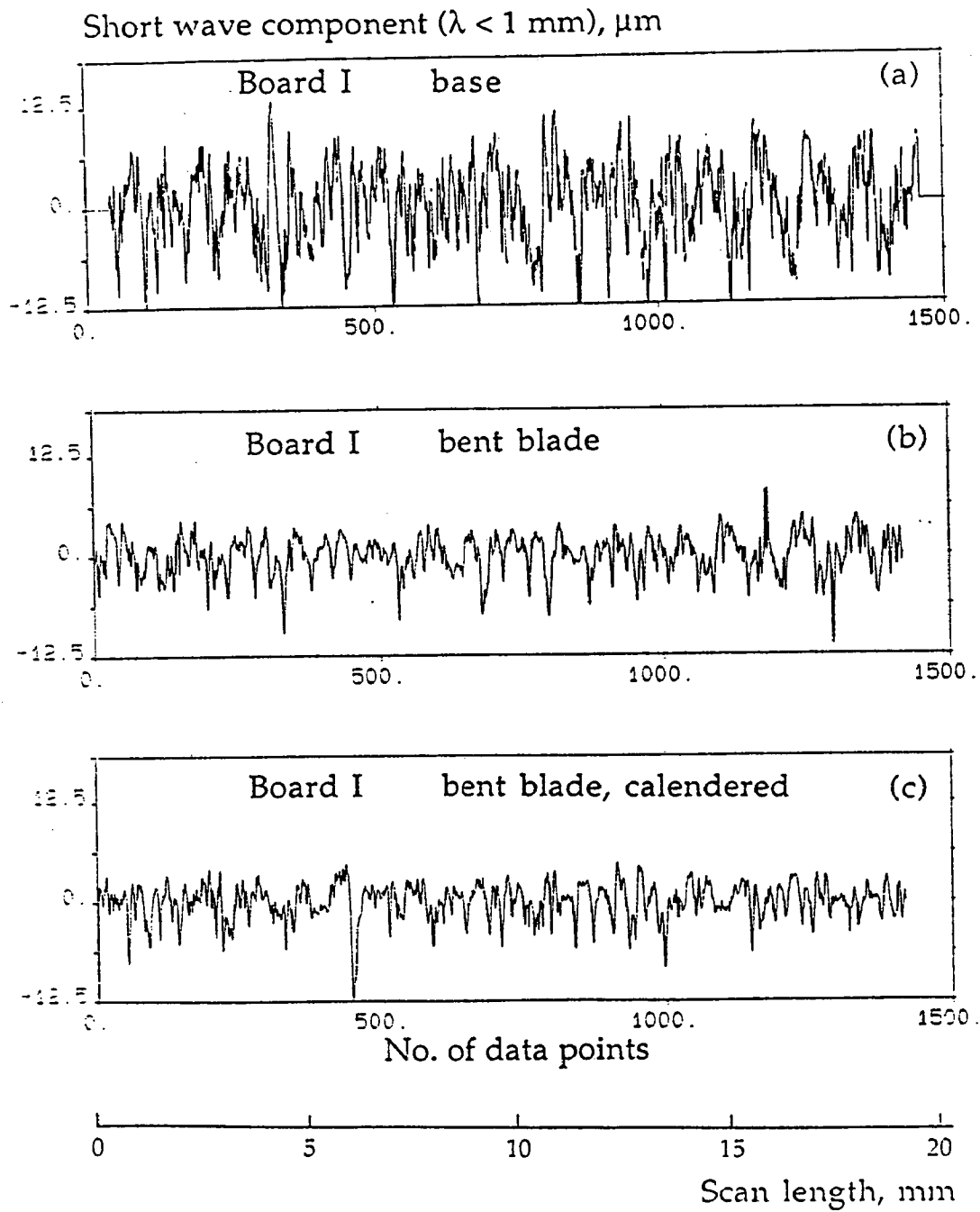


Figure 4.29 Surface profiles of board I
 (a) base board (b) bent-blade coated
 (c) bent-blade coated and calendered

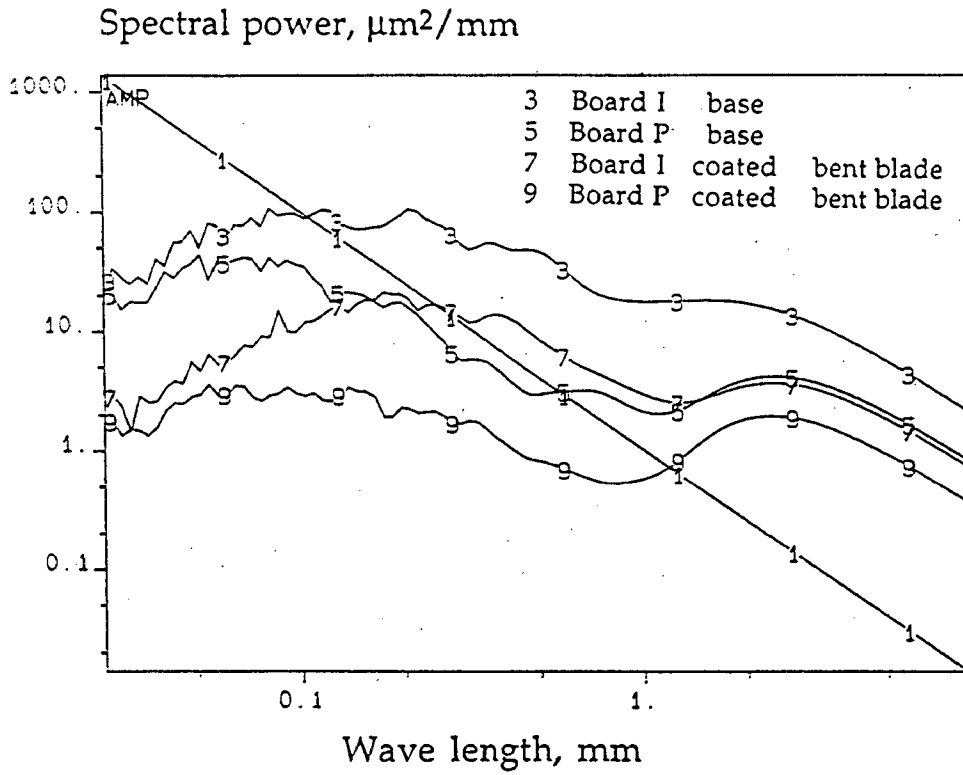


Figure 4.30 Effect on the autospectra of bent-blade coating on two boards

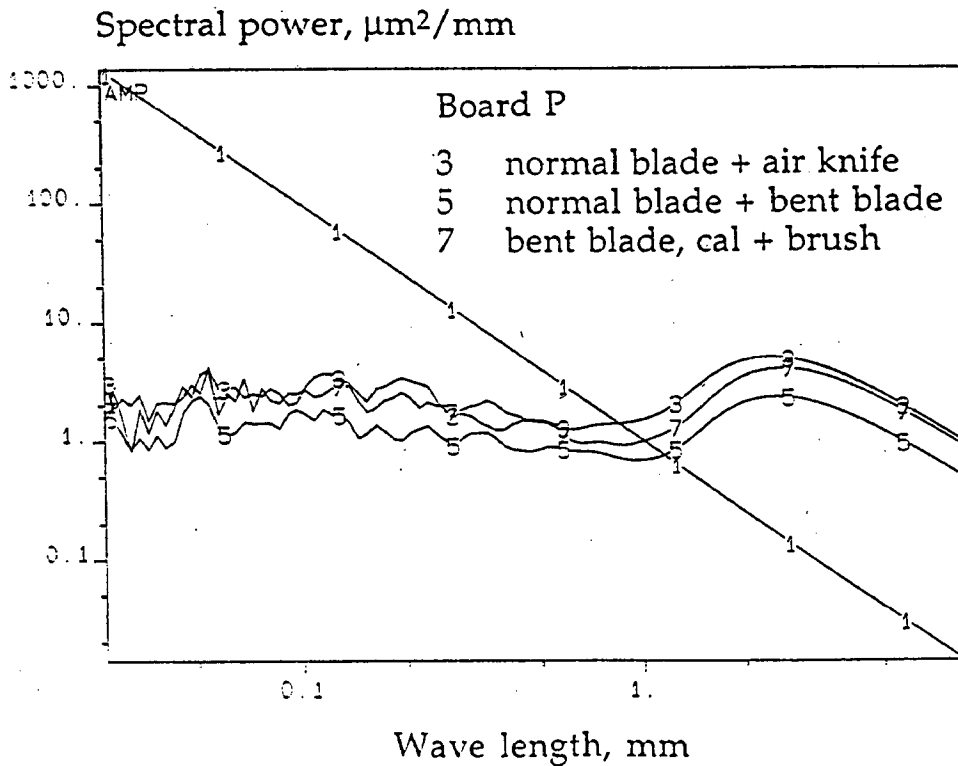


Figure 4.31 Autospectra of three boards having nearly the same PPS-value

6. PROBABILITY DENSITY FUNCTION OF SURFACE PROFILES

6.1 Scope

The autospectra show the spatial distribution of variance of the profiles but they do not account for the nature of the distribution of the profile heights about their mean. There is a tendency to assume this distribution to be normal (Gaussian). In this study of surface profiles of papers and boards of various grades, it was however observed that most profiles deviate from Gaussian behaviour and show skewness in their distribution. In such cases the autospectra do not completely characterize the surface structure and probability density analysis of the profile data is necessary. The nature of the probability density function of the roughness component of a profile and its dependence on coating and calendering is discussed in this section.

6.2 Determination of Probability Density Functions

Since the information about the roughness of the surface is contained only in short-wave components, the probability density functions were determined for the profiles after filtering off the components with wavelengths longer than 1 mm.

The filtered profile data were transformed to a zero mean and unit standard deviation. The probability density function was calculated from these data using equations [4.20] and [4.21]. The probability densities were calculated between $\beta = 3$ and $\alpha = -3$, the data being divided into 100 classes ($K = 100$). The minimum number of class intervals required for a sample size of 1500 data points is 35 to ensure that discrepancy between the calculated probability density and its expected value in any class is significant at a probability level of less than 5 per cent (Bendat and Piersol, 1958).

6.3 Results and Discussion

Figure 4.32 shows the effect of air-knife coating and subsequent calendering on the probability density functions of the profiles of board I. The uncoated board has a positive skewness i.e. the profile data were generally found slightly above the mean line with occasional data falling away from the mean in the negative

direction. On coating the board, the skewness was reduced but subsequent calendering tended to introduce a skewness again.

Since these distributions are expressed in relation to unit standard deviation, they show only the pattern of and not the magnitude of deviations about the mean.

A study of similar profiles shows that this type of analysis can reveal differences in the effects of, for example, bent-blade and air-knife coating or calendering and brushing.

PROBABILITY DENSITY FUNCTION

BOARD I

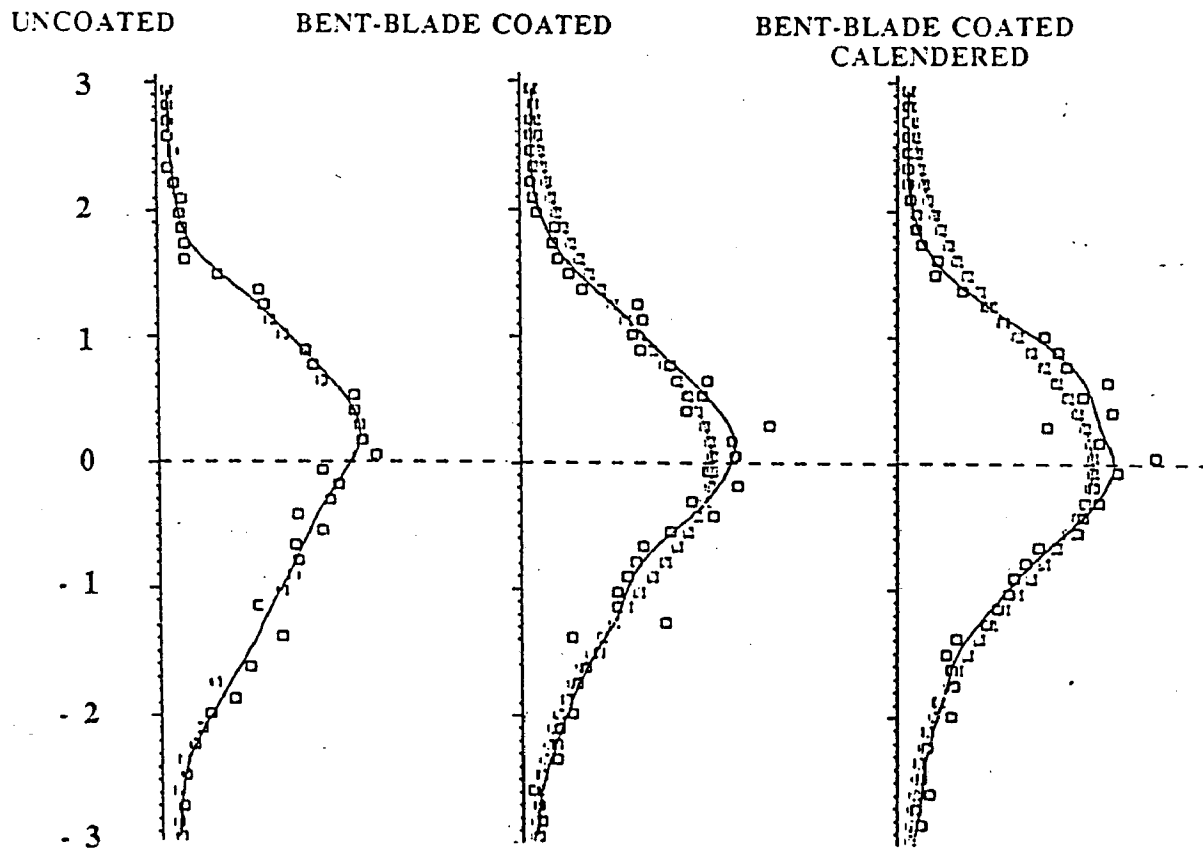


Figure 4.32 Effect of air-knife coating and subsequent calendering on the probability density functions of profiles of board P. A Gaussian distribution is shown in the background

CHAPTER V

EFFECT OF TYPE OF MECHANICAL PULP ON SURFACE PROPERTIES OF HANDSHEETS

1. SCOPE

The surface smoothness and compressibility of paper are highly dependent on the type of pulp from which it is made. It has been reported (Bradway, 1973) that the smoothness-bulk relationship is more strongly influenced by the type of pulp than by any of the papermaking processes. The present work was undertaken to study the effect of different mechanical pulps, which are the major furnish constituents of newsprint and magazine grades of paper, on the smoothness of handsheets made under standard conditions. The effects of wet pressing against a gloss plate and calendering on the smoothness-bulk relationship have been investigated. The study has also involved a comparison of various methods of surface characterization including those which have been developed in the present work and described in chapters II - IV.

It is accepted that it is meaningful to characterize pulps with respect to their surface properties in this way, since the degree of conformability of the pulp to the gloss plate in the sheet-making process does affect the roughness of the sheet and is affected by the properties of the fibers and by unit operations in the pulping process.

2. EXPERIMENTAL

2.1 Pulps

Handsheets were prepared from three different pulps, viz. mill samples intended for newsprint of stone groundwood (SGW) and thermomechanical pulp (TMP), and a chemithermomechanical pulp (CTMP) prepared in a pilot refiner. The pulps were hot disintegrated at 85 °C with a total of 3000 revolutions in a laboratory disintegrator. The pulp samples were analysed for freeness and other properties in the STFI optical pulp analysis system. The characteristics of the pulps are given in Table 5.1.

Table 5.1 Characteristics of Pulps

	SGW	TMP	CTMP
Freeness, CSF	94	143	82
Mean fiber length, mm	1.48	1.86	1.66
Mean fiber diameter, μm	8.53	9.75	9.73
Coarse fiber fraction, %	45.1	58.7	51.5
Middle fiber fraction, %	19.6	14.1	16.2
Fines, %	35.3	27.2	32.3

2.2 Sheet Formation

The sheets were made according to the standard procedure described in SCAN-C 26:76 in a Finnish sheet former of square cross-section, 165 mm x 165 mm. The white water was recirculated so that an equilibrium white water composition was established for each grammage. For each pulp, the preparation of handsheets was started at the highest grammage and then changed to lower grammages. The first 10 sheets were discarded to obtain a constant white water composition. The next 10 to 20 sheets were saved for subsequent evaluation. The same white water was used for the preparation of the sheets of lower grammage, but 6 sheets were discarded after every grammage change to establish new a white water equilibrium.

The sheets were couched and then pressed and dried against gloss plates in air at 50 % RH and 23 °C.

2.3 Wet Pressing, Calendering

Most of the sheets were wet pressed against the gloss plate at 400 kPa in accordance with SCAN-C 26:76 but half the sheets of 60 g/m² for each type of pulp were pressed at a higher pressure of 800 kPa to see the effect of wet pressing on the smoothness of these sheets. Half the sheets of each pulp at each grammage and wet pressing condition were calendered in a laboratory calender in a steel-steel nip at a linear load of about 50 kN/m.

2.4 Determination of Sheet Properties

The following properties were determined on the glossy side of the hand sheets.

- a. Parker-Print-Surf roughness was determined as a function of clamping pressure between 1 MPa and 7 MPa (Bristow 1983). The thickness of the sheet was also measured at these clamping pressures in a modified PPS-tester (Bristow, 1986).
- b. Optical contact area was measured at 2.5, 5 and 7.5 MPa by the FOGRA-KAM tester.
- c. Surface characteristics were studied by the partial coverage printing method described in Chapter II.
- d. Autospectra of surface profiles were determined as described in Chapter IV.

The density of the handsheets was determined by dividing the grammage by their thickness. The density of the solid phase was determined by displacement of a low viscosity non-swelling oil (Bristow 1986).

3. RESULTS AND DISCUSSIONS

3.1 Parker-Print-Surf Measurements

Figure 5.1 shows the Parker-Print-Surf (PPS) roughness values plotted against the clamping pressure in the PPS instrument for the 60 g/m² handsheets of TMP, SGW and CTMP, both before and after laboratory calendering. At a clamping pressure of 1 MPa the CTMP sheet prior to calendering was slightly less rough than SGW and TMP but at higher clamping pressures the SGW and TMP sheets were slightly smoother than the CTMP, indicating that the sheets of SGW and TMP had a greater surface compressibility than the CTMP. The PPS values for all the three pulps were, however, very close to each other. After calendering, all the sheets are smoother and less compressible. The curves confirm that the sheet of SGW pulp has become the smoothest and that, as a result of its greater surface compressibility, this pulp has shown the best response to calendering.

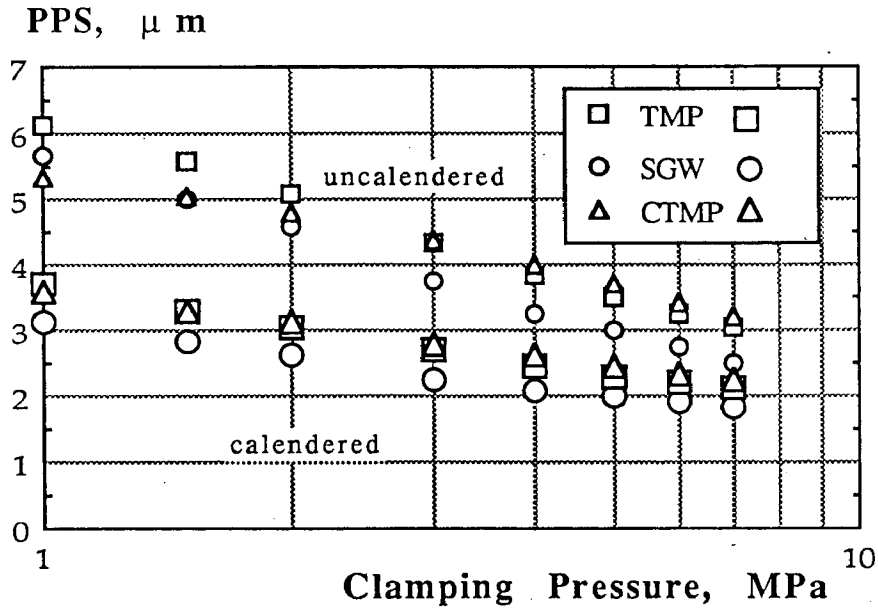


Figure 5.1 Parker-Print-Surf roughness as a function of clamping pressure (cf. Bristow 1982)
 a) handsheets after wet-pressing against a gloss plate
 b) handsheets after laboratory calendering

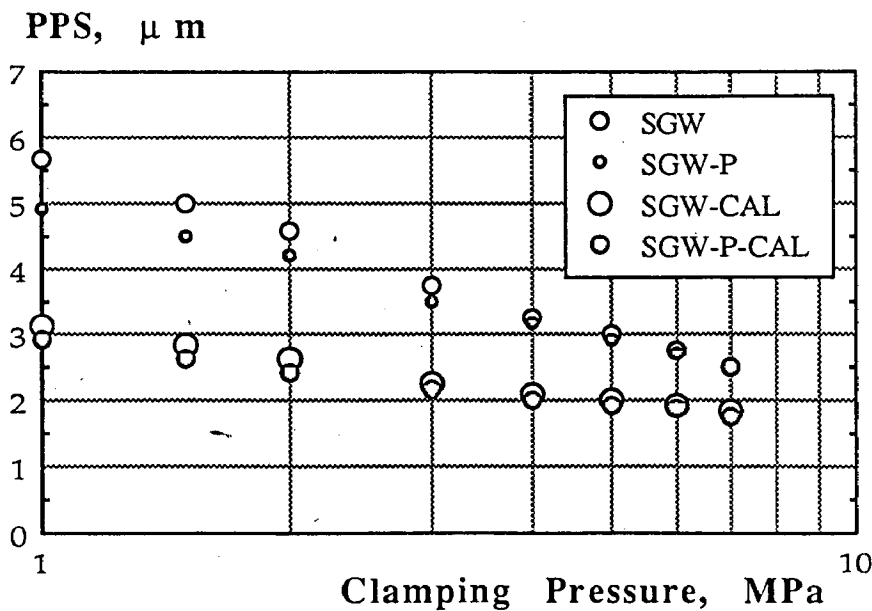


Figure 5.2 Parker-Print-Surf roughness as a function of clamping pressure showing the effect of wet-pressing and calendering on the SGW pulp

The effect on the PPS and surface compressibility of wet pressing against a gloss plate and of calendering is shown in Figure 5.2, for the SGW. The pattern of behaviour was the same for the other pulps. The wet pressing leads to a slight improvement in the smoothness at low clamping pressures but this difference diminishes at higher clamping pressures. The effect is much less than that of calendering, which leads to a significant reduction in roughness which is maintained at higher pressures also.

All the surface smoothing processes such as wet pressing and calendering result in a significant reduction in thickness of the sheet. It is therefore often more important to consider the smoothness vs thickness relationship rather than the smoothness alone since the improvement in the smoothness is generally achieved at the cost of reduced bulk. The void ratio (void volume/solid phase volume) was used instead of bulk since it eliminates effects of differences in the density of solid phases of different pulps.

Figure 5.3 shows plots of PPS against void ratio for SWG, TMP and CTMP pulps. For a given void ratio, the sheet made of SGW is smoother than that made of TMP and both the sheets of SGW and TMP are much smoother than that of CTMP. The relationship between PPS and void ratio shown in Figure 5.3 is nearly linear with the lines for all three pulps passing through the origin. The straight line relationship deviates slightly however at higher values of void ratio in the case of SGW and CTMP. The curvature of the lines gives some indication that the SGW is initially more compressible in the surface than in the bulk whereas the CTMP is initially more compressible in the bulk than in the surface.

Another reason for the deviation in the case of SGW is that there may be a slight error in the PPS measurement for bulky sheets due to transverse flow of air through the sheet as indicated by Mangin and De Grace (1984).

Figure 5.4 shows the effect of wet pressing and calendering on the compressibility of surface and void volume recorded in the modified PPS-instrument. There appears to be a more or less constant relationship between the PPS roughness and the void ratio, regardless of whether the sheet is compressed by wet pressing, calendering or pressing under the PPS measuring head. There is however a slight indication that the wet pressing alters the initial conditions prior to the PPS-testing by reducing the void ratio relatively more than the surface roughness.

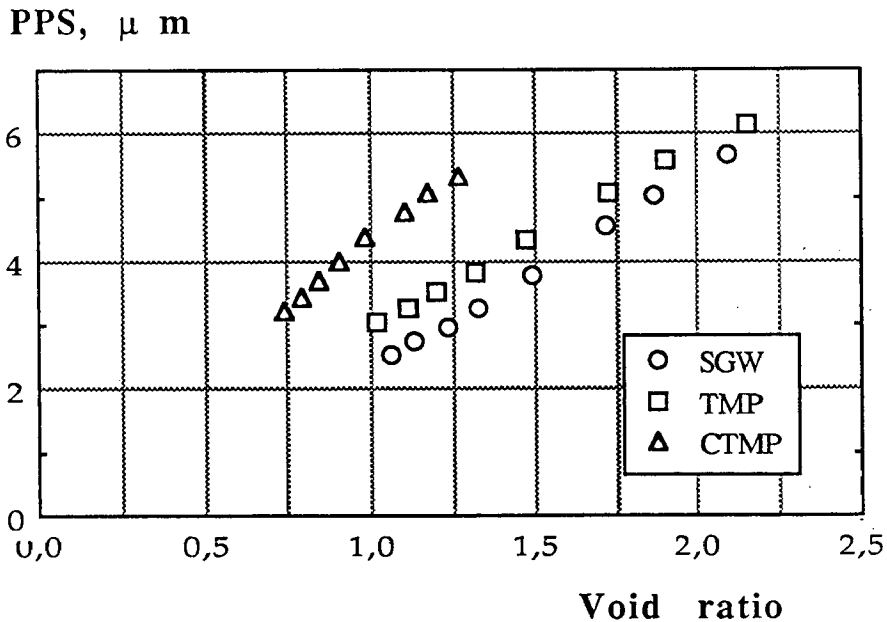


Figure 5.3 The PPS-value versus the void ratio during compression of the sheet for SGW, TMP and CTMP pulps

Figure 5.5 shows a similar relationship for the sheets of different grammage made of SGW pulp. At void ratios lower than 1.5, the PPS vs void ratio relationship is nearly the same for all grammages, but initially the PPS roughness at a given void ratio was found to be higher for higher grammage sheets than for low grammage sheets. This is perhaps due to the greater possibility for transverse air-leakage to occur in the thicker sheets.

3.2 FOGRA-KAM

The optical contact area was measured at three pressures, 2.5, 5.0 and 7.5 MPa in the FOGRA-KAM instrument. Figure 5.6 shows the FOGRA-KAM values as a function of pressure for SGW, TMP and CTMP pulps. It is interesting to note that the SGW sheets were shown to be the roughest by the FOGRA-KAM whereas they were found to be the smoothest by PPS (cf. Figure 5.1). The TMP has been found to be the most smooth of the three pulps with regard to contact fraction whereas it has the highest PPS roughness value at least at lower pressures. After extra wet pressing the SGW becomes the smoother.

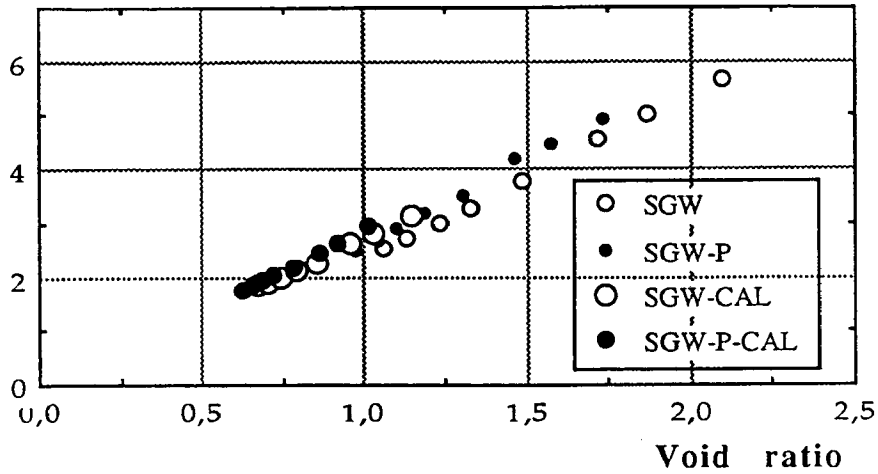
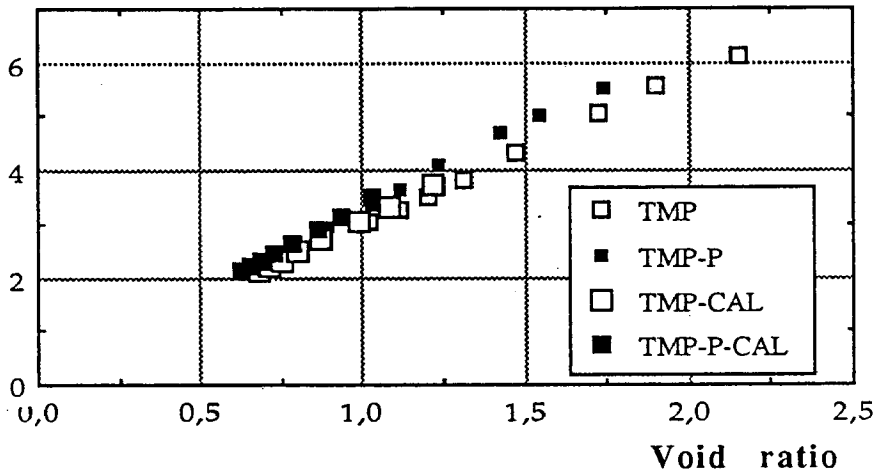
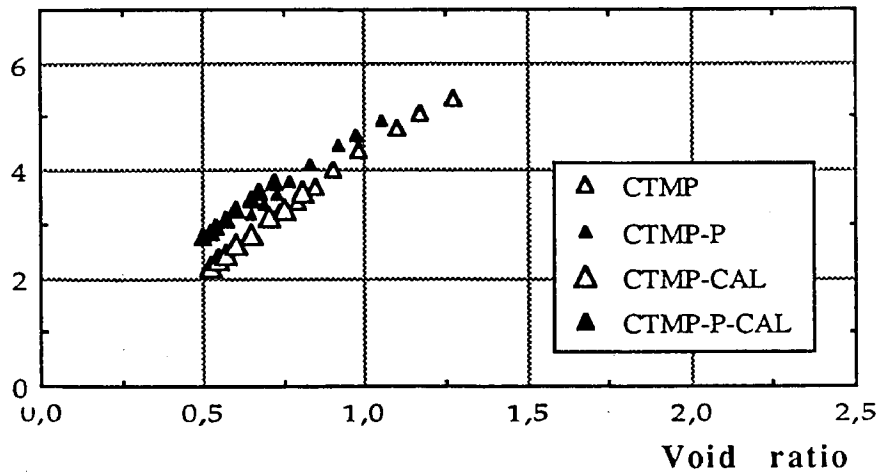
PPS, μm PPS, μm PPS, μm 

Figure 5.4 The relationship between PPS and void ratio during compression in the PPS-instrument. The graphs show for SGW, TMP and CTMP pulps how the relationship between roughness and bulk may be influenced by wet-pressing and/or calendering

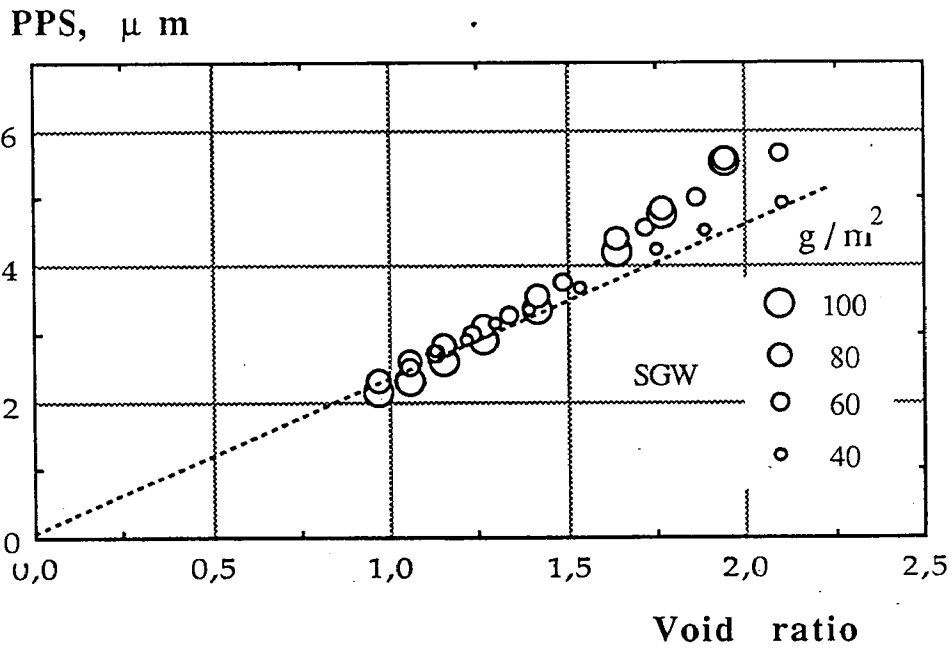


Figure 5.5 The relationship between PPS and void ratio during compression for sheets of different grammage (SGW)

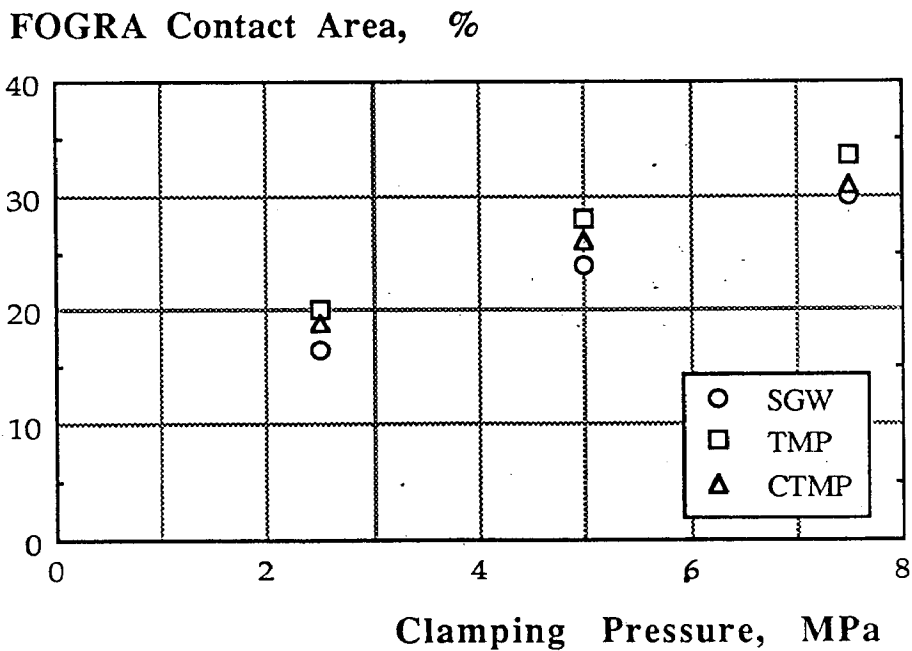


Figure 5.6 The FOGRA contact area as a function of pressure for the handsheets of SGW, TMP and CTMP pulps

3.3 Partial Coverage Printing

The sheets were evaluated by the method of partial coverage printing described in Chapter II. The values of ink requirement for 50 % coverage, $x_{0.5}$, and the slope of the curve of area versus ink on the printing disc at 50 % coverage, $(dA/dx)_{0.5}$ were calculated for the three pulps. It was observed that the effects of change of grammage of the handsheets and of wet pressing of the sheets were not significant. The values for the three pulps are shown in Table 5.2.

Table 5.2 Surface characteristics of the handsheets (60 g/m²) evaluated by the partial coverage method

	CTMP	SGW	TMP
k	0.17	0.48	0.32
n	2.48	2.12	2.04
$x_{0.5}$	2.12	1.44	1.75
$(dA/dx)_{0.5}$	0.29	0.38	0.29
Z	2.7	1.95	2.46

The amount of ink required for 50 % coverage, $x_{0.5}$, is least for SGW and most for the CTMP. These values suggest that SGW has the best printing surface among these handsheets, with TMP in second place and CTMP third.

3.4 Microcontour Ink Stains

The ink-stain data for the calendered samples are shown in Figure 5.7 for the sheets of different grammages. There is considerable variation at different grammages which may be indicative of the precision of the method but there is clearly a significant difference between the CTMP-sheets and those of SGW and TMP.

Microcontour value

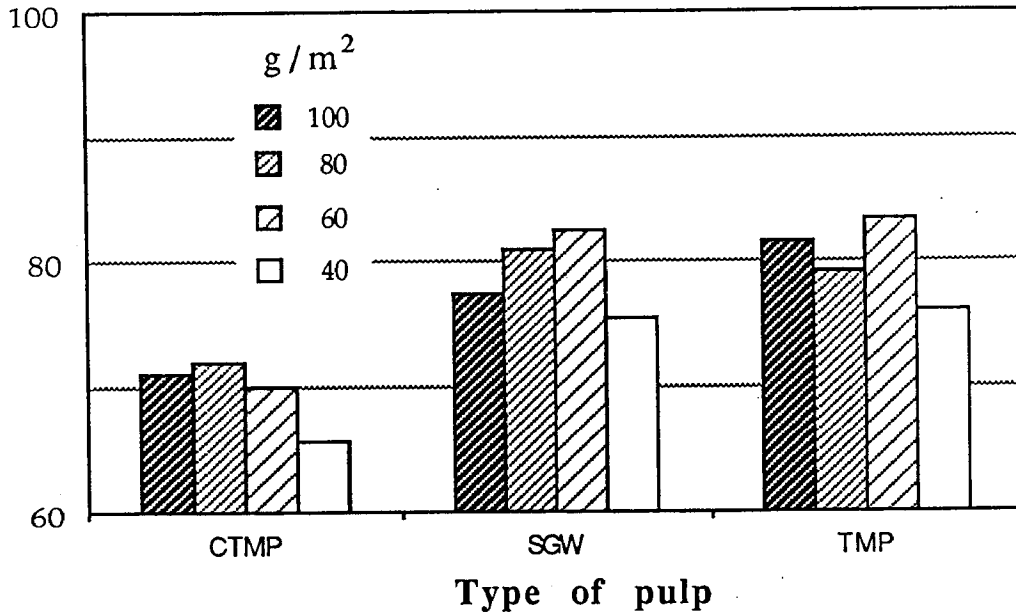


Figure 5.7 Microcontour values for sheets of the three pulps at four different grammages

3.5 Autospectra of Surface Profiles

The autospectra of the surface profiles recorded on the glossy side of the handsheets of 60 g/m² of each pulp are shown in Figure 5.8. The variance of the sheets of TMP pulp was found to be largest in all the wavelength ranges, whereas the variance values of CTMP and SGW sheets were very close to each other with CTMP having a slightly lower value than SGW. The same order was maintained when the profiles were recorded after calendering the sheets, although the variance in each category was of course less than that of the uncalendered sheets.

Figure 5.9 shows the effect of wet pressing and calendering on the autospectra of the SGW handsheets. The wet pressing did not result in any significant improvement in the surface smoothness of the sheets whereas the calendering resulted in a reduction in variance of the profiles at all wavelengths.

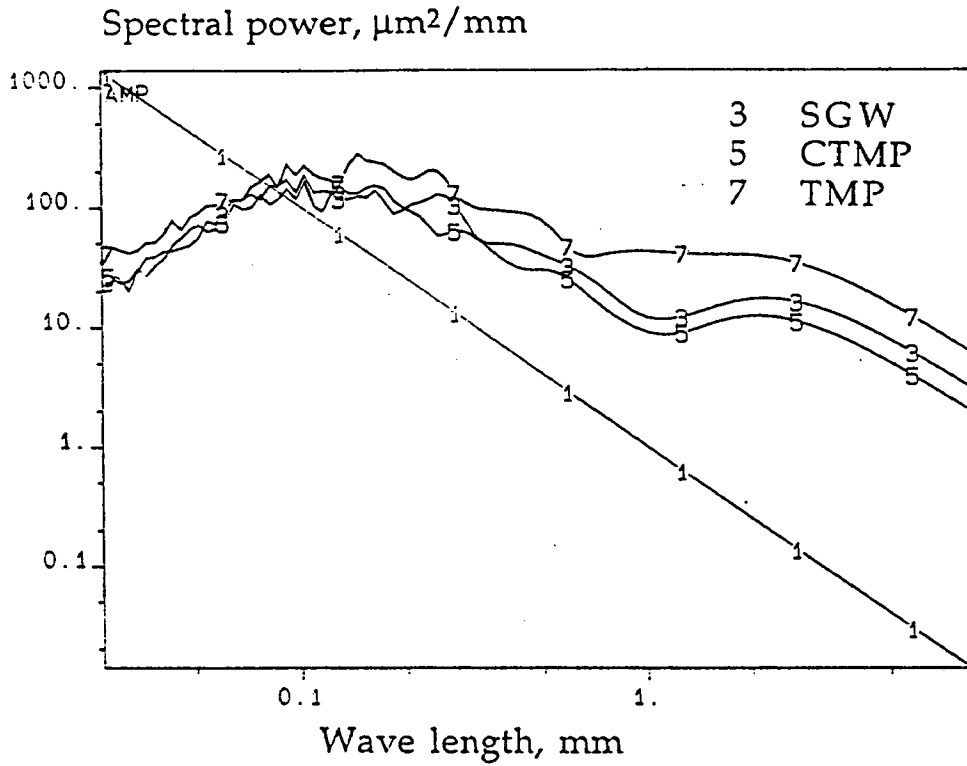


Figure 5.8 The autospectra of the surface profiles of handsheets of SGW, CTMP and TMP

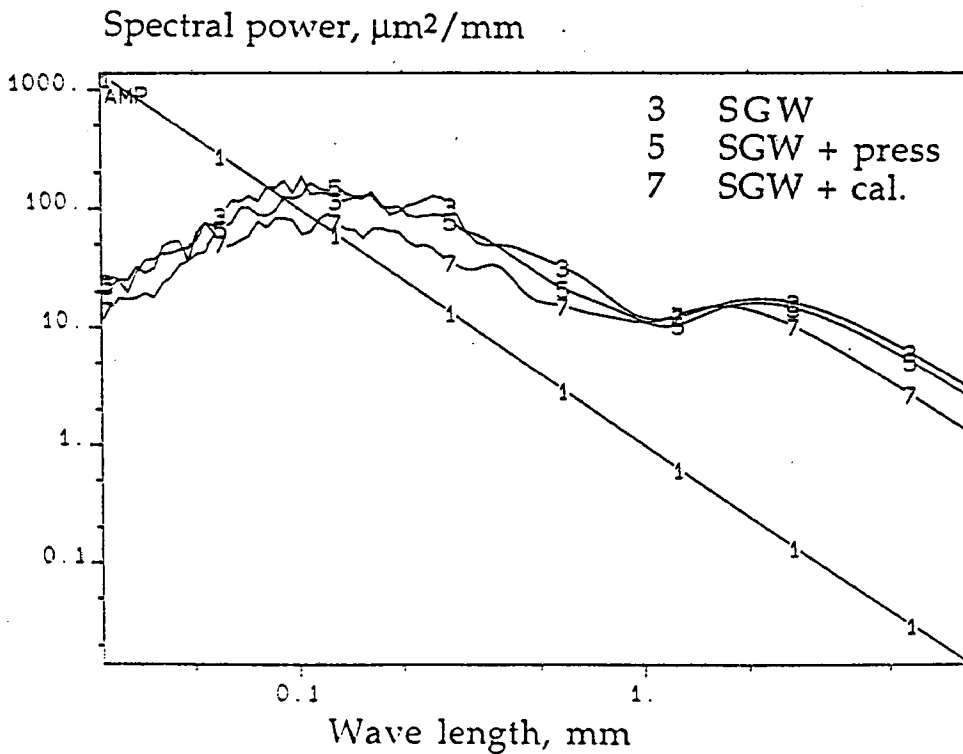


Figure 5.9 The autospectra of the surface profiles of handsheets of SGW pulp showing the effect of wet-pressing and calendering

4. CONCLUSIONS

This study has been an interesting exercise in the application of various surface characterisation techniques to a practical situation, although the material has been limited and the differences in properties have been small.

The methods employed for the evaluation of the surface properties of these handsheets rank them differently, as shown in Table 5.3.

Table 5.3 Smoothness rankings* of handsheets by different methods

	CTMP	SGW	TMP
1 PPS calendered	2	1	3
2 FOGRA-KAM	2	3	1
3 Partial coverage print	3	1	2
4 Microcontour	1	2.5	2.5
5 Autospectra of profile	1.5	1.5	3

* 1 = smoothest

The lack of agreement between PPS and FOGRA-KAM is probably indicative of the fact that the TMP, which shows the better conformability to a flat surface than the other pulps nevertheless has deeper depressions which lead to a higher PPS-value. The PPS-studies showed that the SGW-sheets had the higher surface compressibility.

Clearly more work needs to be done before the complexity of the relationship between these various tests can be explained. It may be that the important thing is to note that they do indeed measure different properties and that the various tests must always be used with caution and with thought in order to derive the best possible interpretation.

SUMMARY OF CONCLUSIONS

The smoothness of paper surface is an important requirement for its good printability. Although the smoothness of a surface is simply defined as its closeness to a plane surface but the quantitative determination of this closeness is not easy. Therefore a large number of methods and instruments have been developed over the years but all of these methods measure the surface structure of the paper to only a limited extent. Since quite often these methods measure different aspects of surface structure they do not give identical results but provide complementary information to each other. No single method is capable of describing the paper surface structure completely.

Any one of these methods can be successfully adopted for routine quality control purpose but a difficulty arises in the evaluation of the surface of papers having very close differences in their smoothness, especially papers made by different processes and from different furnishes. The air-leak and optical methods lack resolution in such cases and quite often the measurements do not relate to the printing performance of the papers. In such cases, it is necessary to obtain more detailed information about those features of the surface structure which are also related to the behavior of paper in a printing process. The methods of surface evaluation based on test printing resembles most closely the actual printing of paper, and surface profilometry provides the most exhaustive description of the surface. These two methods have been studied in detail in the present work.

The main conclusions of this study are summarized in the following paragraphs.

Partial Coverage Printing and Image Analysis

1. If a paper is printed with small amount of ink and at a low printing pressure so as to allow only a partial coverage of the paper surface, the printed pattern thus obtained allows a useful visual examination of the surface. The following information is readily available from an observation of these prints.
 - i). The contrast between adjacent areas. A low contrast signifies smoother surfaces.
 - ii). Clarity of marks/defects. Wiremarks, calender or coater streaks or any other type of marks are clearly visible.
 - iii). The degree of orientation of uneven features in the surface. A pronounced orientation may indicate a poor printing surface.
 - iv). Fineness or coarseness of surface structure.

2. If a surface is printed under given conditions with a given quantity of ink, the degree of coverage of the surface will depend on the degree of contact between paper and printing forme. The degree of coverage is therefore a measure of the surface roughness. The main feature of the present method is to achieve partial coverage and then to use image analysis as a tool to characterize the nature of the surface patterns revealed.
3. At any specified set of printing conditions (speed, force, type of ink etc.) the fractional coverage of the paper surface, A , depends on the amount of ink on the disc, x . The values of x and dA/dx at $A = 0.5$ represent the depth and the slope of the cavities in the paper surface respectively. The value of the square root of the product of x and $1/(dA/dx)$, both evaluated at $A=0.5$, has been found to be approximately equal to the Parker-Print-Surf (PPS) value.
4. The analysis of chords provides information about the coarseness or fineness of the structure. The number of chords and the mean chord length at a given coverage area provide information about the surface texture.
5. The analysis of variance in the greyvalues of the printed image yields a typical wavelength for the pattern which is a characteristic of the surface. The value of typical wavelength for a paper surface was found to be relatively insensitive to the calendaring of paper suggesting that this is also related to the formation of the paper or to textural features of the surface which survive the calendaring operation.
6. The advantage of the present method is that it characterizes the surface in terms of several parameters. These parameters are different measures of the surface features and describe the surface structure much more exhaustively than any of the methods which give only a single quantity for the total surface structure.

Analysis of Microcontour Ink Stains

7. Microcontour ink stains provide an assessment of surface roughness, which may be different from other roughness measuring methods. The coated and uncoated paper show marked difference in the intensity of colouration even though they have the same PPS roughness. Presumably the absorptivity of the paper significantly affects the results and some pigment also penetrates into the pores of the paper along with the oil.
8. The test is good only for the visual comparison of papers which have nearly the same absorptivity and optical properties. The microcontour value defined in terms of reflectance values measured by the Elrepho may be misleading.

9. The image analyzer (IBAS) gives nearly the same information as that obtained by the Elrepho. However the image analyzer provides additional information on the coefficient of variation of the intensity of stains and a typical wavelength for stain patterns. These provide a better basis for evaluating roughness of surface.

Analysis of Surface Profiles

10. Paper surface profiles contain random variations and often periodic variations superimposed thereon. Some of the predominant wavelengths in a surface profile must have arisen due to characteristic sizes of the furnish components or to features of specific process steps.
11. The contribution of short wavelength variations ($< 100\mu\text{m}$) to the total variance in profiles is much less than that in a random profile, presumably because of the finite size of fiber and other furnish components.
12. The autospectrum function gives the distribution of the total variance of the profile data in its various wavelength bands. In general, smooth papers have less variance than that of rough papers in all the bands.
13. A wavelength spectrum appears to be more informative than a frequency spectrum for the study of paper profiles because it gives a better feel of the sizes of the irregularities. When a frequency spectrum is transferred into a wavelength spectrum, however, the shape of the spectrum is distorted and the periodicity of periodic components do not show up at their correct wavelengths. The distortion is dependent on the number of lags used in the calculation of the autospectrum. An increase in the number of lags brings the peaks towards their exact wavelengths but, at the same time, reduces the accuracy of the estimated power of the spectrum.
14. An autocorrelation function gives more accurate information than the wavelength spectrum about the frequency of a periodic component if its existence is very obvious.
15. A bandpass filtration technique based on moving averages is fairly accurate in decomposing a profile into its components in different wavelength bands. The autocorrelation function of these components can be determined to check for periodicity in these components.
16. The longwave oscillations in the paper surface profiles recorded by the Perthometer are due to the flocs or thickness variations in paper rather than to a roughness variation as such. Variations at shorter wavelengths up to about 1mm are probably the type of roughness related to the surface to which the printing forme or cylinder is sensi-

tive and are responsible for the inability of the forme to achieve perfect contact with the paper.

17. The application of air-knife and bent-blade coater results in a reduction of variance of the profile. In case of air-knife that of the base board, whereas the bent-blade coater is able to fill up the narrow deep cavities better leading to a better smoothing effect.
18. Calendering leads to a further reduction of the amplitude of the variations but it affects the peaks of the surface topography more than the cavities and leads to a skewed distribution of the surface. The profile for bent-blade coated board is less skewed because of the better filling of the cavities by the coating colour.
19. The brushing of the coated and subsequently calendered board does not seem to show any significant reduction in the amplitude variations.
20. Two-stage coating in general produces a smoother surface than a single-stage coating for the same coat weight. Bent-blade and then air-knife appear to be the best combination since the bent blade fills the deep narrow cavities and the air knife levels up the surface, finally filling the wider valleys.
21. The differences in the surface smoothness of the boards coated by different processes are clearly discernible in the autospectra of their surface profiles.
22. The autospectra show the spatial distribution of variance of the profile but they do not account for the nature of the distribution of the profile heights about their mean. There is a tendency to assume this distribution to be Gaussian. From the study of surface profiles of papers and boards of various grades, it has been observed that most profiles deviate from the Gaussian behavior and show skewness in their distribution. In such cases the probability density analysis of the profile data is necessary.

Surface Smoothness and Compressibility of Handsheets of Mechanical Pulps

23. All the surface smoothing processes such as wet pressing and calendering result in a significant reduction in thickness of the sheet. It is therefore more important to consider the smoothness versus thickness relationship rather than the smoothness alone since the improvement in the smoothness is generally achieved at the cost of reduced bulk.
24. For a given void ratio (void volume / solid phase volume), the sheet made of the stone groundwood pulp (SGW) is

smoother than that made of the thermomechanical pulp (TMP) and both the sheets of SGW and TMP are much smoother than that of the chemithermomechanical pulp (CTMP). There is some indication that the SGW is initially more compressible in the surface than in the bulk whereas the CTMP is initially more compressible in the bulk than in the surface.

25. There appears to be more or less constant relationship between the Parker-Print-Surf roughness and the void ratio, regardless of whether the sheet is compressed by wet pressing, calendering or pressing under the PPS measuring head. There is a slight indication that the wet pressing alters the initial conditions prior to the PPS testing by reducing the void ratio relatively more than the surface roughness.
26. It is interesting to note that when the optical contact area was measured by the FOGRA-KAM instrument the SGW sheets were shown to be the roughest whereas they were found to be the smoothest by the PPS tester. The TMP has been found to be the most smooth of the three pulps with regard to contact fraction whereas it has the highest PPS roughness value at least at lower pressures. This lack of agreement is probably indicative of the fact that the TMP, which shows the better conformability to a flat surface than the other pulps nevertheless has deeper depressions which lead to a higher PPS roughness value.
27. Different methods of surface evaluation, namely the PPS, the FOGRA-KAM, the partial coverage printing, the microcontour ink stains and the autospectra of surface profiles grade handsheets of SGW, TMP and CTMP pulps differently confirming the multidimensional nature of the surface structure and that no single method is sufficient to describe it completely.
28. More work needs to be done before the complexity of the relationship between these various tests can be explained. It may be that the important thing is to note that they do indeed measure different properties and that the various tests must always be used with caution and with thought in order to derive the best possible interpretation.

REFERENCES

- Albrecht, J. and Brune, M.
Evaluation of paper surface by contact ratio measurement.
In Adv. Print. Sci. Technol. Vol. 10 311-320(1971).
- Andersson, H.J.
Apparatus for topographic studies of paper and paperboard surfaces.
Tappi 42(6):518-520 (1959).
- Aschan, P.J., Engström, G., Bristow, J.A., Johansson, P-Å,
Hoc, M. and Ekman, H., STFI
Influence of coating variables on the printability and gluability
of coated paper board (in Swedish).
STFI Report B 571 (1980).
- Aschan, P.J., Makkonen, T. and Pakko, J.
Board surface structure and gravure printability.
Paperi Ja Puu - Papper och Trä, 1(30) (1986).
- Back, E.L., Matakı, Y., Bristow, J.A. and Ekman, H.
Potentials of hot calendering for printing papers
Part 2. Printability and its relation to gloss and smoothness.
Nordic Pulp and Paper Research Journal, Special Issue, 4 (1988).
- Barber, E.J.
Defining the surface smoothness of paper with the Brush surface
analyser.
Tappi 36(11):158A (1953).
- Bekk, J.
Apparatus for measuring smoothness of paper surfaces
Paper Trade Journal 104(12):62(1937).
- Bendat, J.S. and Piersol, A.G.
Measurement and Analysis of Random Data
John Wiley & Sons, Inc. (1958).
- Bikerman, J.J. and Whitney, W.
Superficial Imbibition by paper
Tappi 46(11):689 (1963).

Bliesner, W.C.

Dynamic smoothness and compressibility measurements on coated papers.

Tappi 53(10):1871 (1970).

Blokhuis, G. and Blogg, A.E.

Dynamic smoothness of paper.

Proceedings of the 12th International Conference of printing research institutes. Guildford, IPC, 53-60 (1974).

Blokhuis, G. and Kalff, P.J.

Dynamic smoothness measurement of papers and print unevenness.

Tappi 59(8):107 (1976).

Bradway, K.E.

Factors which affect the printing smoothness of handsheets.

Tappi 56(8):118-120 (1973).

Bradway, K.E.

Comparison of smoothness evaluation by different test methods.

Tappi 63(11):95 (1980).

Bristow, J.A.

Liquid absorption into paper during short time intervals.

Svensk Papperstidning, 70(15):623-629 (1967).

Bristow, J.A.

The surface compressibility of paper

Sven. Papperstidn. 85(15):127(1982).

Bristow, J.A.

The paper surface in relation to the network.

In Paper Structure and Properties (eds. Bristow, J.A. and Kolseth, P.) Marcel Dekker Inc., pp.169- (1986).

Bristow, J.A. and Bergenblad, H.

Interpretation of ink-stain tests on coated papers.

In Adv. Print. Sci. Technol. (Banks W.H., ed.). Vol 16. Printech Press (1982).

Casey, J.P.

Paper and Pulp. Chemistry and Chemical Technology, Vol 3, 3rd ed., Interscience Publishers Inc., New York (1981).

Chapman, S.M.

The measurement of printing smoothness.

Pulp and Paper Mag. Can. Convention issue 140 (1947).

Climpson, N.

3-Dimensional Paper Surface Profilometry.

Research and Development Dept. ECC International (1984).

Davis, M.N.

US. Patent No. 2050486, Aug 11(1936).

Fetsko, J.M.

Printability Studies on a Survey Series of Paperboards and Coated Papers.

Tappi 41(2):49 (1958).

Fetsko, J.M.

Evaluation of smoothness and absorbency tests for white patent coated paperboard.

Tappi 42(2):110-121 (1959).

Fetsko, J.M., Witherell, F.W. and Poehlein, G.W.

Relationship between gloss and surface roughness of paperboard samples and prints.

Proc. 12th Int. Conf. of Printing Res. Inst., Guildford, IPC, 67 (1974)

Gate, L., Windle, W. and Hine, M.

The relationship between gloss and surface microtexture of coatings.

Tappi 56(3):61 (1973).

George, H.F., Oppenheimer, R.H. and Marrara, C.G.

Gravure print smoothness scanner.

Tappi 59(9):110-113 (1976).

Ginman, R., Makkonen, T. and Nordman, L.

Profile measurement on printing paper.

Proc. 12th Int. Conf. Printing Res. Inst. (Ed. W.H. Banks).
Guildford, IPC Press, 46-52 (1974).

- Ginman, R., Panigrahi, P. and Nordman, L.
Evaluation of the smoothness of coated papers,
in Adv. Print. Sci. Technol., Pergamon Press. Vol 3, pp. 249-262
(1955).
- Glassman, A.
Predicting paper printing quality by the battery of test methods.
Tappi 44(1):7 (1961).
- Gunning, J.R.
A comparison of smoothness testers.
Tappi 55(12):1678-1683 (1972).
- Gunning, J.R. and Farrell, W.R.
A device for measuring mottle in coated papers.
Tappi 59(8):92 (1976).
- Harris, F.J.
On the use of windows for harmonic analysis with the discrete
fourier transform.
Proc IEEE, 66(1):51 (1968).
- Hartig, W.
Testing of optical smoothness with the K.L.-Device in the paper
industry (in German).
Das Papier, 39(1):1 (1985).
- Hawkes, C.V. and Bedford, T.
Patra Printing Lab Report No 51 (1963).
- Hendry, I.F.
Some techniques for the assessment of coated art papers.
Tappi 44(10):725 (1961).
- Hsu, B.S.
Distribution of Depressions in Paper Surface - A method of
determination. Brit. J. Appl. Phy. (13):155 (1962).
- Hsu, B.S.
The surface structure of paper under rolling pressure.
Brit. J. Appl. Phy. (14):301 (1963).

Hull, H.H. and Rgers, M.C.

New method of observing properties of paper which influence printability.

Tappi 38(8):468-472 (1955).

Hung, J.Y., Nelson, R.W. and van Eperen, R. H.

Remarks on the surface receptivity and roughness of paper as these relate to liquid film application.

Tappi 52(9):1732-1734 (1957).

Huynh, V.M. and Peticca, G.

An optical technique for roughness measurement of printing papers.

J. Imaging Technol. 16(1):22-26 (Feb 1990).

Janes, R.L.

Surface configuration of paper and paperboard and its measurement.

Tappi 42(6):172A-176A (1959).

Jenkins, G.M. and Watts, D.G.

Spectral Analysis and its applications

Holden-Day (1968)

Johansson, P.Å.,

Evaluation of grey-tone evenness using bandpass-filtering on a video-scanning image analyser,

Proc. 3rd Scandinavian conference on Image Analysis, Denmark, pp 188-193 (1983).

Kapoor, S.G.

A stochastic Approach to Paper Surface Characterization and Printability Criteria

Ph.D. Thesis, University of Wisconsin-Madison (1977).

Kapoor, S.G. and Wu, S.M.

Predicting printability of gravure and embossed papers by time series analysis.

J. Phys. D. Appl. Phys., Vol. 2, 2005-2017 (1979).

Kapoor, S.G. and Wu, S.M.

A stochastic approach to paper surface characterisation and printability criteria.

J. Phys. D. Appl. Phys., Vol. 11, 83 (1978).

Kapoor, S.G., Wu, S.M. and Pandit, S.M.

A new method for evaluating the printing smoothness of coated papers.

Tappi 61(6):71 (1978).

Karttunen, S.

Contact smoothness and ink transfer of paper.

Paperi Ja Puu 52(4a):159 (1970).

Karttunen, S., Ginman, R. and Makkonen, T.

Printability of light weight coated papers.

14th EUCEPA Conf., Budapest (1971).

Karttunen, S.

Printability and the surface structure of paper.

Papper och Trä No 11, 617 (1971).

Kent, H.J.

The influence of the coating structure on the printability of LWC-paper (in German).

Wochenblatt für Papierfabrikation 112(7):243 (1984).

Kohl, A.

Smoothness measured on-line.

Pulp and Paper Int. 45 (Feb. 1983).

Larsson, L.O. and Sunnerberg, G.

Optically covered area of solid prints related to paper properties.

Tappi 59(8):96 (1976).

Lashof, T.W., Mandel, J. and Worthington, V.

Use of the sensitivity criterion for the comparison of the Bekk and Sheffield smoothness testers.

Tappi 39(7):532 (1956).

- Lashof, T.W. and Mandel, J.
Measurement of the Smoothness of the paper.
Tappi 43(5):385 (1960).
- Leekley, R.M.
In Discussion of the paper of Albrecht and Brune (1971).
- Luey, A.T.
Smoothness measurement with ink films.
Tappi 42(3):185 (1959).
- Luey, A.T.
Effects of board compressibility on printing smoothness.
Tappi 42(6):176A (1959).
- Lyne, B.
Measurement of the distribution of surface void sizes in paper.
Tappi 59(7):102-105 (1976).
- Lyne, L.M. and Copeland, D.
Print quality evaluation by magnetic scanning.
Tappi 51(2):363 (1968).
- Mangin, P.J. and De Grace, J.H.
An analysis of the accuracy of measuring paper roughness with the
Parker Print-Surf.
Tappi Proc. of Int. Printing and Graphic Arts/Testing Conf. 125
(1984).
- Nordman, L. and Aschan, P.J.
Evaluation of coated board surfaces by profile measurements (in
German)
Das Papier 34(10A):v 149-155 (1980).
- Norman, B. and Wahren, D.
A comprehensive method for the description of mass distribution in
sheets and flocculation and turbulence in suspensions.
Sven. Papperstidning 75(20):807 (1972).

O'Neill, J.R.

The printing smoothness of paper - A new method of measurement.
Appita 201 (May 1959).

Parker, J.R.

An air leak instrument to measure printing roughness of paper and board.

Paper Technology 6(2):126 (1965).

Parker, J.R.

Development and application of a novel roughness tester.

Tappi 54(6):934 (1971).

Parker, J.R.

The measurement of printing roughness.

Tappi 64(12):56 (1981).

Perthometer, Feinprüf GmbH, Göttingen

Pritchard, E.J. and McFarlane, D.

Patra Printing Lab. Report No 57 (1964).

Ragan, R.O.

Photographic examination of paper and paperboard surface to predict halftone printing quality.

Tappi 42(6):486 (1959).

Roehr, W.W.

Effect of smoothness and compressibility on the printing quality of coated paper.

Tappi 38(11):660-664 (1955).

Rosen, A. and Hemstock, G.A.

A method of determining the surface roughness and receptivity characteristics of blade coated raw stock.

Tappi 50(1):7 (1967).

Ruckdeschel, F.R. and Hauser, O.G.

Yule-Nielsen effect in printing: a physical analysis

Applied Optics, 17(21), 3376 (1978).

Sankey, C.A. and White, P.H.

Pulp and Paper Mag. Can 49(C):99 (1948).

SCAN C-26:76R

Preparation of laboratory sheets for physical testing.

SCAN P21:67.

Roughness determination with the Bendtsen tester

Schmidt, S.

Smoothness measurement in paper making and printing.

Paper (19 April 1982) pp. 24.

Sheid, L.J. and Hupp, A.H.

An approach to the evaluation of coated paper smoothness.

Tappi 36(10) 177A (1953).

Stout, K.J.

Surface Roughness - Measurement, Interpretation and Significance of Data. Part I - Statistical parameters.

Materials in Engg. Vol. 2, 260 (1981).

Part II - Experimental consideration and significance of data.

Materials in Engg. Vol 2, 287 (1981).

Sweerman, A.J.W.

A new approach to the measurement of roughness and porosity of paper.

Tappi 44(7):172A-174A (1961).

TAPPI T 479 om - 86,

Smoothness of paper (Bekk method)

Tappi Test Methods, vol.1 (1989).

Tappi T 538 om-88

Smoothness of Paper and Paperboard (Sheffield method),

Tappi Test Methods, vol. 1 (1989).

Tollenaar, D. and Ernst, P.A.H.

Optical density and ink layer thickness.

In Adv. in Print. Sci. Technol. (Ed. Bank, W.H.), Pergamon Press, Vol 2, pp. 214-234 (1962).

Tollenaar, D. and Ernst, P.A.H.

Uneven Ink Transfer on Smooth surfaces

In Adv. Print. Sci. & Technol. (Ed. Banks W.H.), Pergamon Press, Vol. 6, 139-149 (1971).

Tollenaar, D., Sweerman, A.J.W., Blokhuis, G. and Van Gastel, L.A.,

Printing blackness as a characteristic for paper quality
Tappi 49(12):532 (1966).

Trice, W.H., Friend, W.H. and Trader, C.D.

Test method for printing smoothness.

Tappi 56(12):151 (1973).

Ullman, U. and Qvarnström, I.

Influence of surface smoothness and compressibility on print unevenness.

Tappi 59(4): (1976).

Verseput, H.W. and Mosher, R.J.

A simplified printing smoothness test using magnetic ink.

Tappi 54(8):1309 (1971).

van der Vloodt, P.C.

A new method for measuring the surface roughness of paper.

In Adv. in Print. Sci. Technol., Vol. 3 191-201 (1964):

Walker, W.C. and Carmack, R.F.

The Printing Smoothness of Paper

In. Adv. in Print.Sci. Technol. (Ed. Banks W.H.), Pergamon Press,

Vol. 3, 203-219 (1964).

Walker, W.C.

Determination of ink transfer parameters.

Tappi 64(5):71 (1981).

Walker, W.C. and Fetsko, J.M.

A concept of ink transfer during printing.

Am. Ink Marker 33(12):38 (1955).

Wieslander, J.

IDPAC Commands - User's Guide

Lund Institute of Technology, Department of Automatic Control,

Lund, Sweden (1980).

Wink, W.A. and van den Akker, J.A.

A new approach and procedure for studying the surface receptivity and roughness of paper as these relate to liquid film application.

Tappi 40(7):528-536 (1957).

Wyszkowski, S.W.P.

Printability testing - A critical review.

Proceedings of TAPPI Printing Reprography Testing Conf. (1979).

APPENDIX A

IMAGE ANALYSIS ROUTINES**Equipment used**

The image analysis investigations were carried out using a commercial Kontron IBAS2 image analyser (A1.1). This system digitizes a standard video signal into an image of 512 • 512 picture elements (pixels) each with 256 possible grey level values ranging from 0 (= black) to 255 (= maximum white) proportional to the local reflectivity times the local illumination. One image thus contains 256 KBytes of information which can be processed in the image analyser's computer memory or stored on magnetic media. A range of standard routines for image enhancement and analysis are available on the system and others can be programmed into it by the user.

The images were captured using a black and white Pasecon tube video camera with a Zeiss Tessovar macrophotography zoom lens. The image width can be adjusted within the 1-50 mm range and the spatial resolution in the digitized image becomes 1/512 of the width chosen.

Contact fraction analysis

The routine for this can shortly be described as an image contour enhancement to sharpen the transition between printed and unprinted areas followed by a thresholding at a grey level corresponding to a reflection level half way between those of fully inked areas and unprinted areas. This creates a binary (strictly black or white) image in which black corresponds to printed areas, while white corresponds to background, i.e. unprinted areas. The proportion of black pixels was counted to give the area of coverage.

In more detail the contour enhancement works as follows. Grey level transition zones (boundaries printed/unprinted) are first detected using a Laplace filter(A1.2). Within these zones a moving window checks each pixel to see whether its grey level is closest

to the local maximum or minimum grey level in the window at its present position around the checked pixel. This pixel is replaced with either the maximum or the minimum level which is the closest in grey level. This procedure leads to a sharper transition between the typical printed and unprinted reflectance values. The subsequent segmentation into a binary image is then less ambiguous and leaves less noisy edges.

The segmentation level was determined in the following way. First the grey levels of the lightest and darkest 1/1000 area fractions were determined. These levels are considered to correspond to typical unprinted and printed areas and the threshold for objective/background was then set to the average of the two levels. This latter procedure leads to an inherent stability of the segmentation against artifacts such as changing illumination, camera, response etc.

Clearly this routine relies on the image to contain at least a 1/1000 area fraction each of printed and unprinted regions. In, for example, a completely ink-covered image area, the threshold would be forced to lie within the grey levels of the inked paper and might result in a area fraction in magnitude of 50 % while the true value was 100 %. Care was taken to ensure that this type of artifact never occurred.

It should not be forgotten that the choice of a specific image processing routine like that here outlined in itself introduces a certain amount of subjectivity. The validity of the routine must be evaluated by the operator according to how well it seems to reveal the interesting features of an image. Once this is done, however, the routine should be automatic and robust against irrelevant factors like illumination changes, as already mentioned.

Chord length analysis

An estimate of the texture coarseness was made using chord length analysis. This means that a binary image of the printed paper is first created according to the previous section. A line grating is then superimposed and the chords are observed that appear where the lines overlap the ink-covered regions of the paper.

The mean length of these chords is then an estimate of the typical dimensions of the inked patches on the printed paper. In a pattern consisting of equally sized circular features, the distri-

bution of chord lengths ranges from a maximum equal to the circle diameter down to zero, but values close to the diameter are much more common than the very low ones. In a pattern of worm-shaped features, the chords are mostly of a length greater than the average diameter of the worm. In a pattern of inked regions made up of several different shapes, both circular and entangled worm-like, it is fair to say that the average chord length gives an indication of the typical dimensions of the speckled or mottled texture of a partially ink-covered paper surface. More information on chord length analysis can be found in textbooks on stereology (A1.3).

Grey-level variance

Unevenness in local reflection ("print mottle") can be quantified as the standard deviation of several readings of the reflection of small enough spots on the printed surface. In the case of image analysis, the recorded image itself consists of 512^2 ordered pixel readings whose grey values can be transformed into reflectance values. The standard deviation (sd) of these is readily available as a standard function on the image analyser. The coefficient of variation (cv) can be calculated as $cv = sd/\text{mean value}$. Since the camera response is proportional to the light level, a change in illumination level will affect both the sd and the mean with the same factor and thus leave the cv unchanged and equal to the cv of local reflectance. The true mean reflectance level can be evaluated with normal equipment like the Elrepho reflectometer.

The value of sd (or cv) is dependent on the spot size in the measurement. In our case the spot size equals the pixel size, p , i.e. $p = \text{image width}/512$. The smaller the spot size the more fine scale variations are picked up and the greater is the sd. Typically one can say that variations of a spatial wavelength longer than twice the spot size can be detected. At the long wavelength end of the spectrum, only variations with a spatial wavelength smaller than the size of the image edge will give a full contribution to the sd.

This discussion indicates the approximate wavelength range that a straight forward image grey level sd analysis covers. It is useful to remember that this and similar measurements involve an inherent bandpassing action in feature sizes.

It is often interesting to go a step further to obtain more detailed information of the texture sizes (wavelength components)

which contribute the most to the overall unevenness pattern. This is analogous to the general application of spectral signal analysis in fields like noise or vibration analysis etc.

Signal analysis of this type can be performed at different frequency/wavelength resolutions.

High resolution studies are typically performed with FFT algorithms (FFT = Fast Fourier Transform). Such high resolution power spectra are useful for the detection of narrow-band periodical variations e.g. variations derived from wiremarks in the paper. The drawback of a high resolution spectrum is that it provides too little data reduction. Most of the time it is better to have fewer numbers, preferably only one, to describe a certain quality property. An intermediate level of resolution between the full FFT-spectrum and a single sd reading can be achieved by studying the variation in a few coarser wavelength bands. Such bands can be calculated by merging together suitable numbers of classes in a high resolution power spectrum, but also by applying bandpass filters on the image and then studying the sd of the filtered image. The latter technique has been used in the present case and is described in greater detail below.

We have here chosen to work mainly with a wavelength notation. It is of course possible to use spatial frequencies instead. The spatial frequency expresses the number of cycles per unit length and thus has the dimension of inverted length. The relation to wavelength is simply an inversion of the value.

Bandpass filtration by moving averages

Low pass filtration

The application of a moving averaging window to a profile leads to a low-pass filtration, meaning that high frequency (short wavelength) components are suppressed while low frequencies pass through the filter. The action can be quantified by studying the response to sine wave functions of different frequencies.

Consider a profile signal of cosine shape with amplitude A_0 and wavelength λ .

$$P_0(x) = A_0 \cos 2\pi x/\lambda \quad [A1.1]$$

If an averaging window of width W is applied, the resulting profile will also be a cosine function but with a different amplitude, A_1 , depending on the relation of W to λ .

This amplitude can be found by calculating the average within the window when the window is centered above a peak of the cosine, for instance around $x = 0$.

$$\begin{aligned}
 A_1 &= \frac{1}{W} \int_{-W/2}^{W/2} P(x) dx = \frac{2}{W} \int_0^{W/2} A_0 \cos(2\pi x/\lambda) dx \\
 &= \frac{2A_0}{W} \int_0^{W/2} \frac{\sin(2\pi x/\lambda)}{(2\pi/\lambda)} \\
 &= \frac{2A_0 \lambda}{W 2\pi} (\sin 2\pi W/2\lambda) = A_0 \frac{\sin(\pi W/\lambda)}{\pi W/\lambda} \\
 &= A_0 \operatorname{sinc}(\pi W/\lambda) \tag{A1.2}
 \end{aligned}$$

with the notation $\operatorname{sinc}(x) \equiv \frac{\sin(x)}{x}$

The amplitude transmission T is therefore:

$$T = A_1/A_0 = \operatorname{sinc}(\pi W/\lambda) \tag{A1.3}$$

The variance or power transmission is however affected by the square of the amplitude and thus T^2 , see the broken line in Figure 1. It can be seen in the figure that

- a wavelength equal to the width of the window W is completely suppressed.
- a certain leakage of energy (variance) from shorter wavelengths is present.
- the filter does not cut off sharply at $\lambda = W$. Instead it has fallen to 0.5 transmission at a wavelength of $\lambda_{0.5}$ determined by $\operatorname{sinc}^2(\pi W/\lambda_{0.5}) = 0.5$. An approximate solution yields $\lambda_{0.5} \approx 1.658 W$, which can be taken as a more representative limit than $\lambda = W$.

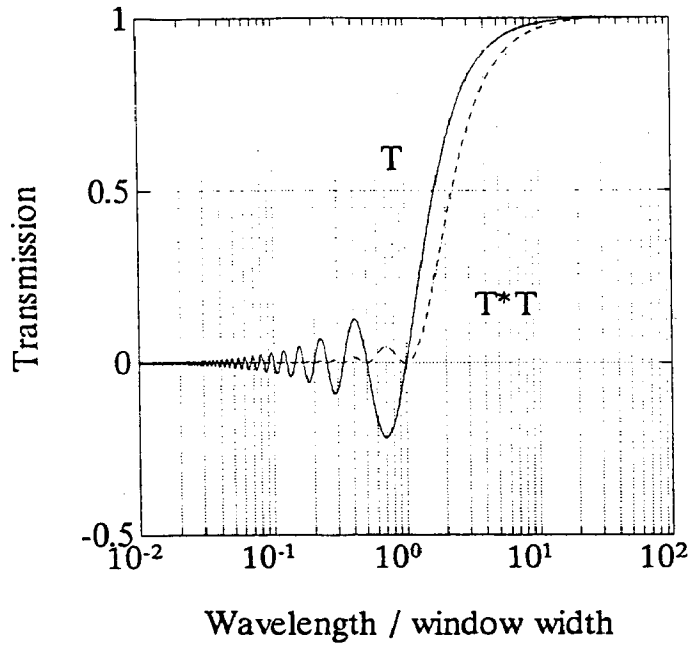


Figure A1.1 Lowpass filter amplitude transmission T (solid line) as function of λ/W , i.e. λ is expressed in units of the window width W and T^2 (broken line)

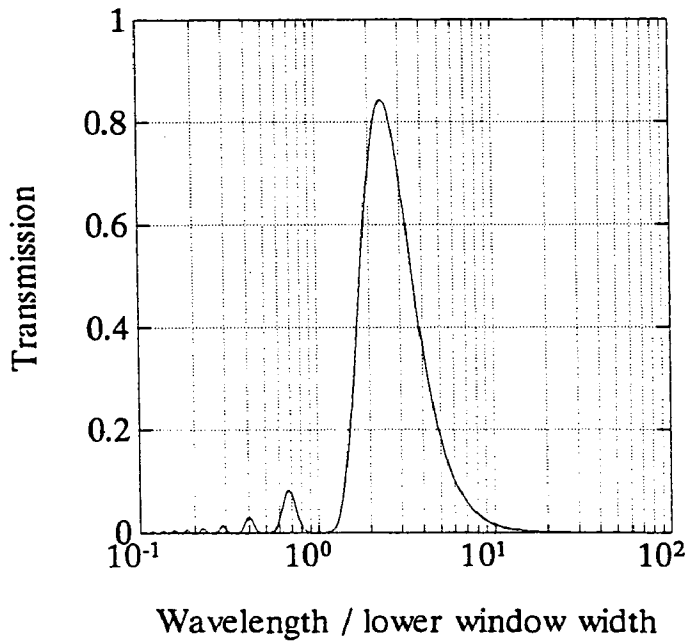


Figure A1.2 Bandpass filter variance transmission T_{bp}^2 as a function of the wavelength expressed in units of the smallest window W in the pair W and $3W$

Bandpass filtration

For the bandpass filtration, we have used the difference between profiles filtered by two windows of widths W and $3W$ respectively. The difference in amplitude response of the two filters constitutes the amplitude of the bandpassed image. The variance or power transmission T_{bp}^2 is then:

$$T_{bp}^2 = (\text{sinc}(\pi W/\lambda) - \text{sinc}(\pi 3W/\lambda))^2 \quad [A1.4]$$

A plot of T_{bp}^2 is given in Figure 2. A numerical solution yields:

Max transmission at $\lambda_{\max} \approx 2.371$ is $T^2 \approx 0.8432$.
Half max transmission is at $\approx 1.71 W$ and $\approx 3.77 W$.

This means that the transmission of the W - $3W$ window combination actually yields a transmission more like an octave filter ($3.77W/1.71W = 2.2$) than the W to $3W$ wavelength transmission that might be assumed without closer consideration.

The typical wavelength

It is often of interest to obtain a quantitative measure of the fineness or coarseness of the patterns in a profile. If a power spectrum has high resolution, any predominant wavelength component as well as the general distribution of the power will be visible.

In a coarser spectrum, such as that obtained from a set of bandpass filters, we can see no sharp peaks but only the power distribution among the bands. One way to assess a characteristic measure, the typical wavelength λ_T , is to calculate "the centre of gravity" of the bands weighted according to the variance in each band.

$$\lambda_T = \frac{\sum V_i \cdot \lambda_i}{\sum V_i} \quad [A1.5]$$

where λ_i is the average wavelength in band No. i
 V_i is the variance in band No. i

The summation is performed over all bands measured. It has been established that this measure reveals the wavelength of a sine wave test profile quite well.

- (A1.1) Manufactured by Kontron Bildanalyse GmbH,
D8057 Eching, Munich, FRG.

- (A1.2) Gonzales, R.C. and Wintz, P.
Digital Image Processing. ISBN 0-201-03045-4.
Addison-Wesley, Reading 1977.

- (A1.3) Russ, J.C.
"Practical stereology". ISBN 0-306-42460-6.
Plenum Publishing, New York 1986.

APPENDIX B

SYNTHESIS OF PAPER PROFILE USING IDPAC

(a) Generation of gaussian white noise (mean = 127, variance = 20)

```

INSI  WNOIS      3000
      > Norm 127 20
      > X

```

(b) Superposition of shortwave sine function (wavelength = 0.6 mm, amplitude = 5)

```

INSI  SIN 6      3000
      > Sine.1414 0.0
      > X
SCLOP SIN65<SIN6 * 5
WECOP WSIN65 < WN015 + SIN65

```

(c) Truncation to give skew distribution

```

RUN   SKEW
      if y > 150 then y = 150
Output:WSINSKEW

```

(d) Filtration of high frequency noise (1st order lowpass filter with cut off wavelength = 0.2 mm)

```

FILT  SYS10 < LP 1 1.4242
DETER LPAP < SY510 WSINSKEW

```

(e) Trimming of profile

```

CUT   CLPAP < LPAP 1501 1500

```

(f) Superposition of longwave sine function (wavelength = 4 mm,
Amplitude = 10)

```
INSI  SINE40  1500
      > SINE  02120  0.0
      > X
SCLOP SINE4010 < SINE40 * 10
VECOP SYNTPAP2 < CLPAP + SINE4010
```